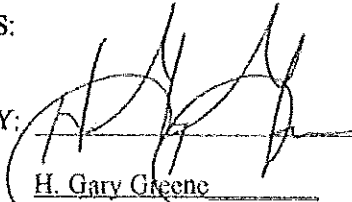
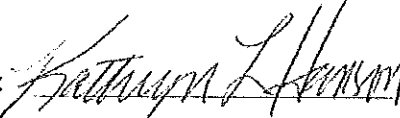


1.0 REPORT TITLE:

DCPP 3D/2D Seismic-Reflection Investigation of Structures Associated with the
Northern Shoreline Seismicity Sublineament of the Point Buchon Region

2.0 SIGNATORIES:

PREPARED BY:  DATE: Jan 4, 2012
H. Gary Greene Consultant
Printed Name Organization

VERIFIED BY:  DATE: 12/06/2012
Kathryn Hanson AMEC
Printed Name Organization

VERIFIED BY: Jan D. Rietman DATE: 12/3/2012
Jan Rietman Consultant
Printed Name Organization

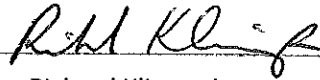
APPROVED BY:  DATE: 12/10/2012
Richard Klimczak PG&E
Printed Name Organization

TABLE OF CONTENTS

1.0	REPORT TITLE:	1
2.0	SIGNATORIES:.....	1
3.0	RECORD OF REVISIONS.....	4
4.0	REPORT VERIFICATION SUMMARIES	5
5.0	INTRODUCTION.....	8
5.1	Purpose	10
5.2	Background.....	10
5.2.1	Regional Stratigraphy	10
5.2.2	Tectonic Setting	12
5.2.3	Key Local Faults	13
5.3	Definition of Study Area	15
5.4	Goals.....	15
5.5	Intended Use of the Results	16
6.0	DATA	17
6.1	Data Acquisition.....	17
6.2	Data Processing and Quality Control	20
7.0	METHODOLOGY	23
7.1	Team-Based Approach	23
7.2	Interpretation Tools	25
7.3	Interpretation Criteria	26
7.3.1	Mapping Horizons (Stratigraphic Beds and Unconformities)	26
7.3.2	Mapping Faults	27
8.0	ASSUMPTIONS	30
9.0	SOFTWARE.....	31
10.0	INTERPRETATION AND ANALYSIS.....	32
10.1	Interpretation	32
10.1.1	Interpretability of Data.....	33
10.1.1.1	<i>Poor Interpretability</i>	33
10.1.1.2	<i>Good Interpretability</i>	36
10.1.2	Stratigraphy.....	36
10.1.3	Structure.....	40
10.2	Analysis	40
10.2.1	Hosgri Fault Zone	42
10.2.1.1	<i>Northern Part of Study Area</i>	43

10.2.1.2	<i>Southern Part of Study Area</i>	45
10.2.2	Point Buchon Fault Zone (Formally called N40°W fault zone)	45
10.2.2.1	<i>Main trace of Point Buchon fault zone</i>	46
10.2.2.2	<i>East Branch Point Buchon fault zone</i>	48
10.2.2.3	<i>Western splays of the Point Buchon fault zone</i>	49
10.2.3	Structures coincident with the northern Shoreline seismicity sublineament 50	
10.2.4	Folds	50
10.2.5	Complex Structural Area	51
10.2.6	Northern extent of the Shoreline seismicity trend at the Hosgri Fault Zone 52	
11.0	CONCLUSIONS	53
11.1	The Hosgri Fault Zone	54
11.2	The Point Buchon Fault Zone	55
11.3	Folding	56
11.4	Northern Shoreline Seismicity Sublineament	56
11.5	Strike-slip Tectonic Models	57
12.0	LIMITATIONS	58
13.0	IMPACT EVALUATION	59
14.0	REFERENCES	60
15.0	LIST OF ACRONYMS	64
16.0	LIST OF FIGURES, FOLDOUTS, PLATES AND TABLES	66
17.0	APPENDICES	68

3.0 RECORD OF REVISIONS

Rev. No.	Reason for Revision	Revision Date
0	Initial Report	

4.0 REPORT VERIFICATION SUMMARIES

Two Independent Technical Reviewers (ITRs) provided reviews of the Technical Report and supporting documents. Ms. Kathryn Hanson reviewed the report for thoroughness and completeness of required sections. Dr. Jan D. Rietman reviewed the report for technical accuracy, including use of proper interpretation methods, and reviewed the Fugro Field and Data Processing reports for completeness and accuracy and as partial QA acceptance of the data collection and processing.

4.1: Report Verification Summary by Independent Technical Reviewer Ms. Kathryn Hanson

Item	Parameter	Yes	No*	N/A*
1	Purpose is clearly stated and the report satisfies the Purpose.	X		
2	Data to be interpreted and/or analyzed are included or referenced.	X		
3	Methodology is appropriate and properly applied.	X		
4	Assumptions are reasonable, adequately described, and based upon sound geotechnical principles and practices.	X		
5	Software is identified and properly applied. Validation is referenced or included, and is acceptable. Input files are correct and accurate.			N/A
6	Interpretation and/or Analysis is complete, accurate, and leads logically to Results and Conclusions.	X		
7	Results and Conclusions are accurate, acceptable, and reasonable compared to the Data, interpretation and/or analysis, and Assumptions.	X		
8	The Limitation on the use of the Results has been addressed and is accurate and complete.	X		
9	The Impact Evaluation has been included and is accurate and complete.	X		
10	References are valid for intended use.	X		
11	Appendices are complete, accurate, and support text.			N/A

* Explain “No” or “N/A” entries. (For example, Items 3 thru 7 would be N/A for a data report that simply presents the collected data.)

This Verification Summary successfully addresses all of the previous technical and editorial comments I made to earlier drafts (August 19, 2011, November 26, 2011, March 18, 2012, June 18, 2012, and December 1, 2012 review comments). As part of the review process I participated in a meeting with the Project team, PG&E, and Jan Rietman on June 29, 2011. I had brief conversations with members of the Project team, chiefly Gary Greene, Project Manager and Hans

Abramson Ward, and Marcia McLaren (Quality Manager) to discuss my review comments to early drafts.

Notes related to items in checklist above:

5. Qualification of the software programs was not included in my scope of work.

11. Review of Appendices was not included in my scope of work.

Verifier (ITR):

Kathryn L. Hanson
 (name/signature)

12/06/2012
 (date)

**4.2 Report Verification Summary by Independent Technical Reviewer
 Dr. Jan D. Rietman**

Item	Parameter	Yes	No*	N/A*
1	Purpose is clearly stated and the report satisfies the Purpose.	X		
2	Data to be interpreted and/or analyzed are included or referenced.	X Comment #3		
3	Methodology is appropriate and properly applied.	X		
4	Assumptions are reasonable, adequately described, and based upon sound geotechnical principles and practices.	X		
5	Software is identified and properly applied. Validation is referenced or included, and is acceptable. Input files are correct and accurate.	X Comment #4		
6	Interpretation and/or Analysis is complete, accurate, and leads logically to Results and Conclusions.	X		
7	Results and Conclusions are accurate, acceptable, and reasonable compared to the Data, interpretation and/or analysis, and Assumptions.	X		
8	The Limitation on the use of the Results has been addressed and is accurate and complete.	X		
9	The Impact Evaluation has been included and is accurate and complete.	X		
10	References are valid for intended use.	X		
11	Appendices are complete, accurate, and support text.	X Comment #5		

* Explain "No" or "N/A" entries.

COMMENTS:

C1: The review process began on June 29, 2011 with an orientation meeting for the data analysis/interpretation team and reviewers. On August 11, 2011 I met with the analysis team to discuss their basic approach using the Seismic Micro-Technology (SMT) program, Kingdom Suite (The present program name, IHS Kingdom, results from corporate changes after August 2011.) Over the next 14 months I held several additional short meetings and discussions with the project manager, Gary Greene. These meetings were primarily to explain or illustrate my comments on the text and illustrations for the three Draft Report versions. Additional meetings were held with Marcia McLaren of PG&E throughout the 17 month period of report review, data corroboration, and software validation for safety-related applications.

C2: All Report Review Comments by me (Jan D. Rietman) to previous Draft Reports were considered and incorporated into the Final Report by the project manager. My final review on December 3, 2012 was of the Report dated December 1, 2012.

C3: The seismic reflection data used for the analysis/interpretation presented in this report are digital SGY files. They reside on a computer in the Geosciences Department of PG&E. These data were incorporated into the analysis/interpretation using the Safety-Related version of IHS Kingdom, Version 8.6, Hotfix4.

C4: The primary software programs used for this analysis/interpretation are Seismic Processing Workshop (SPW), UNISEIS, IHS Kingdom, Rock Solid Attributes (RSA), and ArcGIS. SPW was used by Fugro Seismic Imaging to process the 2D seismic reflection data and UNISEIS is Fugro Seismic Imaging's proprietary program that was used to process the 3D seismic reflection data. IHS Kingdom is a PC-based program for analysis/interpretation of seismic reflection data. Version 8.6 was used in this study. RSA is a separate program or module that provides additional analysis and visualization capabilities to data in IHS Kingdom. ArcGIS is an analysis and mapping program used, in part, to present the results of the analysis/interpretation from the IHS Kingdom program. Data corroboration and software validations for these programs are described in Appendix A.

C5: Appendix A, Qualification of Point Buchon 3D & 2D Seismic-Reflection Profiling Survey Data, discusses the procedures for qualifying the data and validating for safety-related use the software programs used in this study. Reports by Fugro Consultants, Inc. and Fugro Seismic Imaging that provide detailed information on the data collection and processing procedures and software vetting are referenced in Appendix A. I reviewed drafts of the Fugro Reports and my comments were incorporated into their Final Reports.

Verifier (ITR):
2012



December 3

Jan D. Rietman

5.0 INTRODUCTION

Recent studies of seismicity in the vicinity of Pacific Gas and Electric Company's (PG&E) Diablo Canyon Power Plant (DCPP) show a microseismicity alignment sub-parallel to, and 1 kilometer (km) west of, the coastline, suggesting the possible presence of a previously unidentified fault about 1 km offshore of the DCPP (PG&E, 2008; Hardebeck, 2010). This previously unidentified fault was referred to as the Shoreline fault zone (PG&E, 2008). An extensive investigation conducted by PG&E in 2009 and 2010 was undertaken to better constrain the four main parameters of the Shoreline fault zone that are required for seismic source characterization and the assessment of seismic hazard. These parameters consist of geometry (i.e., fault length, fault dip, down-dip width), segmentation, distance from DCPP, and slip rate. The investigation involved the acquisition, processing, and interpretation of new geological, seismological, bathymetric, and geophysical data including USGS seismic-reflection profiles obtained in 2008 and 2009 (PG&E, 2011a, b).

As described in PG&E (2011a, b) the Shoreline fault zone consists of three (North, Central, and South) segments with distinct geologic, morphologic and geophysical characteristics. Based on data available at the time of the study, the North segment was defined primarily by hypocenter alignments of small earthquakes, as there was no clear geological or geophysical evidence for the presence of a fault. The earthquake alignment trends northwest and towards the Hosgri Fault Zone. In contrast, characteristics of the Central and Southern segments were based on a combination of geophysical anomalies, seafloor geology, and geomorphologic characteristics identified in multibeam echosounder (MBES) bathymetry data in addition to earthquake locations.

To determine the shallow geologic conditions along the proposed North segment of the Shoreline fault, PG&E commissioned low-energy, high-resolution 3-Dimensional (3D) and 2-Dimensional (2D) seismic-reflection profiling surveys offshore of Point Buchon. The surveys were undertaken in late 2010 and early 2011 and designed to cover the area

where the proposed North segment of the Shoreline fault zone (PG&E, 2011b) was inferred to trend into the Hosgri Fault Zone (Plate 1). These surveys significantly filled data voids between the previous seismic-reflection data and provided data for refining interpretations. The low-energy sound source restricted penetration to the shallow subsurface, but allowed for high-resolution acoustic imaging that facilitated structural interpretation within a small area offshore of Point Buchon.

While the acquisition, processing, and presentation of the 2010-2011 data analyzed in this report were not performed under a Nuclear Quality Assurance (NQA) program meeting the requirements of 10 CFR 50, Appendix B, "Quality Assurance Criteria for Nuclear Power Plants and Fuel Reprocessing Plants," this Technical Report, which uses the data results has been written, reviewed and approved under the PG&E Geosciences QA program following Geosciences procedure CF3.GE2, Quality Related Technical Reports. The Quality Verification Plan for this report is tracked in System Applications and Products (SAP) in Notification 50427212. Post project, Fugro Consultants, Inc. validated the 3D and 2D data processing software and the software used to interpret the data, and qualified the processed data for use in safety related applications (see Section 9.0 Software). To ensure that the input data presented in this Technical Report are qualified for use in safety related applications, data corroboration of the data inputs was performed by ITR Dr. Jan D. Rietman (per NQA-1-2008, Part 3, Sub-paragraph 3.3, Appendix 3.1, "Guidance for Qualification of Existing Data). Details of the software validations and Dr. Rietman's corroboration is documented in his Verification Summary (Section 4.2) and Appendix A

Section 12.0 of this report addresses the limitations on the use of the results and conclusions presented herein.

5.1 Purpose

The purpose of this technical report is to present initial geologic and geophysical interpretations of the offshore low-energy, high-resolution 3D and 2D seismic-reflection data (referred to here as the 3D/2D dataset) collected in late 2010 and early 2011. The results of this study will be integrated with more extensive and deeper penetration 3D and 2D seismic-reflection investigations, both on land and at sea, which are underway or planned for the future. Therefore, the interpretations presented in this report may be revised when the additional data are acquired and interpreted.

5.2 Background

This section presents a brief summary of the geologic and tectonic setting of the study area to provide a contextual framework for the observations and interpretations made from the newly acquired 3D/2D dataset. The study area consists of two (3D and 2D) overlapping survey blocks and is located offshore along the coastal margin of the Irish Hills, a west-northwest trending ridge within the south central part of the California Coast Ranges, near the city of San Luis Obispo (Plate 1).

5.2.1 Regional Stratigraphy

As part of the work performed to characterize the Shoreline fault zone, PG&E constructed a geologic map of the onshore and offshore areas along the coastline from Morro Bay south to Pismo Beach and west to the offshore shelf break (approximately coincident with the Hosgri Fault Zone) (PG&E, 2011b). The onshore part of this map is based on a compilation of existing geologic maps, which were updated to incorporate new detailed geologic mapping of bedrock exposed in the modern sea cliffs. The offshore part of this map was constructed from the interpretation of seafloor relief and texture exhibited in the MBES imagery and correlation of these seafloor features with drop cores and diver-collected bedrock samples that were obtained in early 2010. The part of this geologic map that covers the 3D/2D study area is reproduced on Plate 1.

Basement rocks exposed in the central California coastal region generally consist of Jurassic to Cretaceous Franciscan Complex rocks (primarily mélangé, metavolcanics, ophiolite, and serpentine) faulted against Cretaceous marine arkosic to lithic sandstone. Along the coastline, the basement rocks are unconformably overlain by the early to middle Miocene Obispo Formation, which consists of tuffaceous marine sandstone, diabase, and resistant zeolitized tuff. Although they are not present along the coastline (on the south limb of the Pismo syncline, the axis of which generally follows the crest of the Irish Hills), the Oligocene Rincon and Vaqueros formations are known to unconformably overlie pre-Tertiary rocks on the north limb of the Pismo syncline in Los Osos Valley. However, the resolution of available geophysical data does not allow for confident differentiation of the Rincon and Vaqueros formations from the basal part of the Obispo Formation. Therefore, in this study Rincon and Vaqueros strata are considered to be part of the basal Obispo Formation. The Obispo Formation is unconformably overlain by marine chert, siltstone, diatomite, and porcelaneous shale of the Miocene Monterey Formation (see Legend, Plate 1). The Monterey Formation is well exposed in sea cliffs along a roughly 5.5-kilometer (km)-long stretch of coastline near Point Buchon. The Late Miocene to Pliocene Pismo Formation unconformably overlies the Monterey Formation and includes, from oldest to youngest, the Miguelito, Edna, Gragg, Bellevue, and Squire members. Onshore adjacent to the study area claystone and siltstone of the Miguelito Member are exposed in sea cliffs between Point Buchon and an area near where the Los Osos fault projects into Quaternary aeolian deposits near Morro Bay.

Geologic mapping reported in PG&E (2011b) shows that the seafloor is underlain by Quaternary marine sediment in a large part of the study area (Plate 1). Where this sediment is absent, most of the seafloor is composed of Tertiary strata exposed in stratigraphic sequences from south to north, including Obispo Formation, Monterey Formation, and the Miguelito Member of the Pismo Formation. Basement rock of the Franciscan Complex and Cretaceous sandstone locally underlie the southernmost part of the study area.

5.2.2 Tectonic Setting

The central coast of California is characterized by transpressional deformation between the San Andreas Fault Zone to the east and the San Gregorio–San Simeon–Hosgri fault system of near-coastal faults to the west (Figure 1). Transpressional deformation in the region is likely driven by three distinct but interacting processes (Lettis et al., 2004): 1) northward left transfer of slip from the San Andreas Fault Zone to the Rinconada and West Huasna faults to the Hosgri–San Simeon fault zone, 2) clockwise rotation of the western Transverse Ranges domain (transrotational deformation of Luyendyk (1991) and Dickinson (2004a, b), which imparts north-directed strain into the region, and 3) an unknown amount of possible plate-normal convergence across the region.

This transform regime initiated approximately 30 Ma when the transform process between the Pacific and North American plates introduced an episode of strike-slip tectonics, or wrench tectonics as described by Wilcox et al. (1973), that prevails today (Atwater, 1970). An important aspect of strike-slip tectonic settings is the development of “restraining” and “releasing” bends of a strike-slip fault system as described by Mann (2007). The resulting “wrench” deformation is reflected in modern topography and bathymetry of *en-echelon* linear to lens-shaped ridges and rhomboid basins (Howell et al., 1980). In such a dynamic tectonic regime wrench faults express compression and tension through restraining and releasing bends that accompany lateral displacement. This type of deformation has been well illustrated in clay model experiments (e.g., Cloos, 1955; Tchalenko, 1970; Wilcox et al., 1973; Mitra and Paul, 2011) that produced characteristic patterns of drag folds and secondary faults along strike-slip fault zones. Folds form at oblique angles to the strike-slip fault in an *en-echelon* pattern, though if transpression is dominant, the folds are rotated so that they nearly parallel the fault (Harland, 1971). *En-echelon* folds are therefore important indicators in plastic cover rocks of strike-slip faults in more rigid basement rocks at depth (Reading, 1980).

In an *en-echelon* strike-slip fault system left-stepping right-lateral strike-slip faults produce a zone of compression (transpression) resulting from a restraining bend and uplift between two *en-echelon* faults, whereas right-stepping right-lateral strike-slip faults produce a zone of tension (transtension) resulting from a releasing bend and depression between two *en-echelon* faults (Rodgers, 1980). Transtension then forms pull-apart (graben-like) basins, half grabens, or depressions (Buchfiel and Stewart, 1966; Crowell, 1974).

Transpressional deformation has produced several distinct but interacting crustal domains and tectonic structures (Figure 1; PG&E, 1988). The study area lies within the western margin of the Los Osos domain, a triangular-shaped structural terrain consisting of northwest-striking reverse, oblique, and strike-slip faults that border uplifted blocks and subsiding basins within the domain. Locally these include the Santa Maria Valley, San Luis/Pismo, and Los Osos structural blocks, from south to north, respectively (Figure 1). The study area is also located in the western offshore part of the San Luis/Pismo structural block. This structural block is bounded to the north by the 50-km-long Los Osos fault zone, and to the south by faults of the Southwest Boundary zone, which include the San Luis Bay, Pecho, Los Berros, Oceano, and Wilmar Avenue faults (Figures 1 and 2). The Irish Hills forms the structural core of the San Luis/Pismo block (Figure 2). A sequence of uplifted marine terraces preserved along the western and southern margin of the San Luis Range record late Quaternary uplift of the San Luis/Pismo block at a rate of about 0.2 millimeter (mm)/yr in the northwest and about 0.1 mm/yr in the southeast (Hanson et al., 1994).

5.2.3 Key Local Faults

Faults that contribute most to seismic hazard at the DCP.P include the Hosgri, Los Osos, Shoreline, and San Luis Bay fault zones (PG&E, 2011a, b). This report provides information that may be used to better characterize the Hosgri Fault Zone and particularly

the Shoreline fault zone and hence reduce uncertainties in the source parameters (i.e., fault length, segmentation and location with respect to DCP.P).

The Hosgri Fault Zone trends northwest-southeast for 110 km from north of Point Estero, just north of Estero Bay, to a location about 5 km northwest of Point Arguello (Willingham et al., in press; Figure 1). It is considered the southernmost part of the larger 410-km-long San Gregorio-San Simeon-Hosgri fault system (Hanson et al., 2004; Dickinson et al., 2005). The Hosgri and San Simeon fault zones accommodate 1 to 3 mm/yr of right-slip along steeply-dipping to vertical transpressional faults (Hanson et al., 2004). Within the longer connected fault zone the slip rate increases to the north, accommodating 6 to 8 mm/yr of slip on the San Gregorio Fault Zone in the Monterey Bay area and northward (Hanson et al., 2004). In the vicinity of the DCP.P the Hosgri Fault Zone is up to 2.5 km wide and composed of multiple fault traces.

As characterized in PG&E (2011b), the Shoreline fault zone is a vertical right-slip fault with an estimated slip rate ranging from approximately 0.05 to 1 mm/yr, with a preferred range of between approximately 0.1 and 0.6 mm/yr. This fault zone has been divided into North, Central and South segments based on changes in the geologic and geophysical expression of faulting at the surface and in the shallow subsurface (PG&E, 2011b). The South and Central segments of the Shoreline fault zone are associated with geophysical anomalies and have clear expression in the seafloor geology and geomorphology interpreted from MBES bathymetry data (Plate 1). In contrast, no clear geological or geophysical expression of the North segment of the Shoreline fault zone was identified in the available data used at the time of the Shoreline fault zone investigation (PG&E, 2011a, b). Seismicity that defined the northern seismicity lineament, therefore, was not clearly associated with any identified structure. As a result, seismic source models for the Shoreline fault zone included significant uncertainties regarding the extent and location of the North segment of the Shoreline fault zone.

5.3 Definition of Study Area

The study area is bounded by the limits of the two survey blocks (the 3D and the 2D survey blocks), located offshore and directly northwest of the DCP.P., as shown in Figure 2 and Plate 1. The 3D survey covers a T-shaped area within the 2D area and the 2D survey covers a larger rectangular area. The 3D survey block is 18 square kilometers (km²) and is located entirely within the larger 2D survey area (Figure 2; Plate 1). The 2D survey consists of 113 lines spaced at about 100 meters (m) apart covering an area of 46.5 km² (Figure 3; Fugro Consultants, 2012a). An additional 1-km² square 3D survey block is located to the south of the larger 3D survey block (Plate 1). This smaller survey block was not connected to the larger, northern block because of adverse weather conditions and the lack of survey time.

The 3D/2D survey blocks cover the northern segment of the Shoreline seismicity sublineament as defined by PG&E (2011b), as well as adjacent parts of the Hosgri and the herein named “Point Buchon fault zone” (parts of which were formerly called the N40°W fault zone in PG&E, 2011b). The widest part (the cross of the T) of the 3D survey covers a part of the Hosgri Fault Zone where the North segment of the Shoreline fault was inferred to trend into the Hosgri Fault Zone (PG&E, 2011b). The 2D data covers areas in the northern, western and southern part of the study area where traces of the Hosgri Fault Zone have previously been mapped, as well as covering the area between the Hosgri and Shoreline fault zones (Figure 2; PG&E, 1988, 2011b).

5.4 Goals

Specific goals identified to be addressed in this study were to evaluate:

- The character of the 3D/2D data including the “interpretability”, depth of penetration, and resolution of the data.

- The seismic stratigraphy imaged in the data including the general extent of stratigraphic units, and potential correlation of mapped horizons with mapped geologic features or units.
- The locations and patterns of faulting, the nature of the faulting, fault strike, dip, vertical separation, evidence for dip/strike-slip, identification of possible piercing points, and large-offset faults versus minor (i.e., small offset faults) where the geology is resolvable and such information is available.
- The patterns of fold deformation in the dataset. This includes trends of folds parallel or oblique to faults, and continuity of folds.
- The nature and complexity of the Hosgri Fault Zone within the study area.
- The nature of the Point Buchon fault zone (formally called N40°W fault zone) and its relationship with the Hosgri Fault Zone (to the north) and the North and Central segments of the Shoreline fault zone
- The nature of the faulting/folding coincident with the Northern seismicity sublineament.
- The nature of the intersection of the Shoreline fault zone with the Hosgri Fault Zone.
- The nature of geology in areas adjacent to, and between, the Hosgri, Point Buchon and Shoreline fault zones.
- How the results of this study compare to the previous interpretation of the location and character of the North segment of the Shoreline and Hosgri fault zones (PG&E, 2011a, b).

5.5 Intended Use of the Results

The interpretations of the 3D/2D data will be used by PG&E in their ongoing efforts to characterize seismic hazards at the DCP.P. The results of this technical report will be further evaluated and integrated with interpretations of other datasets, including seismicity, previous (and planned) seismic-reflection surveys, potential field (gravity and magnetic) surveys, and geologic and geomorphic mapping. The data inputs and the final

report will be provided to the DCP.P. Senior Seismic Hazard Advisory Committee (SSHAC) Seismic Source Characterization Technical Integration (SSC TI) team.

6.0 DATA

The data interpreted for this report are the offshore low-energy, high-resolution 3D and 2D seismic-reflection profile data collected in late 2010 and early 2011. These data were collected by Fugro Consultants, Inc. specifically for PG&E to use in the evaluation of the Shoreline fault zone and other faults within the offshore area of DCP.P. The data collection and processing are described in the following reports:

- Fugro Consultants (2012a)
- Fugro Consultants (2012b)
- Fugro Seismic Imaging (2012)

The Fugro reports and data, including the 3D and 2D data SGY files, reside in the PG&E Geosciences offices in San Francisco, California.

6.1 Data Acquisition

Data were acquired using standard industry procedures with a low power sound source. Low power (1.5 kilojoules [kJ]), high-resolution (100-700 Hertz [Hz] frequency range with a 200-225 Hz fundamental frequency; Figure 3) seismic-reflection profiles were collected offshore of Point Buchon by Fugro Consultants, Inc. from 24 November 2010 to 5 February 2011 using a triple plate boomer as the acoustical source and four parallel hydrophone streamers for receiving acoustical energy (Figure 4). The boomer plates were towed in a sled with the source 0.3 m beneath the sea surface (see Fugro Consultants, 2012a). A trackline map is presented in Figure 5.

The receivers were four parallel, 16 channel, 50-m long Geometrics™ GeoEel- streamers, with GeoEel™ hydrophones grouped at intervals of 3.125 m (42.5 m to first group from head of cable with center group at 25 m from head), and towed at a depth of 2 m ±0.5 m (see Fugro Consultants, 2012a; Fugro Seismic Imaging, 2012). The

geometry of the 3D hydrophone array was 6.25 m lateral offset between streamers providing a subsurface swath width of 18.75 m (Figure 4). With this configuration a total of 64 channels of data were acquired.

The seismic source (a triple plate boomer AP3000 manufactured by Subsea Systems, Inc. of Ventura, California capable of delivering 0.5 kJ of energy/plate) was placed ahead and in the center of the hydrophone geometry. Precision horizontal positioning of the receivers and source array was accomplished by placing Global Positioning System (GPS) units, which utilized a wide-area Differential Global Positioning System (DGPS), at the head of each hydrophone streamer and the boomer sled (Figure 4). Accuracy of positioning varied throughout the streamer array. Data received at the head of the streamer array were collected at a positioning accuracy of ~1 m while data received near the tails of the streamers were estimated to have been collected at a positioning accuracy of ~3 m (Figure 6).

The seismic source was fired on distance (every 3.125 m), with a group interval of 3.125 m and 16 channels per streamer provides for 8-fold acquisition geometry (Fugro, 2012a, b). Calculations for fold are as follows:

$$\text{Fold} = (1/2) * (\text{Number of Channels}) * (\text{Channel Interval} / \text{Shot interval})$$

$$\text{Fold} = (1/2) * (16 * (3.125\text{m} / 3.125\text{m}))$$

$$\text{Fold} = (1/2) * (16 * 1)$$

$$\text{Fold} = 8$$

The returning signals along with positioning data were digitally transmitted to the recording equipment onboard the recording vessel M/V *Michael Uhl*. For the 3D data acquisition line spacing was 12.5 m (see Fugro Consultants, 2012a). However, in some cases winds, waves, and currents resulted in uneven streamer separations, thus preventing the intended coverage (Figure 7).

Vertical resolution of the 3D/2D data is estimated to be 1.8-2 m based on a dominant (fundamental) frequency of ~200-225 Hz at an assumed velocity of ~1600-1650 meters per second (m/s) (Figure 3). Vertical resolution is calculated as follows:

$$VR = TT = 0.25\lambda \text{ (of dominant frequency)}$$

Where:

$$VR = \text{Vertical resolution, } TT = \text{Tuning thickness and } \lambda = \text{wavelength}$$

The seismic vertical resolution is the minimum (or tuning) thickness of a bed that can be distinguished. The tuning thickness is a bed that is 0.25λ in thickness from which reflectors from its upper and lower surfaces interfere. The interference is constructive when the contrasts of the two interfaces are of opposite polarity, often resulting in an exceptionally strong reflector (Sherrif and Geldart, 1995).

In January and February, 2011 infilling of seismic data gaps were undertaken (Figure 7). The 2D data were collected at 100-m spacing (see Fugro Consultants, 2012b). Nominal fold was 8 with a sample rate of 0.5 milliseconds (ms) and a record length of 1 second (s) for both 3D and 2D data. The bin nominal size was 1.5625 m in the in-line direction and 3.125 m in the cross-line direction. A total of 2,019.47 km of 3D and 2D data were collected. The 3D swath mapping (4 streamer width) provided a full-fold area or volume (cube) of 17.51 km^2 , which is divided into a large 16.51-km^2 rectangular block and a small 1.0-km^2 -square block. In addition to the 3D data, 113 2D lines were collected (see Fugro Consultants, 2012b). Survey deliverables to PG&E that are used in this report are based on World Geodetic System 84 Universal Transverse Mercator WGS 84 UTM Zone 10 (N) meter grid coordinates (see Fugro Consultants, 2012a).

6.2 Data Processing and Quality Control

The 2D and 3D data were processed in a similar manner but at two different locations. Fugro Consultants, Inc. in Ventura, California processed the 2D data (see Fugro Consultants, 2012b for complete processing procedure).

Fugro Seismic Imaging, Inc. of Houston, Texas, undertook processing of the 3D data. The 3D and 2D data processing was performed following industry standards (industry standards refer to those standards and procedures of data collection and processing used by petroleum and geophysical companies to assure continuous high quality and consistency in their data acquisition methods) practices for data collection and processing (Fugro Consultants, 2012a, b) and followed procedures described in the Handbook of Offshore Surveying (Lekkerkerk et al., 2006). For every processing stage, the output data and log files were checked to ensure that the data were correct. Quality control checks were recorded in the project files. The data were processed using Fugro Seismic Imaging's proprietary seismic processing software in UNISEIS™.

Stacks and gathers were created and reviewed at each stage of the processing for every line. The 3D volume time slices were created and viewed at the following processing milestones: surface related multiple-elimination (SRME) volume, signature deconvolution volume, cross-line statics solution, pre-stacked time migration, final filtered, and scaled volume. Velocities were checked in Fugro Seismic Imaging's proprietary analysis software package UNISEIS using an iso-velocity viewer and display of normal move out (NMO) corrected common depth point (CDP) gathers. In addition, time-slices of the first pass velocity volume and migration velocity volume were created and viewed. These data are displayed in a 3D volume, or cube, that can be used in a similar manner as a medical cat-scan to view internal structures and stratigraphy. The data can be viewed in cross-sectional vertical profiles arbitrarily (user-defined) selected in any direction, or in horizontal time slices that are useful for developing maps and measuring true strikes of features. This 3D processing provides substantially more information than can be obtained from conventional 2D seismic-reflection profile

interpretations and removes considerable uncertainty from the interpretations and analyses.

Velocity analysis was also performed with Fugro Seismic Imaging's proprietary analysis software package in UNISEIS (see Fugro Seismic Imaging, 2012); for this report, depth is reported in two-way travel time (TWTT) in seconds (s) on seismic-reflection profiles and milliseconds (ms) in 3D volume time slices with sea surface being zero, however a tidal range of from +2.1 m to -0.5 m occurred during the surveys, which was determined by the tidal cycles recorded by the National Oceanic and Atmospheric Administration (NOAA) at Port San Luis. However, no tidal corrections were made (P. Hogan, written communication to Gary Greene, e-mail dated November 15, 2011). A swell/static filter was applied so that the data bins would match as best as possible, but not corrected to a vertical datum such as mean-low-low-water (MLLW). Estimates of depths are given in this report based on an assumed shallow subsurface sediment velocity of 1600 m/s (Fugro Consultants, 2012b).

The seismic stratigraphy immediately beneath the seafloor is masked by the "bubble pulse", the train of seismic energy produced by the sound source and exhibited in seismic-reflection profiles as a series of closely spaced artifact reflectors. Even though deconvolution processing has been applied, this masking by the bubble pulse prevents complete resolution of weak legitimate reflectors parallel to the seafloor for ~5 ms (~4 m at 1600 m/s) beneath the seafloor reflector (Figure 8).

Processing of the 3D seismic-reflection data was done in many steps as illustrated in Figure 9 with a quality control assessment made at the end of each step. Parameter (e.g., gain, signal-to-noise ratio, etc.) testing was initially applied to the data followed by navigation merge and quality control (QC) assessment, initial noise elimination, QC of near trace gathers, application of low-cut filter, and gain recovery (Figure 9). The data were then sorted to CDP and a brute stack for each streamer was produced using a water

dependent brute velocity function. Static corrections were then made to reduce jitter in the data that resulted from the lack of control mechanisms (“birds”) on the streamer to regulate depth and orientation. Noise due to swell, boomer misfires, and other sources was attenuated from the data using a time frequency de-noise algorithm (TFDN). Surface related multiple-elimination (SRME) that included the bubble-pulse train to reduce repeated surface reflectors was undertaken and velocity analysis was performed on a 125 m (in-line direction) by 250 m (cross-line direction) grid.

The binned SRME were stacked and then a dip-model was constructed using Fugro Seismic Imaging’s interpolator that uses a similarity-based dip analysis (see Fugro Seismic Imaging, 2012). Another dip model was then created using a full stack of the data. Migration velocity analysis was then undertaken and signature deconvolution using a statistical deconvolution approach, which involved the design of a wavelet-shaping operator for each individual shot record. Lines were migrated post-stack 2D to be used as input into the cross-line solution. This was followed with offset plane regularization and interpolation and 3D pre-stack Kirchhoff time migration. The final nominal 8-fold binned gathers were output from the 3D migration as NMO and the binned gathers stacked. Unwanted noise that lies outside of the frequency range of the desired reflection data was attenuated by the application of a series of zero-phase Butterworth Filters and time-variant decibel scaling was applied to the stack to balance the amplitudes in the final section (Fugro Seismic Imaging, 2012).

The 2D data were collected in the same manner and with the same parameters as the 3D data and processed in a similar way with one exception being that the 2D data line spacing of 100 m was too far apart to be included in a 3D volume. Therefore, 3D processing was not undertaken on these lines. The 2D data were collected at 100 m spacing with the intent to fill in between these lines at 12.5 m spacing so that a 3D volume could be constructed that would cover the entire planned survey area. However, due to lack of time and weather problems these fill lines were not completed and only the

northern and central survey area were covered in the density required for the construction of a 3D volume.

7.0 METHODOLOGY

This section describes the methodology used to interpret the 3D/2D seismic reflection data. The extent of data collection is shown in Figure 5 and described in Section 5.3 above. The post-processed 3D/2D data extend vertically to about 500 ms or 0.50 s (~400 m), with better imaging (interpretability) generally in the upper 350 ms or 0.035 s (~280 m) to 100 ms or 0.10 s (~80 m).

7.1 Team-Based Approach

The interpretation of the 3D/2D data was conducted using a team-based approach. The term interpretation, as used in the analysis and presented in this technical report, means that the visual observation and recognition of features or acoustic signals (reflectors) in the 3D/2D dataset, assisted by standard software used in the geophysical community, industry, government, and academia to interpret 3D/2D seismic-reflection data, were used to map stratigraphic layers and geologic structures. The team approach for this project consisted of an initial stage wherein each team member interpreted the same set of seismic-reflection profiles that were later compared to determine differences in interpretive styles and identification of acoustic structures. It is notable that all team players consistently interpreted structures and acoustic anomalies in the same fashion with few differences among the team member interpretations. Results of the first stage led to the confidence of the team to undertake the second stage of team interpretation in which several individuals independently interpreted and mapped the 3D/2D data in different parts of the study area, yet collaborated as a team to successfully integrate the findings into a collectively agreed upon (consensus) interpretation. An objective of the team approach was to minimize the introduction of model-based interpretive bias that could occur should one individual perform all of the interpretations. Additionally, the team approach facilitated the understanding of how convergent or divergent each individual's mapping and interpretations were with respect to one another. This provided

insight into the possible range or alternatives in the mapping interpretation, and thus the variability of the geologic conditions imaged by the 3D/2D data.

The individuals comprising the interpretation team and their key roles are:

- Technical Coordinator – Dr. Stuart Nishenko (PG&E)
- Interpretation (Lead Coordinator) and technical report preparer – Dr. H. Gary Greene (Moss Landing Marine Laboratory)
- Interpretation – Michael Angell (Fugro Consultants)
- Interpretation – Justin Pearce, Certified Engineering Geologist (CEG)
- Interpretation – Hans Abramsonward, CEG (Lettis Consultants International)

The interpretation team met regularly to discuss independent interpretations of the seismic-reflection dataset (e.g., profiles, time slices) and derivative datasets (e.g., similarity maps), and develop criteria for mapping structures, promote consistent mapping across the dataset, ensure that there was a relatively even distribution of map interpretations within the data set, and ultimately develop consensus interpretations.

The methodology for data interpretation was consistent with the geological and geophysical interpretation of seismic-reflection data outlined by Sheriff (1982), Yilmaz (2001) and Brown (2004). The interpretation tasks included:

- Mapping of selected stratigraphic layers (horizons) that are either locally prominent or laterally extensive within the 3D/2D dataset, including stratigraphic unconformities.
- Mapping of structural features, including faults, folds, and/or acoustical anomalies.
- Correlation of faults and fold axes from one line to another, and using user-selected slices through the 3D cube to confirm orientation and trends.

- Distinguishing areas of relatively good and poor data interpretability (zones of no reflectors or chaotic acoustic returns) by delineating areas of poor interpretability, those areas where interpretation is not possible or is inferred (Figure 10).

Mapping of selected seismic stratigraphic layers (horizons) provided an initial framework that was used to evaluate patterns of deformation in well-imaged seismic strata, including areas of deformed, but unfaulted strata. This was undertaken primarily to determine presence of faulting and not for the construction of structural contour or isopach maps.

7.2 Interpretation Tools

Seismic Micro Technology's (SMT) Kingdom Suite™ software Version 8.5 package was used to view seismic-reflection data. The software package allows the user to view and map on vertical profiles (3D and 2D datasets, cross-sections and user-selected cross-sections), as well as on horizontal time slices (3D dataset, plan view, user-selected). The vertical cross-sectional profiles and horizontal time slices are primarily displayed as seismic-reflection amplitudes. Some similarity time slices (the presentation of similar acoustic characteristics such as wave forms) generated in SMT are also displayed.

Seismic attributes (i.e., derivative) volumes, commonly referred to as cubes, obtained from the time-amplitude 3D dataset were developed by Fugro (Fugro Seismic Imaging, 2012) using SMT. Seismic attributes (e.g., wave forms) are derived from the seismic-reflection data and provide information relating to the amplitude, shape, and/or position of the seismic waveform, which is then compared to similar adjacent waveforms. Seismic attributes may reveal features or patterns that otherwise might not be noticed. The similarity time slice, or derivative, maps show subtle structural features that may not be observable on the amplitude time slice maps. Derivative maps used in this investigation consist of amplitude and similarity time slice maps (Foldout A).

Interpretations were performed on each 2D line (at approximately 100 m line spacing), with emphasis on those 2D lines outside of the 3D dataset. Within the 3D dataset, mapping was conducted initially on 3D line numbers evenly divisible by 20 to develop an overall understanding of the dataset. In areas of interest, or areas having complicated fault geometry, increased density of interpretation to every 10th line, or every 5th line as appropriate, was undertaken. In some cases interpretations were made on every other line to better define continuity of a structure or feature. User-selected profiles were used to provide different apparent (oblique to structural trends) and true view angles (perpendicular to structural trends) across features to evaluate and aid in interpretations. Cross-lines were interpreted as necessary to develop accurate mapping and interpretation of shallow structures. Furthermore, numerous time slices, which include data from every in-line and cross-line profile, were interpreted.

7.3 Interpretation Criteria

This section describes the criteria used by the interpretation team to develop technically consistent mapping within the 3D/2D dataset. Criteria are specific to the geological features mapped such as horizons (stratigraphic marker beds and unconformities) and structure (faults and folds).

7.3.1 Mapping Horizons (Stratigraphic Beds and Unconformities)

Selected stratigraphic beds or layers were mapped based on one or more of the following criteria:

- Vertical sequence of distinct low- and high-amplitude reflectors, either as a low-high pair (doublets) or as low-high-low or high-low-high triplets.
- Correlation over several hundred meters in lateral extent (Foldout B)

Angular unconformities were mapped based on one or more of the following criteria:

- Presumed younger sediments overlying an angular-eroded surface of tilted/folded older rocks.

- Reflector onlap, downlap, or toplap against upper or lower bounding surfaces, commonly indicating a hiatus in deposition.

7.3.2 Mapping Faults

Faults were identified based on one or more of the following criteria:

- Abrupt lateral truncation of reflectors.
- Displaced, offset, or broken reflectors.
- Correlations of offset reflectors across a fault plane.
- Direct fault plane reflections.
- Acoustical anomalies (e.g. presence of diffractions, especially at a reflector termination, or presence of laterally short and bright reflectors adjacent to a plane that appear as “flags” or contrasting acoustic signals separated by a plane.
- Visible drag and rollover of reflectors.
- Loss or substantial decrease in acoustic coherence beneath a fault plane, or distorted dips observed through a fault plane.

To track faults within the SMT Kingdom Suite software program that were interpreted and mapped by the various team members, and to correlate these with previously mapped faults, a coding scheme based on colors and a five digit numbering system was developed (Table 1) and stored on the PG&E 3D/2D SMT Kingdom Suite project. The intent of the scheme is to recognize associations within the spatial fault patterns and map preliminary correlations of each fault identified with known fault zones (e.g., Hosgri Fault Zone) or groups of faults (e.g., closely-spaced, north-south-trending faults). The numbering system provides information on a fault’s attitude (orientation, dip, sense of displacement, if any) and allows for tracking of the various fault “picks” each member of the team makes. Different colors are assigned to clearly associate each mapped structure with the various fault zones or groups shown on Plate 2 and discussed herein. This scheme is discussed in more detail below:

Four different fault zones, four different fault trends, a one set of unassigned faults listed in Table 1 have been mapped and assigned a unique set of five-digit numbers as noted below:

First digit – Name or trend of main trace of fault

Second digit – Differentiates a primary strand (digit equals zero) from secondary strand of a fault zone or group of faults (digit equal to or greater than 1)

Third digit – Fault attitude and direction of movement

0 = Strike-slip – vertical to near vertical fault

1 = Normal – east dipping or down on east

2 = Normal – west dipping or down on west

3 = Reverse – east dipping or up on east

4 = Reverse – west dipping or up on west

5 = Uncertain – data interpretability is not sufficient to resolve

Fourth and fifth digits – Individual Fault ID number (up to 99 faults can be listed)

Faults that are continuous and change in dip along strike are given different numbered fault codes along those segments that dip differently.

The code for the eight fault zones and fault trends, plus the unassigned faults, and colors assigned in the SMT project is presented in the following table:

Table 1. *Numbering system and colors used to distinguish fault types and association with fault zones and groups (trends) of faults in the high-resolution 3D/2D seismic reflection survey area offshore of DCP.P.*

<i>Fault Name or Trend</i>	<i>Five-Digit Code</i>	<i>Color in SMT Project</i>
Hosgri Fault Zone	10000	Red
Point Buchon fault zone	20000	Blue
Western splays of Point Buchon fault zone	30000	Dark green
East branch Point Buchon fault zone	40000	Gold
N-S-trending faults	50000	Light green
NW-SE-trending faults	60000	Maroon
E-W-trending faults	70000	Pink
Other faults	80000	Violet/purple
Unassigned faults	No numbers	Black

Example:

A west-dipping reverse fault mapped as a secondary strand of the Hosgri Fault Zone would be written as “12401”.

The numbering scheme represents the team’s current interpretation of which faults are associated with a fault zone or stand alone, based on the spatial patterns of the faults. The fault numbering code does not necessarily represent the final fault names as the initial interpretations presented in this report may change once additional data, such as seismicity, gravity, magnetic, or deep penetration seismic reflection profiles, are considered. Any future changes made to the coding of the faults will be recorded and explained.

Fold axes were identified and mapped based on one or more of the following criteria:

- Both limbs of a fold are present or in the case of a monocline beds consistently dip one direction.
- The amplitude of the fold is greater than several tens of ms (~20 m).

- The greatest curvature of a sequence in upturned or downturned reflectors.

8.0 ASSUMPTIONS

Initially, assumptions were made in regard to adequate QA/QC oversight of the data collection and processing having been done, but subsequently PG&E's QA/QC validation of all data and software used to produce this report has been completed (see Appendix A). However, specific assumptions are presented below:

1. The 3D/2D seismic data were acquired and processed at specified standards as stated in the survey data reports (Fugro Consultants, 2012a, b) and seismic data processing report (Fugro Seismic Imaging, 2012). It was assumed that QC requirements as stated in the reports were rigorously applied.
2. The previous studies by PG&E (2011a, b) of the Shoreline fault zone are acceptable for use in this report based upon the approval of the report by the NRC.
3. Navigation was of the accuracy specified in NCS SubSea Navigation Final Report J00344-FR-001 DCP.P. 3D Geophysical Survey Job Documents (NCS SubSea, 2011). This assumption is supported where georeferenced datasets overlap showing the same structures within the limits of each survey dataset (Figure 11).
4. All seismic stratigraphy imaged by the low-energy data is assumed to have an average bedrock velocity range of 1600-1650 m/s (see Figure 3) to be used when converting time to depth and for estimating depths and inclinations (dips). This velocity is based on a seismic source frequency spectrum (Figure 3) and the processing parameters (NMO correction using a brute velocity function of 1600 m/s applied to the seismic data in the CDP domain) used by Fugro Consultants, Inc. (Fugro Consultants, 2011a, b) in the processing of the seismic-reflection data. This assumption provides

reasonable estimated depth calculations down to ~400 m although faster velocities would be expected at the deeper depths.

5. Multibeam echosounder bathymetric data collected and processed (2 m grids, with $\sim\pm 1$ m resolution) by the Seafloor Mapping Lab of California State University Monterey Bay were maintained at IHO S-44 Special Order specifications. Across the entire MBES swath an average of 95.8% of cross-line soundings fall within IHO Special Order tolerances, with 99.7% within IHO Order 1 (P. Iampietro Written Communication, 2010 to S. Nishenko) and PG&E Multibeam Bathymetry Survey 2009 Quality Control Report (PG&E, 2011b, Appendix F; [http:// Seafloor.csumb.edu/projects. html](http://Seafloor.csumb.edu/projects.html)). See 2006-07 Multibeam Bathymetry Survey of Morro Bay and Point Buchon, Center for Integrative Coastal Observation Research and Education. This assumption is validated through the comparison of various geophysical datasets including the 3D/2D seismic reflection data that precisely overlay each other as a georeferenced product (Figure 11; see Appendix A).
6. The seismic reflection data used in the Long Term Seismic Program (LTSP) report (PG&E, 1988) were collected to industry standards at the time.
7. The USGS 2D seismic reflection profiles (Sliter et al., 2009) were collected using industry and scientific standards.

9.0 SOFTWARE

The primary software programs used for this analysis and interpretation of the 3D and 2D seismic reflection data are Seismic Processing Workshop (SPW), UNISEIS, IHS Kingdom, Rock Solid Attributes (RSA), and ArcGIS. SPW was used by Fugro Seismic Imaging to process the 2D seismic reflection data and UNISEIS, Fugro Seismic Imaging's proprietary program, was used to process the 3D seismic reflection data. IHS Kingdom is a PC-based program for analysis and interpretation of seismic reflection data. Version 8.6 was used in this study. IHS Kingdom was used in the interpretation and construction of structure maps, cross-sections and time slices. RSA is a separate program

or module that provides additional analysis and visualization capabilities to data in IHS Kingdom. Similarity time slices from RSA were compared to amplitude time slices from IHS Kingdom. Data corroboration of the data interpretations in the validated version of IHS Kingdom (version 8.6 Hotfix 4) and data from RSA used in selected figures, software validations for SPW, UNISEIS and IHS Kingdom, and qualification of the data processed using SPW and UNISEIS are documented in Appendix A.

ArcGIS by the Economic and Social Research Institute (ESRI) Version 10 is an industry, government and academia acceptable software package commonly used to collate and map spatial data in an accurate georeferenced manner. This software was used to construct maps presented in the Shoreline fault zone report (PG&E, 2011b), some of which were duplicated in this report, and was used for the construction of maps (plates and figures) for presentation purposes only in this report. Previously interpreted geologic and structure maps in ArcGIS from PG&E (2011b) are used here as base maps for comparison purposes. No calculations were performed on the data using ArcGIS. Therefore, ArcGIS was not validated under NQA.

10.0 INTERPRETATION AND ANALYSIS

The interpretation and analyses of the low-energy, high-resolution 3D/2D seismic-reflection data were compared with previously mapped geology described in the PG&E (2011b) report. Key observations and interpretations of the data are presented in the following section (Section 10.1), followed by analyses of the implications of the observations for characterizing faults in the study area (Section 10.2).

10.1 Interpretation

Interpretations of the strata and structure were made from a 3D volume and 2D seismic-reflection profiles. The volume was viewed in vertical profiles (consisting of in-lines, cross-lines, and user-selected lines) and horizontal time slices. Consensus interpretations are compiled and presented as a map on Plate 2. Data examples illustrating relevant

findings are presented in figures of cross-sectional profiles and various time slices in plan view.

As discussed above the seismic-reflection profiles used in the 2D interpretations and to construct the 3D volume were collected in an identical manner and processed in similar ways (see Fugro Consultants, 2012a, b; Fugro Seismic Imaging, 2012). The difference between the 3D and 2D data sets is primarily the line spacing and the more sophisticated processing needed to produce the 3D volume. The 3D lines spaced 12.5 m apart was necessary for the production of a 3D volume. The 2D lines at 100 m spacing are too far apart to permit construction of a 3D volume and, therefore, the 2D seismic-reflection profiles were interpreted without benefit of horizontal time slices and user-selected cross-sections.

10.1.1 Interpretability of Data

The variability in lithology, water depth, and the occurrence and rugosity of bedrock seafloor exposures, result in zones of variable interpretability. In zones where acoustic energy is either scattered or absorbed, resulting acoustic returns are typically opaque or chaotic, making them difficult to impossible to use for interpreting geologic structures. Alternatively, in zones where the energy is reflected in a conformable manner, resulting records show relatively coherent reflectors, facilitating interpretation. To provide insight into the uncertainties of the 3D/2D interpretations, zones of poor and good data interpretability are shaded in color (Figure 10; Plate 2). Generally the boundaries between the poor and good interpretability zones are often controlled by structure (e.g., faults). Criteria used for defining these zones are described in the following sections.

10.1.1.1 *Poor Interpretability*

In this report, “interpretability” refers to the expression of seismic reflectors in the data as strong or weak, and weak or chaotic reflectors are considered to be of “poor interpretability.” The expression of reflectors is a function of: 1) the type and character of rock imaged by the acoustics (sound), and 2) artifacts or noise in the final 3D/2D data

that may be introduced by the seismic-reflection survey design or post processing of the seismic data. With respect to (1) above, seismic data typically are better suited to imaging bedded sedimentary units than crystalline rock or massive sedimentary units. In bedded sedimentary units the impedance contrasts are inherently stronger between beds of sedimentary rocks. Crystalline rock or massive sedimentary units generally do not have planar internal seismic reflectors and thus generally produce zones of “poor data interpretability”. As an example, massive sandstone may have undergone fold-related deformation, but this may not be expressed in a seismic-reflection profile due to the lack of internal planar surfaces (such as bedding or cleavage) that would have localized the deformation. Similarly, highly deformed or steeply dipping beds and reflectors also are difficult to interpret.

The 3D/2D data are characterized as having poor data interpretability in most of the eastern and shallower water depth parts of the study area, particularly adjacent to bedrock outcrops (Plate 2, Figure 10). Other smaller regions of poor data interpretability are located adjacent to, and among, various strands of the Hosgri Fault Zone (Plate 2). Within these regions, reflectors are generally discontinuous or not recognizable in most profiles and time slices. Faults mapped within these regions are generally inferred from lineaments evident in some time slices, lateral continuity of acoustic anomalies in adjacent profiles, and alignment with the projections of structures mapped elsewhere. As a result, the interpretation and mapping of faults in these regions have varying degrees of uncertainty.

Areas of poor data interpretability were identified based on one or more of the following criteria:

- Relatively chaotic acoustic character (Figure 10).
- Abrupt loss of lateral acoustic quality (Figure 10).
- Parabolic effects and artifacts (Figure 12).
- Bedding “ray” effects and artifacts from upturned beds (Figure 12).

In the seismic-reflection profiles it is more difficult to interpret structure and stratigraphy in two areas: 1) at depth and 2) in shallow areas where bedrock is exposed because strong seafloor reflectors mask weaker deep reflectors. Poor interpretability areas are also located where poor acoustically responsive rock types (e.g., highly fractured or heterogeneous rock) occur.

For many of the faults mapped within zones of poor interpretability, *interpretation uncertainty* of whether an observed anomaly or lineament may be the acoustic expression of a fault or some other alternative interpretation, such as a resistant bed or a geologic contact, exists. If numerous acoustic anomalies or lineaments exist in a region, the interpretation uncertainty may also include uncertainty in the correlation of individual anomalies or lineaments along strike from one line to another. If a feature cannot be correlated across two to three lines, then it is uncertain in its presence and location.

An interpretive *measurement uncertainty* is the uncertainty of the mapped position and geometry of a fault or fold. Uncertainty in the interpreted position of a fault or fold is based on the width and variability of the lineament or acoustic anomaly used to interpret the structure. The measurement uncertainty in the position of faults mapped within the zones of poor data interpretability is estimated to range up to $\sim \pm 50$ m horizontally, as measured from the variability in reflectors imaged on the seismic-reflection profiles and the line spacing (100 m for 2D and 12.5 m for 3D profiles) across which a structure could be confidently mapped. Following the criteria described in Section 7.3, faults are mapped as vertical unless clear evidence for fault dip is evident in the seismic-reflection profiles.

As significant uncertainties are associated with the mapping of faults in zones of poor data interpretability, most faults mapped within these zones are shown on Plate 2 as dashed and queried lines, indicating they are approximately located and inferred.

10.1.1.2 *Good Interpretability*

The 3D/2D data are characterized as having good data interpretability in most of the western, and deeper water depths, part of the study areas underlain by folded sedimentary rocks, east of the Hosgri Fault Zone. Within these areas reflectors are readily identifiable and commonly may be traced for kilometers, facilitating the interpretation of fold axes and the presence or absence of faults. Faults are interpreted based on abrupt lateral truncation of reflectors and by displaced, offset, or broken reflectors. Correlations of offset reflectors with similar characteristics are also possible across many fault planes, and could be used in the measurement of vertical separation once reflectors are correlated, as well as horizontal separation once good piercing points are established. Similarly, where continuous reflectors are observed to cross the projection of a fault mapped elsewhere, the continuity of reflectors may be used to limit the potential length of that fault, and provide information about viable geometric connections among faults in the study areas. Faults mapped within the zones of good data interpretability are typically associated with much less interpretation uncertainty than those in zones of poor data interpretability. Uncertainty in the position of faults in these zones is estimated to be about ± 25 m, as a structure may be mapped with confidence across two lines spaced at 12.5 m apart. Faults and structures mapped in the zones of good interpretability that are based on well-defined lineaments evident in time slices, and that correlate well to other faults, are mapped as well-defined and shown as solid lines on Plate 2.

10.1.2 Stratigraphy

This section addresses the acoustic stratigraphy observed in the 3D/2D dataset. Six basic seismic stratigraphic features and units are identified: 1) the seafloor, 2) a surficial unconsolidated sediment layer, 3) an unconformity on top of rock including buried wave-cut platforms, 4) stratigraphic marker beds in the Tertiary rocks, 5) unconformities within the Tertiary section, and 6) the top of Mesozoic basement.

The seafloor is a distinctly recognizable feature in the 3D and 2D data. The seafloor horizon is mapped as the first high-amplitude reflector encountered directly beneath the water bottom (e.g., Figures 8, 12 and 13a). Vertical bathymetric relief of the seafloor horizon (as mapped) is commonly associated with two things: 1) rugged bedrock at the seafloor, and 2) the margins of mobile sand sheets (Figure 13). The sand sheets exhibit relief of up to a meter locally, and this relief similarly is reflected in the seafloor horizon in cross-sectional views. Hence, apparent bathymetric steps in the seafloor from migrating sand may be expressed as a lineament or tonal contrast in the plan view in the MBES bathymetric image rather than as a flat homogeneous tonal feature (Figure 13b). Mapping the seafloor horizon provides a marker for evaluating any possible seafloor expression of a fault, as well as paleo-geomorphic features such as paleo-seacliffs.

In the Point Buchon to Lion Rock offshore area a package of thin (<1 m thick) mobile sand sheets is imaged in the MBES bathymetry along a zone that extends from the outer margin of the exposed eroded bedrock platform to the Hosgri Fault Zone further offshore (Plate 1). These sand sheets exhibit a distinct morphology of a dune form with sharp distinct down drift (lee side) lobe fronts and gradational less distinct up-current (stoss) side margins. Scour-like depressions are interspersed with the sand sheets.

Although stringers of sand and gravel fill crevices and fractures in the extensive bedrock outcrops exposed on the inner continental shelf and nearshore areas east of the western boundary of the bedrock outcrops, the most prominent unconsolidated sediment packages in the study area are the late Pleistocene and Holocene sediments and the extensive mobile sand sheets that cover much of the central and outer continental shelf. These sand sheets are separated by rippled scour depressions (as observed from USGS camera drops, B. Edwards, Personal Communication, 2009) that are floored by gravels or smooth bedrock surfaces. From the 3D seismic reflection profiles it can be seen that together with the underlying late Pleistocene and Holocene unconsolidated sediment, many of the sand sheets cover irregular, differentially eroded sedimentary bedrock with more resistant beds that project up into the overlying sediments (Figure 13a) and may cover evidence of

faulting expressed on the bedrock surface. These more resistant beds, along with other bedrock relief locally appear to dam and stabilize the basal part of the mobile sand sheets. Commonly the fronts of the sheets mimic pronounced bedrock relief, especially in areas where the bedrock feature is perpendicular or sub-perpendicular to the sediment transport direction.

Although not the focus of this analysis and report, wave-cut platforms on Tertiary and older rock are recognizable in both the 3D and 2D seismic reflection profiles as sub-planar and gently west-dipping reflectors directly beneath the surficial unconsolidated sediment, which is acoustically transparent. An example of a wave-cut platform is shown in Figure 12. Wave-cut platforms for the area of this study have been previously investigated (PG&E, 2011b, Appendix I, “Identification, mapping and analysis of offshore wave-cut platforms and strandlines (Paleoshorelines) in the Shoreline fault zone study area”) and it is anticipated that results from this survey will be integrated into a later report on the subject and used to augment previous investigations.

Much of the bedrock exposed at the seafloor in the study area was identified as Tertiary sedimentary rocks in PG&E’s Shoreline fault zone report (PG&E, 2011b, Section 5.2.1 of that report) (Plate 1). Specific stratigraphic layers imaged have not yet been correlated to specific known formations, members, or beds in either shallow water or deep water due to an absence of direct geologic data (i.e., drill cores). Within the 3D/2D study area, selected horizons in Tertiary bedrock were mapped to establish stratigraphic horizons (beds) that are relatively extensive across the study area. An example of the extent and character of several laterally continuous horizons as imaged in 3D seismic-reflection profiles is shown on Foldout B. The correlation of the various horizons, arbitrarily numbered horizon H05 through horizon H40, to onshore geologic units is not known. These marker horizons are notably displaced in some locations but also are conspicuously unbroken in other locations (Foldout B). Thus, these marker horizons may be relevant for estimating offsets and possible long-term slip-rates, but cannot confidently be used at this

time for this purpose because of the uncertainties of their stratigraphic assignment and age. Much more work needs to be done to correlate the many horizons observed in the seismic-reflection profiles to known age markers.

Several unconformities are imaged in the 3D/2D data. Besides wave-cut platforms (described above in this section) angular unconformities are present within the Tertiary section (e.g., horizon H35 in Foldout B), however, their regional extent and geologic relationship with known stratigraphic formations are not yet established. Furthermore, no attempt has been made to correlate these unconformities to the angular unconformities in the Tertiary sedimentary rocks that were previously mapped and assigned ages as reported in PG&E (1988) and by Willingham et al. (in press). Moreover the unconformities were not systematically mapped for this study. However, preliminary analysis of the unconformities present in sedimentary deposits west of the primary western trace of the Hosgri Fault Zone suggests an unknown component of vertical displacements along this fault (see Foldout C for example). Systematic and complete mapping and analysis of the unconformities may yield information to help evaluate timing of late Cenozoic deformation periods.

The contact between top of Mesozoic “basement” and Tertiary strata is difficult to identify in the 3D/2D data, likely due to the combined effects of decreasing interpretability with depth in the seismic profiles and potentially low velocity contrasts across lithologic contacts. Generally, Mesozoic basement (e.g. Cretaceous sandstone or Franciscan Complex rocks) in lateral contact with Tertiary sedimentary rock at the bedrock surface does not produce a distinct sharp or abrupt marker that can be used to define the depth below the Tertiary sequence and dip of the contact. A lateral change in acoustic signal (e.g., increase in reflectors) is observed locally, but does not necessarily mark a lithologic contact or boundary (Figure 10a).

10.1.3 Structure

Plate 2 shows folds and faults identified and mapped in the study area based on the interpretations of the 3D/2D seismic-reflection profiles in conjunction with the MBES bathymetry. This interpretation represents the current consensus interpretation of the structures in the study area. A comparison of the current structural mapping with previous interpretations of offshore structural trends based on seismic-reflection data and onshore and offshore geologic mapping as described in the Shoreline fault zone report (PG&E, 2011b) is presented in Plate 3.

The faults and folds mapped in the Study Area are divided into the following structural components:

- Major long-length (likely on the order of hundreds of meters to kilometers) faults of the Hosgri Fault Zone.
- Other long-length (likely on the order of tens to hundreds of meters), fairly continuous faults (Point Buchon fault zone).
- Moderate-length (likely on the order of several tens of meters), discontinuous faults that splay westward from the Point Buchon fault zone.
- Minor faults with short lengths that are related to specific larger faults and folds (north trending and east trending).
- Minor faults associated with small, intra-formational deformation.
- A prominent, fairly continuous NW-SE trending syncline/anticline pair that lies above the deeper northern Shoreline seismicity sublineament of PG&E (2011b) and monocline that strikes NE-SW.

10.2 Analysis

The overall geologic structure within the study area consists of the northwest-southeast-trending Hosgri Fault Zone in the west, the Point Buchon fault zone on the east and in between a zone of distributed deformation characterized by discontinuous faulting and

folding (Plate 2). West of the Hosgri Fault Zone, in the offshore Santa Maria Basin, the seismic reflectors are relatively flat lying to gently west-dipping in attitude. East of the Hosgri Fault Zone, on the continental shelf, well-imaged seismic reflectors are gently deformed into a system of folds that trend northwest across the majority of the study area. In the northern part of the study area, this system of folds transitions into a northeast-trending, north-dipping monocline.

Several additional minor faults are identified within the dataset. These faults typically extend only a few tens of meters in plan view and are localized within the folded strata east of the Hosgri Fault Zone (Foldout B) and may not be faults at all, but acoustic anomalies, as they appear to be aligned along the data collection tracklines and anomalous stripping observed in various time slices. Not all potential intra-formational faults observed were mapped as the team concentrated on defining and mapping the more prominent continuous and better defined faults.

There are broad areas that are acoustically opaque and/or contain distorted reflectors that hamper interpretability, particularly in the eastern part of the study area (Plate 2). Based on sharp contrasts or differing acoustic signatures to the north, the zone of poor interpretability is bounded by, and in some places coincides with, the East Branch and western splays of the Point Buchon fault zone (Figure 10b; Plate 2). In the central area the poor interpretability zone is more complex and lies between Point Buchon fault zone and the coded 30000 series fault splays. In the central part of the study area, the zones of poor interpretability lie between the western splays of the Point Buchon fault zone and a broad anticline, and in the southeastern part of the 2D survey area they coincide with areas where bedrock is exposed at or near the seafloor.

The following sections describe the locations, extents, geometries, and geometric connections of faults in the study area (Plate 2). Where possible, sense of displacement and/or relative direction of vertical fault separation is given.

10.2.1 Hosgri Fault Zone

The Hosgri Fault Zone is the most prominent, continuous and complex fault zone in the region. Previous mapping (PG&E, 1988; Willingham et al., in press) of this structure in the area offshore of Point Buchon indicates that the structure consists of a zone of faults that generally coincides with the shelf break. Previous detailed mapping of this part of the Hosgri Fault Zone, which was based on the interpretation of high-resolution 2D seismic reflection profiles spaced about 800 meters apart collected by the USGS in 2008 and 2009 (Sliter et al., 2009), and reported in PG&E (2011b), indicated that it is an active transpressional right-slip fault zone (Plates 1 and 3a). As shown by PG&E (2011b) the fault zone generally consists of three to four major strands and associated sub-parallel splays within a zone that ranges in width from about 1 to 2.5 km. The fault zone trends northwest-southeast (about N25-30°W); however, traces within the fault zone exhibit a left-restraining bend to the south and west of the study area (Plate 3a).

Interpretation of the 3D/2D data reveal that the geometry of the Hosgri Fault Zone within the shallow section is more complex than previously mapped (PG&E, 2011b), and has a slightly different geometry than was previously interpreted. This increased complexity is now recognized because of the reduced line spacing of the 2D survey (i.e., 100 meters for the current survey compared to 800 meters for the previous USGS surveys) and the availability of the 3D volume for part of the area that permit a much more detailed examination of the fault zone. As currently mapped, the Hosgri Fault Zone consists of a relatively simple, linear zone of faults in the center of the study area that spreads out into more diffuse and complex zones of faults both in the northern and the southern parts of the study area (Plate 2). Many of the strands within the fault zone are restricted to the Tertiary sedimentary bedrock sequence (Foldout C) identified previously in the PG&E Shoreline fault study (PG&E, 2011b), some extend to the bedrock surface and are buried beneath surficial sediment, whereas others extend to the seafloor (Figure 14) cutting the Quaternary sedimentary package.

10.2.1.1 *Northern Part of Study Area*

The Hosgri Fault Zone at the northern end of the study area is expressed as a system of faults that bound a small (~375 m wide) graben (Foldout C), herein called Graben A. Faults along the inferred western margin of this graben (faults coded 10005 and 11205 are approximately aligned with the primary strands of the Hosgri Fault Zone to the south in the central part of the study area (e.g., fault coded 10002 shown on Plate 2 and discussed in more detail in this section and following Section 10.2.1.2 below). The fault that bounds the eastern margin of the graben (faults coded 11006, 11208) separates gently dipping and folded reflectors (probably Pliocene Miguelito Member of the Pismo Formation) from faulted well-layered graben-fill sediment of unknown age (Foldout C).

West of the Graben A-bounding faults, another set of north-trending normal faults (the coded 50000 series faults) is observed in the 3D/2D data. These include both east-dipping and west-dipping faults that typically exhibit normal displacements within a sequence of relatively flat-lying reflectors. Three of these faults (faults coded 51202, 51203, and 51111) extend upward to an unconformity that occurs about 0.03 s (~24 m) below the seafloor (Foldout C). At least one of the faults (fault coded 51202) appears to disrupt this unconformity. This unconformity is shown at a depth of about 0.16 s (~128 m) below the 0 datum, which is approximately sea level, on Foldout C. These faults occur at about the same location as the previously mapped west strand Hosgri Fault Zone Trace A2 (PG&E, 2011b) (Plate 3a).

In the northern part of the 3D survey block the Hosgri Fault Zone is characterized by a single dominant fault strand (fault coded 10002), which locally is accompanied by associated secondary splays (Plate 2). The primary strand is acoustically defined by the distinct truncation of folded reflectors on the east with flat-lying reflectors on the west (Figure 14). Locally, in the northwestern part of the 3D survey area bedrock is elevated as a northwest-southeast linear ridge (pressure ridge) projecting above the sediment-covered seafloor. The pressure ridge is bounded by faults having seafloor expression

including a fault coded 10002 on the west and a secondary splay of the Hosgri Fault Zone (fault coded 11003) that splits and bounds the ridge on the east (Figure 14). As shown on Figure 14, chaotic acoustic reflectors are present between the central and eastern faults in the profile, in contrast to more organized and coherent reflectors on the opposite sides of the faults.

Another secondary splay, fault coded 11001, lies about 20-30 meters west of the primary strand, and is buried about 0.05 s (40 m) beneath the seafloor (Figure 14). As shown in the figure, bright spots of folded and truncated reflectors are imaged along the west fault and in a synclinal fold between the two most western faults of this strand. The bright spots most likely represent gas-charged sediments where gas migrating up along the faults has been trapped. Fault coded 11001 is a persistent feature in the northern part of the 3D survey, and also in the 2D profiles to the north, running parallel to the primary fault coded 10002 for a distance of about 1.4 km.

South of the pressure ridge, fault coded 10002 extends to within a few milliseconds (a few meters) of the seafloor (the upward termination of the fault strand in profiles is obscured by the bubble pulse), but no seafloor scarp is evident in the MBES image near the upward projection of this fault (Plate 2). This fault extends southward beyond the limit of 3D dataset, and is expressed in 2D profiles in the shallow subsurface as a single fault that truncates steeply-dipping, well-defined parallel reflectors on the east and an acoustically opaque zone on the west. The fault appears to extend into and displace unconsolidated Quaternary sediment beneath the seafloor.

The 3D data indicate that within the shallow section no through-going strand of the Hosgri Fault Zone east of fault coded 10002 exists. At depth other faults may exist but these are difficult to define as acoustic “wipe-outs” from shallow-lying gas-charged sedimentary layers may be masking deep structure and stratigraphy. East of faults coded 10002 and 11003 is a sequence of steeply-dipping and locally tightly-folded, relatively

thin-banded reflectors (Figure 14). These reflectors cross the previously mapped location of Trace C2 of the Hosgri Fault Zone and are not faulted, indicating that Trace C2 either does not extend into the uppermost 200 meters of section or does not exist at this location (Plate 3).

10.2.1.2 *Southern Part of Study Area*

South of fault coded 10002, the Hosgri fault zone widens and becomes more disorganized (fragmented or less continuous) with several strands splaying to the east in the area where the 3D/2D survey areas meet and could be the result of less resolution in the spacing of the seismic-reflection survey lines (Plate 2). Numerous sub-parallel discontinuous faults that strike about N20°-40°W, most of which are only a few hundred meters in length, can be correlated on only a few adjacent seismic profiles. In the southernmost part of the study area, traces of the Hosgri Fault Zone strike distinctly more westward, about N40°-70°W and extend approximately parallel to the strikes of fold axes and bedding inferred from the MBES bathymetry (Plate 3).

In contrast to the sharp juxtaposition of folded reflectors against relatively flat-lying reflectors associated with fault coded 10002 (in the north), the acoustic stratigraphy and structure evident in the 2D seismic-reflection profiles in the southwestern part of the study area become choppy in appearance. More and tighter folding is present to the east, whereas to the west the folds are broader and gently dipping. Outcrops of bedrock are evident in MBES imagery to the west of the southern part of the study area, suggesting that surficial sediments are thin, and that the rocky part of the continental shelf extends west of the study area.

10.2.2 *Point Buchon Fault Zone (Formally called N40°W fault zone)*

The Point Buchon fault zone (called the N40°W in PG&E, 2011a, b) is a structurally complex feature that cuts through and deforms Tertiary strata in the central and northern

part of the study area. This fault zone is well defined on Plate 2 and its component structures are described below:

- The main trace is a continuous linear fault that extends northwest from the southeast corner of the 3D survey to near the northern end of the study area where a graben, herein called Graben B, has been mapped. This fault zone includes the faults coded in the 20000 series and individual faults coded 40001, 40003, 40002, and may also include shorter, less well-defined faults mapped along the same trend to the southeast (Plate 2).
- An East branch that splits from the primary fault at the southern end of fault coded 40001 extends northwestward beyond the northern limit of the 3D study area. This branch also includes other faults coded in the 40000 series.
- Several short faults that splay westward from the main fault trace in the center part of the study area (the coded 30000 series faults).

The Point Buchon fault zone is characterized in both the 3D/2D and MBES datasets. Good correlation between the two datasets, even in areas of poor seismic reflection interpretability, allow for confident mapping of this structure (Figures 10 and 11).

Parts of the Point Buchon fault zone that were originally described as the N40°W fault zone in the PG&E Shoreline fault zone report (PG&E, 2011b) were mapped as a less complex fault zone than interpreted herein. These include the southern part of the main trace of the Point Buchon fault zone and associated faults, which trend approximately N45°W, and the East branch of the Point Buchon fault zone, which trends approximately N35°W (Plate 2).

10.2.2.1 *Main trace of Point Buchon fault zone*

The south end of the Point Buchon fault zone bounds seafloor rock exposures that are characterized by poor data interpretability (Plate 2). Seafloor geology reported in PG&E (2011b) indicates that in this area the fault zone consists of up to two closely spaced (i.e., up to ~150 m apart) discrete fault traces that locally are associated with distinct seafloor

bedrock scarps (Plate 1). The fault separates relatively resistant blocky Obispo Formation on the east from a less blocky rock type on the west, probably of the same formation (Plates 1 and 3b).

The main trace of the Point Buchon fault zone is expressed in the seismic-reflection profiles as an acoustic anomaly and abrupt change in acoustic character from one side of the fault to the other. However, time slices from the 3D amplitude volume show the fault as a continuous sharp lineament within an acoustical chaotic zone, which coincides with the well-imaged bathymetric scarp along the coded 40000 series faults, specifically the coded 40003 fault (Figures 15 and 16, Plate 3b). South of the bedrock exposure, the fault zone trends towards, and may converge with, the Central segment of the Shoreline fault zone, although a direct connection could not be identified within this zone of poor data interpretability (Plate 2).

The north end of the main trace of the Point Buchon fault zone is shown to continue as a fairly linear fault zone buried beneath surficial Quaternary sediments (Foldout D). Acoustically, for most of its length, the structure is characterized as a narrow zone of chaotically disrupted and offset reflectors to the east that are truncated against well-imaged, gently dipping reflectors to the west (Foldout Db).

The northwestern end of the Point Buchon fault zone widens and includes north- and northwest-trending faults (in Figure 17 from left-right, faults coded 21101, 21201, 21202) that exhibit normal displacement and these faults along with fault coded 20005 bound and cut Graben B. These faults separate folded and dipping reflectors of probable Tertiary sedimentary rock from thinly bedded, seafloor-parallel to sub-parallel acoustic layers that probably represent graben fill. The age of the probable graben-fill sediment is unknown. However, the graben-filling reflectors are nearly parallel to the seafloor and are bounded by Tertiary bedrock suggesting that the graben-fill sediment may be

significantly younger than the surrounding materials, possibly Quaternary to Holocene in age (i.e., $< \sim 2.6$ Ma).

The lowermost part of the graben-fill sequence is offset by faults in the Point Buchon fault zone. The northwest end of the graben appears to be truncated by a north-south-trending fault (fault coded 11008) that exhibits displacement down to the east. This fault is parallel to, and may be part of, a set of normal faults that branch northward from the central trace (fault coded 10001) of the Hosgri Fault Zone and bounds Graben A (described in Section 10.2.1.1 and shown as fault coded 11208 on Figure 17b and Plate 2). From the northern end of Graben B (defined by fault coded 11008) to the southern extent of the Point Buchon fault zone, the total fault length is about 7.5 km (Plate 2).

10.2.2.2 *East Branch Point Buchon fault zone*

The East Branch of the Point Buchon fault zone splits northward and east of the main trace of the fault zone at approximately in-line number 1480 of the 2D survey (Figure 5, Plate 2). It is oriented $\sim N35^\circ W$ compared to the main trace, which is oriented $\sim N45^\circ W$. Much of the East Branch Point Buchon fault zone is mapped on the basis of the linear $N35^\circ W$ -trending seafloor scarp that separates bedrock on the east from unconsolidated sediment on the west (Plate 3b). In the northern part of the 2D study area, north of the 3D survey block, along the East Branch faults are imaged on only a few 2D seismic-reflection profiles and mapped based on bent and truncated acoustic reflectors (Figure 10a). The faults of this branch may be more continuous at depth, as they lie in areas of poor interpretability and it was not possible to interpret their deeper extent. To the south, in the 3D survey block, the East Branch Point Buchon fault zone is exhibited in the 3D/2D data as a narrow zone up to 100 m wide that clearly truncates a broad open syncline on the east and separates this broad fold from a series of folded and disrupted reflectors on the west (Foldout D). Here, the fault zone extends vertically to the top of bedrock, but is buried by an acoustical transparent layer of surficial sediment.

The East Branch Point Buchon fault zone is about 6 km long and if the main trace of the Point Buchon fault zone within the study area is included, the total length of the fault zone is about 9 km. The fault may extend beyond the northern limit of the study area, projecting toward a fault mapped from the 2008/2009 USGS data (Plate 3a) as the easternmost trace of the Hosgri Fault Zone. To the south, the Point Buchon fault zone may connect with the central segment of the Shoreline fault in the vicinity of Lion Rock (Plate 2).

A complex fault intersection occurs where the East Branch Point Buchon fault (fault coded 40008 on Figure 16b) splits from the main fault (fault coded 40001 on Figure 16b). Figure 16b is a time slice at 74 ms through the 3D similarity volume that shows the faults at this intersection as subtle lineaments (light intensity) cutting through acoustically opaque bedrock (dark intensity). The light intensity lineaments appear to be troughs in the top of bedrock that are filled with sediment resulting from differential erosion into bedrock (dark areas) along the faults. Other faults (the coded 31000 series faults) can be seen in the time slice splaying northwestward from the main trace of the Point Buchon fault zone. These splay faults are discussed in the following section (see Section 10.2.2.3 below).

10.2.2.3 *Western splays of the Point Buchon fault zone*

Near the center of the main trace of the Point Buchon fault zone, a series of four to five generally northwest-trending faults (the coded 30000 series faults) that splay west from the main Point Buchon fault zone and step to the north in map view (Plates 2 and 3b). These faults range from about 0.7 to 1.7 km in length and dip steeply (near vertical) to the northeast (Figures 18 and 19). The faults truncate upturned reflectors (possibly sedimentary beds) along the eastern limb of a syncline and juxtapose reflector-rich strata on the west against reflector-poor acoustic returns on the east (Figure 18a). Thus, amounts of displacement and sense of fault slip are not resolvable. Additionally, there appear to be moderate ray effects (piping)/interference (dipoling) on the upturned beds at

the bedrock surface, which may be confused with dipping reflectors. When viewed on the coast-parallel 3D cross-lines, faults within this zone are expressed as northwest-southeast oriented acoustically chaotic zones that range from about 100 to 125 m wide.

The splay faults generally bend gently westward near their northern extent and die out in the cores of asymmetric anticlinal folds south of the Hosgri Fault Zone. The geometry of the fault-fold relationships of the splay faults suggests they may be associated with wrench tectonics (shear couple in a strike-slip fault regime) and faults of the same age and deformation system (conjugate faults).

10.2.3 Structures coincident with the northern Shoreline seismicity sublineament

This section describes the structural features mapped in the vicinity of the northern Shoreline seismicity sublineament (i.e., the northwest trend of epicenters). As shown on Plates 1 and 3a, surficial structures mapped for the Shoreline fault zone report (PG&E, 2011b) along this alignment include a 6.5-kilometer-long, northwest-trending syncline that approximately overlies the seismicity sublineament and three queried nearsurface shallowly buried bedrock faults that intersect the axis and eastern limb of the syncline. For the Shoreline fault zone report, these features were inferred to represent one of several alternative interpretations of the location for the North segment of the Shoreline fault zone (PG&E, 2011b).

10.2.4 Folds

A major structural element within the 3D/2D study area that coincides with the northern Shoreline seismicity sublineament mapped and reported in PG&E (2011b) is an extensive, northwest-trending syncline (Plate 2) that uniformly deforms Tertiary strata. The structural axis of this syncline is almost directly coincident with the synclinal axis interpreted from the USGS seismic reflection profiles and reported in PG&E (2011b) (Plate 3a). The axis of the syncline mapped using the 3D/2D data appears to step easterly in the southeast direction, consistent with mapping reported in PG&E (2011b). The syncline extends from the southeast part of the study area for over 7 km to where the

syncline is intersected by two north-south oriented faults (fault coded 51001 and 51301 in Figures 18a and 19a) that separate this structure from an east-northeast-trending, northwest-dipping monocline (Plates 2 and 3b). The syncline terminates in the northwest and does not connect with the Hosgri Fault Zone. Previous mapping (see Plate 1) showed this syncline as a more continuous structure in the vicinity of the Hosgri Fault Zone (PG&E, 2011b).

Anticlines are mapped directly west of the major syncline described above, formed from the western limb of the syncline, and are represented by two relatively short (~500 m long) anticlinal axes located directly to the west of the western splays of the Point Buchon fault zone (Plate 2). The anticlinal axes west of the syncline are generally consistent with an anticline mapped and reported in PG&E (2011b; Plate 3a). Close examination of the 3D/2D data indicates that the anticlinal axes are sub-parallel to the synclinal axis. The Tertiary rocks east of the anticline and west of the syncline are deformed but not faulted.

10.2.5 Complex Structural Area

Along and near the easternmost inferred and queried fault trace of the North segment of the Shoreline fault zone, as interpreted from the more widely-spaced USGS seismic-reflection profiles (PG&E, 2011b; Plate 3a), the 3D/2D data better resolve the fault geometries (Plate 3b) than previously mapped. In this area a series of four or five generally northwest-trending faults (the coded 30000 series faults in Figures 18a and 19a) splay to the west from the Point Buchon fault zone (Plates 1 and 3a).

The 3D/2D mapping does not show a continuous North segment of the Shoreline fault zone (PG&E, 2011b). However, the 3D/2D data provide evidence for a zone of non-contiguous faults (the western splays of the Point Buchon fault zone) that follow the eastern margin of the major syncline discussed above in Section 10.2.4. The 3D/2D data generally indicate that these faults are vertical to gently east-dipping in the shallow

subsurface. The geometry of these faults at depth is not known, however, these faults may merge at depth, but no evidence of this is seen in the shallow penetrations 3D/2D dataset. Given the location uncertainty (± 0.5 km) of the offshore earthquakes (PG&E, 2011b), the seismicity sublineament may be associated with these merged faults at depth, although no evidence exists for the continuation of these faults below 0.4 kilometers (Plate 3).

West of the western splays of the main Point Buchon fault zone (the coded 30000 series faults), well-imaged well-layered reflectors within the broad syncline are generally uninterrupted by faults (Figure 18), with the exception of two north-trending, east-dipping faults (faults coded 51001 and 51301, Figure 18, Plate 2) that together offset reflectors vertically by about 0.01 s (~8 m) up on the east. Based on the loss of acoustical expression of fault coded 31301 to the north, it appears that the zone of coded 30000 series faults terminates at a structurally complex location where a monocline and the reverse faults, faults coded 31301 and 71401, meet (Figures 18b and 19b).

10.2.6 Northern extent of the Shoreline seismicity trend at the Hosgri Fault Zone

Starting about 600 m south of the northwest extent of the 30000 coded west splay faults of the Point Buchon fault zone the gently north-plunging syncline opens to become a broader fold and is intersected by faults coded series 51000 (Foldout Bb). The map trace of the syncline axis stops where this broad fold terminates and a northwest-dipping monocline occurs (Plate 2, Foldout Bb). Directly northwest of the monocline axis, reflectors dip to the north. In a time slice amplitude map at 0.150 s (Figure 19b), two observations are made: 1) reflectors are laterally continuous and not faulted by the easternmost strand of the Hosgri Fault Zone as shown in Plate 3a (Trace C2) in this area, and 2) reflectors are laterally continuous and unbroken directly northwest of the coded 30000 series faults. Therefore, a shallow (above a depth of 400 m) geometric connection between the Hosgri Fault Zone and the proposed North segment of the Shoreline fault

zone as inferred by the northern Shoreline seismicity sublineament is not possible based on the shallow penetration 3D/2D dataset.

The north end of the main trace of the Point Buchon fault zone is divided into many *en echelon* faults and appears to die out into a fold and cross faults that trend north-south that separate grabens 'A' and 'B' (e.g. fault coded 11008). Also, in the northern study area the East Branch Point Buchon fault zone becomes less continuous than directly to the south, within the 3D survey block, and is primarily characterized by *en echelon* faults and a western splay fault (fault coded 41301) that die out in a zone of extension (Plate 2). The East Branch Point Buchon fault zone appears to extend to the north beyond the study area.

11.0 CONCLUSIONS

The 3D/2D dataset used to evaluate the geology offshore of DCP.P significantly improves the understanding of the geologic structure and represents an important contribution to the knowledge base needed for evaluating the seismic hazards of the region. Despite limited acoustic penetration from the low-energy source in some areas, particularly in shallow water depths, and zones of poor interpretability that are present in the data, the 3D/2D dataset allows for more detailed mapping than had previously been possible. Specifically, the 3D seismic volume and the close spacing of the seismic-reflection profiles permit better correlation of faults and folds to more confidently characterize geology and more accurately determine structural trends and extents resulting in the mapping of more complex structure. This increased complexity is recognized primarily because of the high-resolution of the data and small line spacing of the 3D/2D data (100 m for the 2D survey and 12.5 m for the 3D survey).

The main structural elements mapped in the study area are the Hosgri Fault Zone, the Point Buchon fault zone, and a prominent syncline that deforms Tertiary strata in the southern two-thirds of the study area.

11.1 The Hosgri Fault Zone

The Hosgri Fault Zone consists of numerous fault strands and is the best imaged fault zone in the region. It is also the most continuous and complex fault zone in the study area. The fault juxtaposes folded Tertiary strata on the east against relatively flat-lying reflectors of probable Quaternary age on the west. Locally, strands of the fault zone exhibit seafloor expression, either as erosional fault-line scarps, or as tectonic scarps within young sediment. Several strands of this fault zone are identified in the 3D/2D dataset that show bright spots of associated gas pockets. The 3D/2D dataset shows that this fault zone is more complex at depths less than about 400 m than previously mapped (PG&E, 1988; PG&E, 2011b) (Plate 3). This increased complexity is recognized primarily because of the high-resolution of the data and small (12.5 m) line spacing of the 3D/2D data (12.5 m for the 3D survey and 100 m for the 2D survey).

In the study area the local style of faulting changes along strike of the Hosgri Fault Zone. A graben, Graben A, bounded by right-stepping strands of the Hosgri Fault Zone in the north indicate extensional strike-slip faulting (transtension) (Plates 2 and 3b). A single fault strand characterizes the fault zone in the center of the study area. Numerous, relatively short strands fan out to the southeast and are associated with folds in the south, indicating compressional strike-slip faulting (transpression). Similar morphology and structure is observed along many strike-slip fault systems and various researchers have postulated different terminology and models of formation of such features (e.g., see discussion in Mann, 2007). Reading (1980) reported that along strike-slip fault systems small-scale alternate zones of extension and compression occur. Reading (1980) states that these zones occur along 1) curved parts of strike-slip faults, 2) braided faults within a strike-slip fault system, or 3) side-stepping, *en-echelon* (conjugate) faults. This pattern has been described for the San Andreas Fault System within the region of this study (Kingma, 1958; Quennell, 1958; Crowell, 1974; Dickinson, 2004b). Such relationships will be further evaluated when additional data that can be used to explore the geometry and connection of faults at depth are available.

11.2 The Point Buchon Fault Zone

The Point Buchon fault zone, northwest of the central segment of the Shoreline fault zone, is a northwest-trending fault that disrupts Tertiary strata east of the Hosgri Fault Zone. Segments of the fault zone, including the southern part and the East Branch, were originally mapped as the N40°W fault zone and described in PG&E (2011b).

Both the main and Eastern Branch of the Point Buchon fault zone exhibits probable fault-line scarps, which are clearly evident in the MBES bathymetric images (Plate 2). To the south, the Point Buchon fault zone may connect to the Central segment of the Shoreline fault zone and associated structures, although no identifiable connection has been observed in the 3D/2D data.

Approximately halfway along the mapped length of the East Branch Point Buchon fault zone, a moderately well-defined narrow zone of faults bifurcates toward the north. Here the East Branch is parallel to the Hosgri Fault Zone and likely continues north beyond the study area (Plate 2).

In the northern part of the study area Graben B is associated with the northern end of the Point Buchon fault zone (Figure 17; Plate 2). Although there is no information on the age of the sediment fill in the graben, the occurrence of generally seafloor-parallel and sub-parallel reflectors filling a graben bounded by Tertiary bedrock suggests that the graben-fill sediment may be significantly younger than the surrounding stratigraphy, possibly Quaternary to Holocene in age (i.e., <~2.6 Ma). A north-trending fault (fault coded 11008) that may be part of the Hosgri Fault Zone truncates this graben at its northwest extent (Plate 2). This graben is located about 400 to 500 meters east of the primary traces of the Hosgri Fault Zone. The presence of this graben and Graben A to the northwest is indicative of transtension in the northern part of the study area, but the structural relationship between the two grabens and structures within Estero Bay to the north of the study area needs to be further evaluated.

A system of splay faults branches off to the west of the main Point Buchon fault zone, close to where the East Branch splits from the main trace. These splay faults trend west-northwest and die out in the cores of asymmetric anticlinal folds without observed direct linkage to the shallow (upper 400 m) parts of the Hosgri Fault Zone (Figure 18).

11.3 Folding

The geometry of folding in Tertiary strata indicates a northeast-southwest horizontal direction of maximum shortening. Deformation within the Hosgri and Point Buchon fault zones is predominantly northwest-southeast oriented representative of a strike-slip fault system (Reading, 1980; Mann, 2007). Minor discontinuous faults generally occur as north-trending and east-trending sets (Plate 2), and are localized within the Tertiary folded section, indicating they are related to the folding stress field. These minor faults likely are bending moment faults formed during folding of strata as indicated by bent reflectors. Northeast-trending faults exhibiting minor warping of the fold axes suggest some northeast-southwest directed tearing may have deformed the folds.

11.4 Northern Shoreline Seismicity Sublineament

The 3D/2D dataset shows several faults in the vicinity of the northern Shoreline seismicity sublineament (as defined by Hardebeck, 2010 and PG&E, 2011b). Two postulated (queried) continuous and linear, northwest-trending, *en-echelon* faults along this seismicity trend were reported in the Shoreline fault zone report (PG&E, 2011b) based on the interpretation of widely spaced (800 m) 2D seismic profiles (Plate 3a). The 3D/2D dataset more clearly delineates the locations of structures in this area and provides improved imagery of subsurface geology (Plate 3b). The Point Buchon fault zone is located about 300-750 m northeast of the surface projection of the northern Shoreline seismicity sublineament (Plate 3b), although the ~0.5 km location uncertainty of the earthquakes may reduce this offset. However, as outlined below no well-defined

continuous through going fault coincident with the seismicity sublineament is observed or found from this study to connect directly with the Hosgri Fault Zone.

Four faults that splay westward from the Point Buchon fault zone may overlie the seismicity sublineament. These faults appear to die out to the west in the shallow subsurface (i.e., approximately the uppermost 50 to 400 meters below the seafloor) without reaching the Hosgri Fault Zone. Uninterrupted (unfaulted) reflectors are seen in the 3D/2D data to be continuous across parts of the northward projection of the seismicity sublineament (PG&E, 2011b) (Plates 2 and 3).

A shallow geometric connection between the Hosgri Fault Zone and the proposed North segment of the Shoreline fault zone as defined by the seismicity sublineament was not observed in the 3D/2D dataset (see Section 10.2.3.3). No surface fault structure aligns with the northern Shoreline seismic sublineament, in contrast to what has been observed in the Central and Southern sublineaments (PG&E, 2011b), but rather faults die out within an area of transtension characterized by the small grabens 'A' and 'B' and the monolcine in the northern part of the study area.

Since the 3D/2D data are restricted to the shallow subsurface the mapped surficial faults cannot be extended to the earthquake hypocentral depths. Therefore, no conclusion can be made in regard to these faults being the source of the earthquakes that constitute the northern Shoreline seismicity sublineament (Plate 3a).

11.5 Strike-slip Tectonic Models

The change in faulting style from transtension in the northern part of the study area to transpression in the southern part of the study area is a common feature of strike-slip fault systems (Mann, 2007) as discussed in Section 5.2.2 above. Folding and uplifted bedrock in the southern part of the study area may result from a left-transfer of slip between active traces of the right-lateral Hosgri Fault Zone. This fault configuration suggests that

distinct quadrants of tension (in the north) and compression (in the south) exist with conjugate faults and folds connecting the primary through-going faults of the main traces of the Hosgri Fault Zone in a fashion as described from the mathematical models of Rogers (1980) and clay models of Wilcox et al. (1973). More recent scaled analog clay model experiments provide additional insights into the structural geometry and evolution of releasing and restraining bends (e.g., McClay and Bonora, 2001; Mitra and Paul, 2011).

Harland (1971) states that folds form at oblique angles to the strike-slip fault in an *en-echelon* pattern, though if transpression is dominant, the folds are rotated so that they nearly parallel the fault. Therefore, the nearly Hosgri-Point Buchon fault parallel *en-echelon* folds in the central and southern part of the study area may be inferred to have resulted from a dominant transpressional regime. *En-echelon* folds have been suggested to indicate deformation in plastic (ductile) cover rocks overlying strike-slip faults in more rigid basement rocks at depth (Reading, 1980), and this may be the case in the study area, although ages of folding in the study are not well constrained and need to be determined. To confirm this concept deeper penetration HESS needs to be undertaken.

12.0 LIMITATIONS

A limitation on the use of the data interpretations is that the results presented in this report have not been integrated with other datasets, such as gravity data and the high-resolution magnetic anomaly data.

A second limitation is that no absolute or interval (formational) seismic velocities for the use in the construction of accurate depth sections were available at the time of interpretation and report writing.

Finally, the faults mapped in this study could not be correlated with microseismicity as the penetration depth of the 3D/2D seismic-reflection acoustics did not reach a depth that would have allowed for such a correlation.

13.0 IMPACT EVALUATION

The results presented herein may result in changes to DCP.P's seismic source characterization of crustal fault sources that are presented in the Shoreline Fault Report (PG&E, 2011b) and the LTSP Report (PG&E, 1988). Depth penetration is limited from a low-energy source that provides only shallow time sections and the small area of coverage limits an overall regional perspective.

The results of this study suggest a possible different geometry and relationship between the Hosgri Fault Zone and the Central segment of the Shoreline fault zone and a possible connection to the Point Buchon fault zone. This data will be used as input for development of the seismic source logic trees for the seismic source characterization by the SSHAC SSC TI team. Therefore, the association of seismicity with the Point Buchon fault zone and structural relationships among the Hosgri and Point Buchon fault zones needs further analyses, especially in the area of transtension, in the northern part of the study area.

The interpretations reported here provides results that are relevant to seismic hazard, but does not by itself provide sufficient information to update the seismic hazard model of DCP.P. However, the findings reported here do have implications for certain seismic source parameters that are part of the seismic hazard model. Namely, this report contains information about two seismic sources in the DCP.P seismic source model: the Shoreline and Hosgri faults. The update of the seismic hazard model for DCP.P is being conducted through the SSHAC Level 3 process, which involves a synthesis of all available geologic, seismic, and geophysical information available.

14.0 REFERENCES

- Atwater, T.M., 1970, Implications of plate tectonics for the Cenozoic tectonic evolution of western North America: *Geological Society of America Bulletin*, v. 81, p. 3513-3536.
- Brown, A.R., 2004, Interpretation of three-dimensional seismic data: American Association of Petroleum Geologists, Memoir 42, 6th Edition, Tulsa, OK, 541 p.
- Burchfiel, B.C., and Stewart, J.H., 1966, 'Pull-apart' origin of the central segment of Death Valley, California: *Bulletin Geological Society of America*, v. 77, p. 439-442.
- Cloos, E., 1955, Experimental analyses of fracture patterns: *Geological Society of America Bulletin*, v. 66, p. 241-256.
- Crowell, J.C., 1974, Origin of late Cenozoic basins in southern California, *in*: Dickinson, W.R., ed., *Tectonics and Sedimentation: Society of Economic Paleontologists and Mineralogists Special Publication 22*, Tulsa, OK, p. 190-204.
- Dickinson, W.R., 2004a, Evolution of the North American Cordillera: *Annual Reviews of Earth and Planetary Sciences*, v. 32, p. 13-45.
- Dickinson, W.R., 2004b, Kinematics of transrotational tectonism in the California Transverse Ranges and its contribution to cumulative slip along the San Andreas Transform Fault System: http://seismo.berkeley.edu/~rallen/teaching/SO4_SanAndreas/Resources/BlockRotationTransrotationTectonism.pdf.
- Dickinson, W.R., Ducea, M., Rosenberg, L.I., Greene, H.G., Graham S.A., Clark, J.C., Weber, G.E., Kidder, S., Ernst, W.G. and Brabb, E.E., 2005, Net dextral slip, Neogene San Gregorio-Hosgri fault zone, coastal California: geologic evidence and tectonic implications: *Geological Society of American Special Paper*. 391, 43 p.
- Fugro Consultants, 2012a, Field operations report 2010-2011 high-resolution marine survey offshore Diablo Canyon power plant, central California: Prepared for PG&E, May 2012, Fugro Proj. No. 04.B0992017, 875 p.
- Fugro Consultants, 2012b, 2D seismic data processing report 2010-2011 high-resolution marine survey offshore Diablo Canyon power plant, central California: Prepared for PG&E, May 2012, Fugro Proj. No. 04.B0992017, 13 p.
- Fugro Seismic Imaging, 2012, Seismic data processing report, 3D high-resolution marine survey, California offshore 2011, Diablo Canyon: Prepared for PG&E, May 2012, Rept. No. 2010-4410_Draft01, 36 p.
- Hanson, K.L., Wesling, J.R., Lettis, W.R., Kelson, K.I., and Mezger, L., 1994, Correlation, ages, and uplift rates of Quaternary marine terraces, south-central California, *in* Alterman, I.B., McMullen, R.B., Cluff, L.S., and Slemmons, D.B.,

- eds., Seismotectonics of the Central California Coast Range: Geological Society of America Special Paper 292, p. 45-72.
- Hanson, K.L., Lettis, W.R., McLaren, M.K., Savage, W.U., and Hall, N.T., 2004, Style and rate of Quaternary deformation of the Hosgri fault zone, offshore south-central California, *in* Keller, M.A., ed., Evolution of Sedimentary Basins/Offshore Oil and Gas Investigations—Santa Maria Province: U.S. Geological Survey Bulletin 1995-BB, 33 pp.
- Hardebeck, J.L., 2010, Seismotectonics and fault structure of the California central coast: Seismological Society of America Bulletin, v. 100, 1031-1050, doi: 10.1785/0120090307.
- Harland, W.B., 1971, Tectonic transpression in Caledonia Spitzbergen: Geological Magazine, v. 108, p. 27-42.
- Howell, D.G., Crouch, J.K., Greene, H.G., McCulloch, D.S., and Vedder, J.G., 1980, Basin development along the late Mesozoic and Cenozoic California margin; a plate tectonic margin of subduction, oblique subduction and transform tectonics, *in* Balance, P.F., and Reading, H.G., Sediment in Oblique-slip Mobile Zones: International Association of Sedimentologists Special Publication 4, p. 43-62.
- Kingma, J.T., 1958, Possible origin of piercement structures, local unconformities, and secondary basins in the Eastern Geosyncline, New Zealand: New Zealand Journal of Geology and Geophysics, 1, p. 269-274.
- Lekkerkerk, H-J., van der Velden, R., Roders, J., Haycock, T., de Vries, R., Jansen, P., and Beemster, C., 2006, Handbook of Offshore Surveying, Book Two: Clarkson Research Services Limited, St Magnus House, London, 194 p.
- Lettis, W.R., Hanson, K.L., Unruh, J.R., McLaren, M., and Savage, W.U., 2004, Quaternary tectonic setting of south-central coastal California, *in* Keller, M.A., ed., Evolution of Sedimentary Basins/Offshore Oil and Gas Investigations—Santa Maria Province: U.S. Geological Survey Bulletin 1995-AA, 24 pp.
- Luyendyk, B. P.1991. A model for Neogene crustal rotations, transtension, and transpression in Southern California, Geological Society of America Bulletin 103, p. 1528-1536.
- McClay, K. and Bonora, M., 2001, Analog models of restraining stepovers in strike-slip fault systems: American Association of Petroleum Geologists Bulletin, v. 85, n. 2, p. 233-260.
- McCulloch, D.S., 1987, Regional geology and hydrocarbon potential of offshore central California continental margin, *in* Scholl, D.W., Grantz, A., and Vedder, J.G., eds., North America and Adjacent Ocean Basins – Beaufort Sea to Baja California: Circum-Pacific Council for Energy and Mineral Resources, Earth Science Series, Houston, v. 6, p. 353-401.

- Mann, P., 2007, Global catalogue, classification and tectonic origins of restraining- and releasing bends on active strike-slip fault systems, *in* Cunningham, W.D. and Mann, P., eds., *Tectonics of Strike-slip Restraining and Releasing bends*: Geological Society, London, Special Publications, 290, P. 13-142.
- Mitra, S., and Paul, D., 2011, Structural geometry and evolution of releasing and restraining bends: Insights from laser-scanned experimental models: *American Association of Petroleum Geologists Bulletin*, v. 95, no. 7, p. 1147-1180.
- NCS SubSea, 2011, Navigation Final Report, Diablo Canyon Power Plant 3D Survey: NCS Subsea, Inc., Job Number J00344-FR-001-001, DCP.P. 3D Geophysical Survey, 18 p.
- PG&E, Pacific Gas and Electric Co, 1988, Final report of the Diablo Canyon Long Term Seismic Program: US Nuclear Regulatory Commission Enclosure 1, PG&E letter DCL-05-002, Docket No. 50-275 and No. 50-323.
- PG&E, Pacific Gas and Electric Co, 2008, E-mail to Alan Wang and Vincent Gaddy (NRC) from Bill Guldmond (PG&E), Subject: Preliminary data for seismic discussion, with attachment, DCP.P_Nov 20-2008_v2 (3). ppt.
- PG&E, Pacific Gas and Electric Co, 2011a, Progress report on the analysis of the Shoreline fault zone, central coastal California: Report to the U.S. Nuclear Regulatory Commission, PG&E Letter DCL-10-003, 36 p.
- PG&E, Pacific Gas and Electric Co, 2011b, Shoreline Fault Zone Report: Report on the analysis of the Shoreline fault zone, central Coastal California: Report to the U.S. Nuclear Regulatory Commission, January 2011.
<http://www.pge.com/myhome/edusafety/systemworks/dcpp/shorelinereport/>
- Quennell, A.M, 1958, The structural and geomorphic evolution of the Dead Sea Rift: *Quarterly Journal of the Geological Society of London*, 114, p. 1-14.
- Reading, H.G., 1980, Characteristics and recognition of strike-slip fault systems, *in* Balance, P.F., and Reading, H.G., eds., *Sediment in Oblique-slip Mobile Zones*: International Association of Sedimentologists Special Publication 4, p. 7-26.
- Rodgers, D.A., 1980, Analysis of pull-apart basin development produced by *en echelon* strike slip faults. *in* Balance, P.F., and Reading, H.G., eds., *Sediment in Oblique-slip Mobile Zones*, International Association of Sedimentologists Special Publication 4, p. 27-41.
- Sheriff, R.E., 1982, *Structural Interpretation of Seismic Data*: American Association of Petroleum Geologists, v. 73 p., ISBN 0-89181-172-9.
- Sherrif, R.E., and Geldart, L.P., 1995, *Exploration Seismology*: Cambridge University Press, Second Edition.
- Sliter, R.W., Triezenberg, P.J., Hart, P.E., Watt, J.T., Johnson, S.Y., and Scheirer, D.S., 2009, High-resolution seismic reflection and marine magnetic data along the

- Hosgri fault zone, central California: U. S. Geological Survey Open-File Report 2009-1100. <http://pubs.usgs.gov/of/2009/1100>.
- Tchalenko, J.S., 1970, Similarities between shear zones of different magnitudes: Geological Society of America Bulletin, v. 81, p. 1625-1640.
- Wilcox, R.E., Harding, T.P. and Seely, D.R., 1973, Basic wrench tectonics: American Association of Petroleum Geologists Bulletin, v. 57, p. 74-96.
- Willingham, C.R., Rietman, J.D., Heck, R.G., and Lettis, W.R., in press, Characterization of the Hosgri Fault Zone and adjacent structures, *in* Keller, M.A. ed., The offshore Santa Maria Basin, south-central California: U.S. Geological Survey Bulletin 1995-CC, Evolution of Sedimentary Basins/Onshore Oil and Gas Investigations, Santa Maria Province.
- Yilmaz, O., 2001, Seismic Data Analysis, Processing, Inversion, and Interpretation of Seismic Data; Society of Exploration Geophysicists, Investigations in Geophysics No. 10, 2nd Ed., Tulsa, OK, 2 v., 2027 p.

15.0 LIST OF ACRONYMS

CDP	Common Depth Point
CEG	Civil Engineering Geologist (California)
CMP	Common Mid Point
CRP	Common Reference Point
CSUMB	California State University Monterey Bay
DCPP	Diablo Canyon Power Plant
DEM	Digital Elevation Model
DGPS	Differential Global Positioning System
ESRI	Economic and Social Research Institute
FCL	Fugro Consultants, Inc.
GPS	Global Positioning System
HESS	High-Energy Seismic Survey
Hz	Hertz
IHO	International Hydrographic Office
IPRP	Independent Peer Review Panel
ITR	Independent Technical Reviewer
kJ	kilojoules
km	kilometers
LCI	Lettis Consultants International
LTSP	Long Term Seismic Program

MBES	Multibeam Echosounder
m	meters
MLLW	Mean-low-low-water
MLML	Moss Landing Marine Laboratories
ms	milliseconds
m/s	meters per second
mm/yr	millimeters per year
NMO	Normal Move Out
NQA	Nuclear Quality Assurance
NRC	Nuclear Regulatory Commission
PG&E	Pacific Gas and Electric Company
TWTT	Two Way Travel Time
QA	Quality Assurance
QC	Quality Control
s	seconds
SMT	Seismic Micro Technology
SRME	Surface related multiple-elimination
SSC	seismic source characterization
SSHAC	Senior Seismic Hazard Advisory Committee
TFDN	Time frequency de-noise algorithm
TI	Technical Integration
USGS	United States Geological Survey

UTM	Universal Transverse Mercator
WGS	World Geodetic System
2D	Two-dimensional
3D	Three-dimensional

16.0 LIST OF FIGURES, FOLDOUTS, PLATES AND TABLES

- Figure 1 Regional tectonic setting with faults and structural domains (modified after PG&E, 1988).
- Figure 2 Structural blocks and faults in the DCP.P area (modified after PG&E, 1988).
- Figure 3 Frequency spectrum from 3D/2D seismic-reflection dataset showing dominant (fundamental) frequency of 200-225 Hz and calculation using 1600-1650 m/s to determine vertical resolution (2.00-2.06 and 1.78-1.83 m).
- Figure 4 Streamer layout (layback diagram) for seismic source and receivers used in the collection of 3D/2D data from the M/V Michael Uhl.
- Figure 5 Trackline map of 2D seismic-reflection lines and boundary of 3D survey area.
- Figure 6 Schematic diagram of streamer array showing navigation positioning accuracy during 3D/2D seismic-reflection survey.
- Figure 7 Schematic diagram illustrating skewed geometry of streamer array during times of adverse weather conditions resulting in irregular coverage.
- Figure 8 Example of “bubble-pulse” recorded during 3D/2D seismic-reflection survey showing ~5 ms (~4 m) thick shallow subsurface section not resolvable due to masking of legitimate reflectors by pulse width.
- Figure 9 Flow chart showing procedures and steps undertaken in the processing of the 3D data.
- Figure 10 Examples of data quality (interpretability) shown in (a) 3D seismic-reflection profile line 12120 and (b) on amplitude time slice at 150 ms (TWTT).
- Figure 11 MBES bathymetry overlaid upon 3D amplitude time slice at 138 ms (TWTT) showing a good correlation between the two data sets.
- Figure 12 Example of a wave-cut platform and shoreline angles illustrated in 3D seismic-reflection profile 13340 and showing bedding artifacts.

- Figure 13 Illustrations of mobile sand sheets shown in (a) 3D seismic-reflection profile 12120 and (b) on MBES shaded relief bathymetry map.
- Figure 14 Vertical and horizontal geometry of Hosgri Fault Zone strands in (a) 3D seismic-reflection profile 11180 and (b) on MBES bathymetry map within northern part of survey area.
- Figure 15 Amplitude time slice maps at 95 ms (TWTT) in the southern part of the 3D study area showing (a) uninterpreted and (b) interpreted strands of the Point Buchon fault zone.
- Figure 16 Fault strands associated with the fault intersection of the Point Buchon fault zone shown in (a) uninterpreted and (b) interpreted similarity time slices at 74 ms (TWTT).
- Figure 17 Graben at northern end of Point Buchon fault zone shown on (a) 2D seismic-reflection profile 1120, and (b) MBES bathymetry.
- Figure 18 Structure associated with the northern part of the Point Buchon fault zone shown in (a) 3D seismic-reflection profile 11820 and (b) in amplitude time slice at 150 ms (TWTT).
- Figure 19 Principal structural elements in the northern part of the study area showing faults and folds in (a) 2D seismic-reflection profile 1399 and (b) on amplitude time slice map at 150 ms (TWTT).
- Foldout A Comparison of amplitude and similarity time slices at 150 ms showing uninterpreted data (a and b) and interpreted maps (c and d).
- Foldout B Marker horizons identified in (a) user-selected 3D strike line and (b) mapped on amplitude time slice at 150 ms (TWTT).
- Foldout C Graben associated with Hosgri Fault Zone: (a) 2D seismic-reflection profile 1039 showing fault boundaries and sediment fill and (b) map view showing faults, graben, and MBES bathymetry.
- Foldout D Relationship of the Hosgri and Point Buchon fault zones in the northern part of the survey area: (a) uninterpreted and (b) interpreted 3D profile 11200; (c) uninterpreted and (d) interpreted amplitude time slice at 150 ms (TWTT).
- Plate 1 Geology of Interpreted Offshore Structures from the 2011 Shoreline Fault Zone Report (PG&E, 2011b)
- Plate 2 Structural Interpretation Map Low Energy 3D/2D Seismic-Reflection Data
- Plate 3 Comparison of Interpreted Offshore Structures: a) Shoreline Fault Zone Report (PG&E, 2011b), and b) This Study

Table 1 Numbering system and colors used to distinguish fault types and association with fault zones and groups (trends) on the high-resolution 3D/2D seismic reflection survey area offshore of DCP.P.

17.0 APPENDICES

Appendix A Qualification of Point Buchon 3D & 2D Seismic Reflection Profiling Survey Data (October 2010 to February 2011)

APPENDIX A

QUALIFICATION OF POINT BUCHON 3D & 2D SEISMIC- REFLECTION PROFILING SURVEY DATA (November 2010 to February 2011)

1.0 REASON FOR QUALIFYING DATA

Some of the activities associated with the Point Buchon 3D and 2D seismic-reflection profiling survey were governed by a 10 CFR 50, Appendix B, QA Program, and some activities were not, as follows:

- a. The data collection was not performed in accordance with a QA Program meeting the requirements of 10 CFR 50, Appendix B, “Quality Assurance Criteria for Nuclear Power Plants and Fuel Reprocessing Plants”.
- b. Likewise the data processing software and data interpretation and analysis software were not validated in accordance with a 10 CFR 50, Appendix B, QA Program.
- c. The interpretation and analysis of the survey data were documented in the technical report GEO.DCPP.TR.12.01, “DCPP 3D/2D Seismic-Reflection Investigation of Structures Associated with the Northern Shoreline Seismicity Sublineament of the Point Buchon Region”. The preparation, review (by an independent technical reviewer [ITR]), and approval of this Report were performed in accordance with the Geosciences Procedure CF3.GE2, “Quality-Related Technical Reports”; and this procedure is part of the PG&E’s QA Program, which meets the requirements of 10 CFR 50, Appendix B.

Since PG&E desires to use the survey data results in DCP.P safety-related applications, the data collection and the data processing software and the interpretation and analysis software will be qualified for safety-related applications in accordance with ASME NQA-1-2008, Part III, Subpart 3.3, Non-mandatory Appendix 3.1, “Guidance on Qualification of Existing Data,” using the qualification method of data corroboration.

2.0 QUALIFICATION OF DATA AND SOFTWARE

2.1 Qualification of Data Collection and Processing Software for 2D and 3D Data.

2.1.1 2D Data Collection and Processing

Fugro Consultants, Inc. (FCL) acquired high resolution 2D seismic reflection data offshore Point Buchon and Avila Bay between November 2010 and February 2011 for the PG&E Central Coast Seismic Project (CCSIP). FCL documented the field operations in a report (FCL, 2012a). The report describes the daily operations, navigation and seismic instrumentation, data collection parameters, marine wildlife monitoring activities, and the required permits and notices. This report was reviewed by PG&E's ITR Jan D. Rietman (see Table A.1 for Mr. Rietman's qualifications).

FCL performed and documented the processing of the 2D seismic reflection data using the software Seismic Processing Workshop (SPW). The FCL report (FCL, 2012b) documents the processing flow and the relative parameters used in each step of the processing. Major processing steps included deconvolution, velocity analysis, CMP stack, post-stack Krichoff time migration, filtering, scaling, and merging of the navigation data. The output of the processing was SEG Y files for each line that was used as input to the IHS Kingdom program. The report also discusses the quality control procedures followed during the processing. This report was reviewed by PG&E's ITR Jan D. Rietman.

FCL subsequently performed and documented, in accordance with the FCL QA Program that meet the requirements of 10 CFR 50, Appendix B, the validation of the commercial SPW for safety-related applications and the qualification of the 2D seismic reflection data processed by the program (FCL, 2012e). To satisfy the data processing software validation requirements, FCL used processing exercises from a published seismic processing textbook written specifically for SPW. The processing exercises were successfully completed. The 2010/2012 2D survey data were qualified for use in safety-related applications through successful data corroboration with USGS high-resolution 2D single-channel mini-sparker data collected in the same area in 2008 and 2009.

The Fugro report (FCL, 2012e) was reviewed by PG&E's ITR Jan D. Rietman and accepted by the Geosciences Quality Manager. Acceptance of this Project Report by the Geosciences Quality Manager is documented in SAPN QVP 50405898.

2.1.2 3D Data Collection and Processing

FCL acquired high resolution 3D seismic reflection data offshore Point Buchon and Avila Bay between November 2010 and February 2011 for the PG&E Central Coast Seismic Project (CCSIP). FCL documented the field operations in a report (FCL, 2012a). The report describes the daily operations, navigation and seismic instrumentation, data collection parameters, marine wildlife monitoring activities, and the required permits and notices. FCL acquired 3D seismic data using a triple-plate boomer sound source and a four-streamer array of hydrophones beginning in November 2010 and ending February 2011. NCS Subsea, Inc. provided differential global positioning system navigation and positioning control. Details of the field data acquisition are reported separately in FCL's Field Operations Report (Fugro, 2012a). The operations report was reviewed by PG&E's ITR Jan Rietman.

Fugro Seismic Imaging (FSI) was subcontracted by FCL to process the data using their proprietary seismic processing software Uniseis. The 3D processing report (FCL, 2012c) documents the processes and parameters used to process the 3D data. Major processing steps for the 3D data included merging seismic and navigation data, noise reduction, filtering, brute stack, static corrections, multiple elimination, velocity analysis, binning, dip models, deconvolution, 3D Pre-stack Kirchhoff time migration, mute, band-pass filter and post-stack scaling. This report was reviewed by PG&E's ITR Jan D. Rietman.

FCL requested FSI to validate the software Uniseis for safety-related applications and to qualify the collected data in accordance with the FCL QA Program. To satisfy the data processing software validation requirements, FSI used a series of exercises to compare the 3D seismic survey data to three public datasets generated by others in the same area. Uniseis was validated to be functioning properly, given that the results are comparable to the three public datasets, which have been accepted and used by government agencies and others for seismic hazard analyses and other purposes. The collected survey data were qualified by data corroboration – i.e., comparison to the three public datasets as follows: 1) comparison of the seafloor horizon on the 2010-2011 data with the multibeam bathymetric data (MBES), 2) geologic interpretation comparisons (e.g. compare a mapped fault to a fault feature in the 3D data, and 3) comparison of the 2010-2011 data processed with Uniseis with a USGS 2009/2010 Mini-Sparker dataset.

The validation and qualification was approved by FCL in their project report (FCL, 2012d). This report was reviewed by PG&E's ITR Jan D. Rietman and accepted by the Geosciences Quality Manager. Acceptance of this Project Report by the Geosciences Quality Manager is documented in SAPN QVP 50405898.

2.2 Qualification of the Interpretation Software, IHS Kingdom, Version 8.6, Hotfix 4, for Safety-Related Use.

The software initially used for the interpretation is IHS Kingdom, version 8.6 (formerly called SMT Kingdom Suite when the data analysis and interpretation were done in 2011). At the time the interpretation began, this software had not been validated for safety-related use. PG&E requested FCL to validate IHS Kingdom software for safety-related use in accordance with the FCL 10 CFR 50, Appendix B, QA Program. FCL chose to accomplish the validation of the software IHS Kingdom, version 8.6, by: 1) validating the software HIS Kingdom, version 8.6, Hotfix 4 for use with Windows Version 7 platform with 64-bit processor, and 2) comparing the results of running the same input data using both versions of the software.

FCL validated the commercial software IHS Kingdom, version 8.6, Hotfix Level 4 (Kingdom) for safety-related applications. The Kingdom validation is documented and approved in FCL (2012f) Safety Validation Report (SVR), Kingdom-v8.6HF4-SVR_00, "Validation of the Commercial Software, IHS Kingdom Version 8.6 Hotfix 4 Associated with Converting the Software to Safety-

Related Software”. This Report was reviewed by PG&E’s ITR Jan D. Rietman. Acceptance of this Project Report by the Geosciences Quality Manager is documented in SAPN QVP 50462849.

The Teapot Dome public-domain dataset provided by DOE was used for software and hardware testing. The ability of Kingdom software to accurately load the Teapot Dome SEG Y data was evaluated according to FCL’s validation procedures detailed in their report, in order to evaluate the software’s ability to accurately reproduce interpretations of subsurface geologic faulting and stratigraphic relationships. Two –way travel time plots (TWT) of the Teapot Dome data were compared to published spatially identical seismic TWT plots that were generated independently of the Kingdom software. A dataset of well data with known locations was also independently verified for location accuracy in Kingdom.

As required by FCL’s procedure QAP-03E, to qualify specific hardware (e.g., PC) for use with the IHS Kingdom software, FCL completed the required software installation and checkout process. This process yielded the following QA documentation: IHS Kingdom Software User Manual (SUM), Kingdom-v8.6-HF4-SUM_00; the IHS Kingdom Software Installation and Checkout Plan (SICP), IHSKingdom-v8.6HF4-SICP_00; and the IHS Kingdom Software Installation and Checkout Results Report (SICRR), IHSKingdom-v8.6HF4-SICRR_00. The results of qualifying the specific hardware are in the SICRR.

While the non-validated software IHS Kingdom, version 8.6, was originally used in the interpretation and analysis of the survey data, FCL had validated a different version of the software, namely: the software IHS Kingdom, version 8.6, Hotfix 4. FCL qualified the non-validated software version by running the survey data through the validated software version and comparing the outputs as follows:

- (a) The Point Buchon seismic data set to be corroborated includes four components: 2D survey lines, a large 3D survey volume (amplitude data), a small 3D survey volume (amplitude data), and a large 3D survey volume (derivatives from the RSA program). As shown in the Technical Report Figure 1 the small survey area lies just to the south of the large survey area.
- (b) The four Point Buchon data sets were run using the software HIS Kingdom, version 8.6, Hotfix 4, as described below:
 - The software HIS Kingdom, version 8.6, Hotfix 4, was opened.
 - The four Point Buchon Data sets were loaded into this software.
 - The faults, mapped horizons, and cultural features used in the report figures and/or referenced in the report were transferred to this software.
 - The new version of the Point Buchon interpretation project was saved in the file D:\QAVValidation\Pt_Buchon_Survey_interpretation\Pt_Buchon_Survey_Interpretation_Final Dated October 31, 2012.

- (c) The qualification process was based on data comparisons both from within the validated software and between identical figures produced by the validated and non-validated versions of IHS Kingdom.
- (d) Within the validated version, data comparisons were made between 2D data survey lines and arbitrary lines at the same location created from the 3D data volume. Comparisons were also made between the multibeam bathymetry data (collected separately – see main body of report) and small features such as sand waves and rocks that also show on the 2D survey lines and on inlines, crosslines, and arbitrary lines created from the 3D survey. The coordinates of the 10 common features that were tested were within the relative positional accuracy (<0.5m) between the three surveys (multibeam, 2D, and 3D).
- (e) A comparison was also made between the report figures produced from the non-validated version of IHS Kingdom and identical figures at the same scale produced from the validated version. Figures 10, 12, 18 and foldout B were reproduced to show both the seismic sections and time-slice views. Figure 11 shows correspondence between surface multibeam data and subsurface 3D time-slice data. All mapped faults, horizons, and cultural features were faithfully reproduced from the vetted version. (Note some annotations were made on the report figures using ArcGIS.) Foldout A was reproduced from the validated version to allow for comparison between amplitude and similarity time slices from the two 3D volumes as well as between the validated and non-validated versions.
- (f) The creation of the validated version of the Point Buchon project on IHS Kingdom v8.6 Hotfix 4, was conducted on PG&E’s computer in the Geoscience Department by Hans AbramsonWard and observed by PG&E’s ITR Jan D. Rietman. Data comparisons and the qualification of the data also were made by PG&E’s ITR Jan D. Rietman.

Fugro Consultants, Inc. (FCL) (2012a), Field Operations Report, 2010 - 2011 High-Resolution Marine Survey, Offshore Diablo Canyon Power Plant, Central Coastal California Seismic Imaging Project, Fugro Project No. 04.0992017, Prepared for PG&E, May 2012.

_____ (2012b), 2D Seismic Data Processing Report, 2010-2011 High-Resolution Marine Survey Offshore Diablo Canyon Power Plant, Central Coastal California Seismic Imaging Project; Fugro Project No. 04.B0992017; Prepared for PG&E, May 2012.

**PACIFIC GAS AND ELECTRIC COMPANY
GEOSCIENCES DEPARTMENT
TECHNICAL REPORT**

**TR Number: GEO. DCP.P. TR.12.01
Revision: 0
Appendix A
Page A-1 of 7**

_____ (2012c), 3D Seismic Data Processing Report, 2010-2011 High-Resolution Marine Survey Offshore Diablo Canyon Power Plant, Central Coastal California Seismic Imaging Project; Fugro Project No. 04.B0992017, FSI Report No. 2011-4410 (rev3); Prepared for PG&E, May 2012.

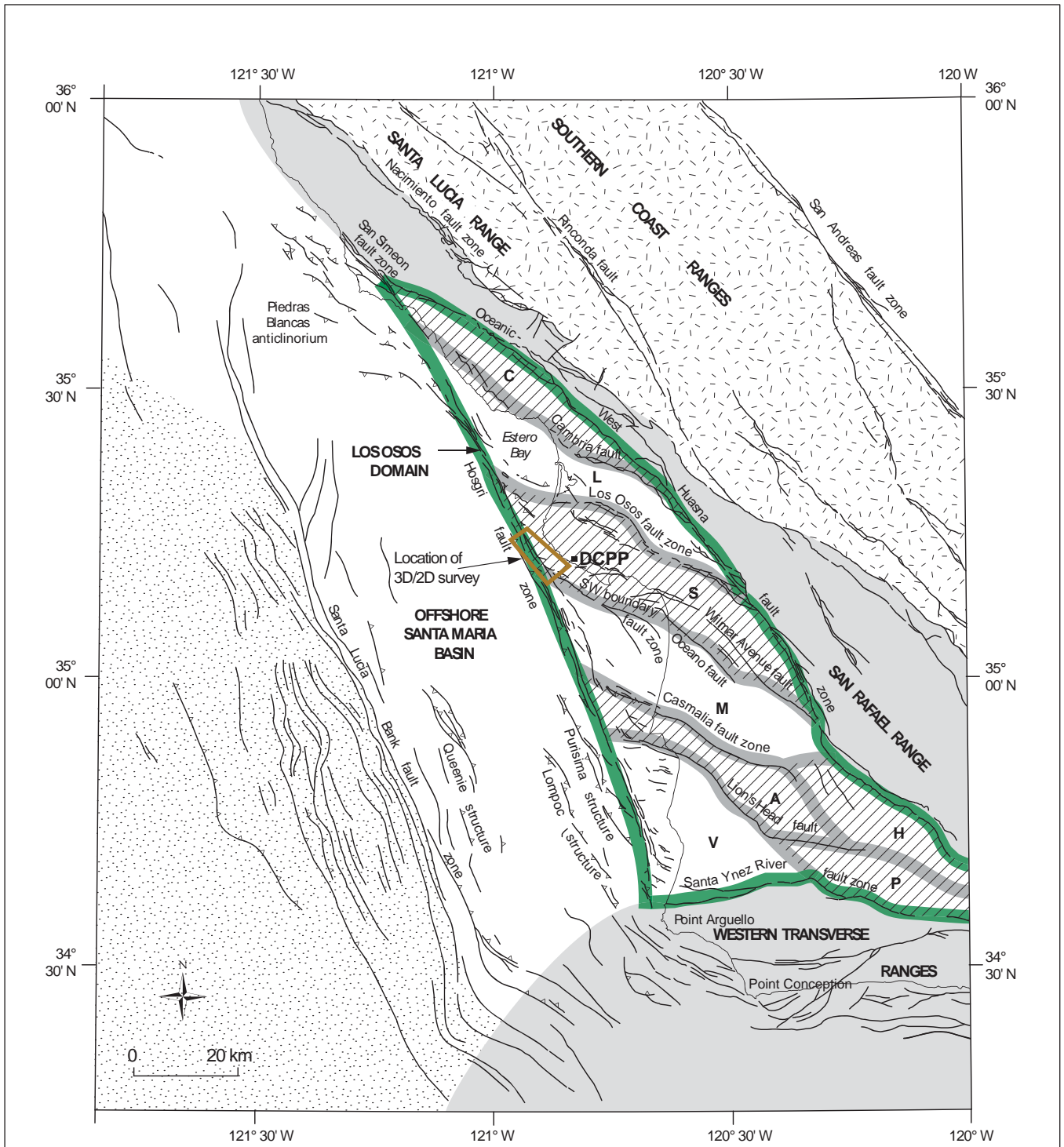
_____ (2012d), Software Validation of Uniseis and 3D Data Qualification of 2010-2011 High-Resolution Marine Survey Data Offshore Diablo Canyon Power Plant, Central Coastal California Seismic Imaging Project, FCL Job No. 04.64110031, FCL Report No. PGEQPR-03 R0, FSI Project No. 2011-4493, Prepared for PG&E, June 2012.

_____ (2012f), Validation of the Commercial Software, IHS Kingdom, Version 8.6 Hotfix 4 Associated with Converting the Software to Safety-Related Software, FCL Report No. Kingdom-v8.6HF4-SVR_00 R0, Prepared for PG&E, July 2012.

_____ (2012e), Software Validation for Seismic Processing Workshop and Qualification of 2010 - 2011, 2D High-Resolution Seismic Reflection Data, for Diablo Canyon Power Plant - Central Coastal California Seismic Imaging Project, PGEQ-PR-06_Rev 1, Prepared for PG&E, November 2012.

TABLE A.1. ITR's AREA OF REVIEW AND QUALIFICATIONS

Name	Company	Area of Review	Qualifications
Jan D. Rietman	Consulting Geophysicist	Point Buchon Interpretation Report. Fugro Field Operations Report. Fugro 2D Processing Report. Fugro 3D Processing Report. Validation Report for HIS Kingdom, v8.6, Hotfix 4. Corroboration of 2D amplitude, 3D amplitude, and 3D attribute data used in IHS Kingdom.	MS (1959) & PhD (1966), Geophysics, Stanford University. California Professional Geophysicist, Gp 53. California Professional Geologist, G 1430. Over 40 years industry experience collecting and interpreting seismic reflection data for exploration and critical facility siting. Over 14 years of experience using IHS Kingdom and its predecessor, SMT Kingdom Suite.



Explanation

- Salinian Terrane
 - Stanley Mountain Terrane
 - San Simeon Terrane
 - Patton Terrane
- Sur-Obispo Composite (McCulloch, 1987)

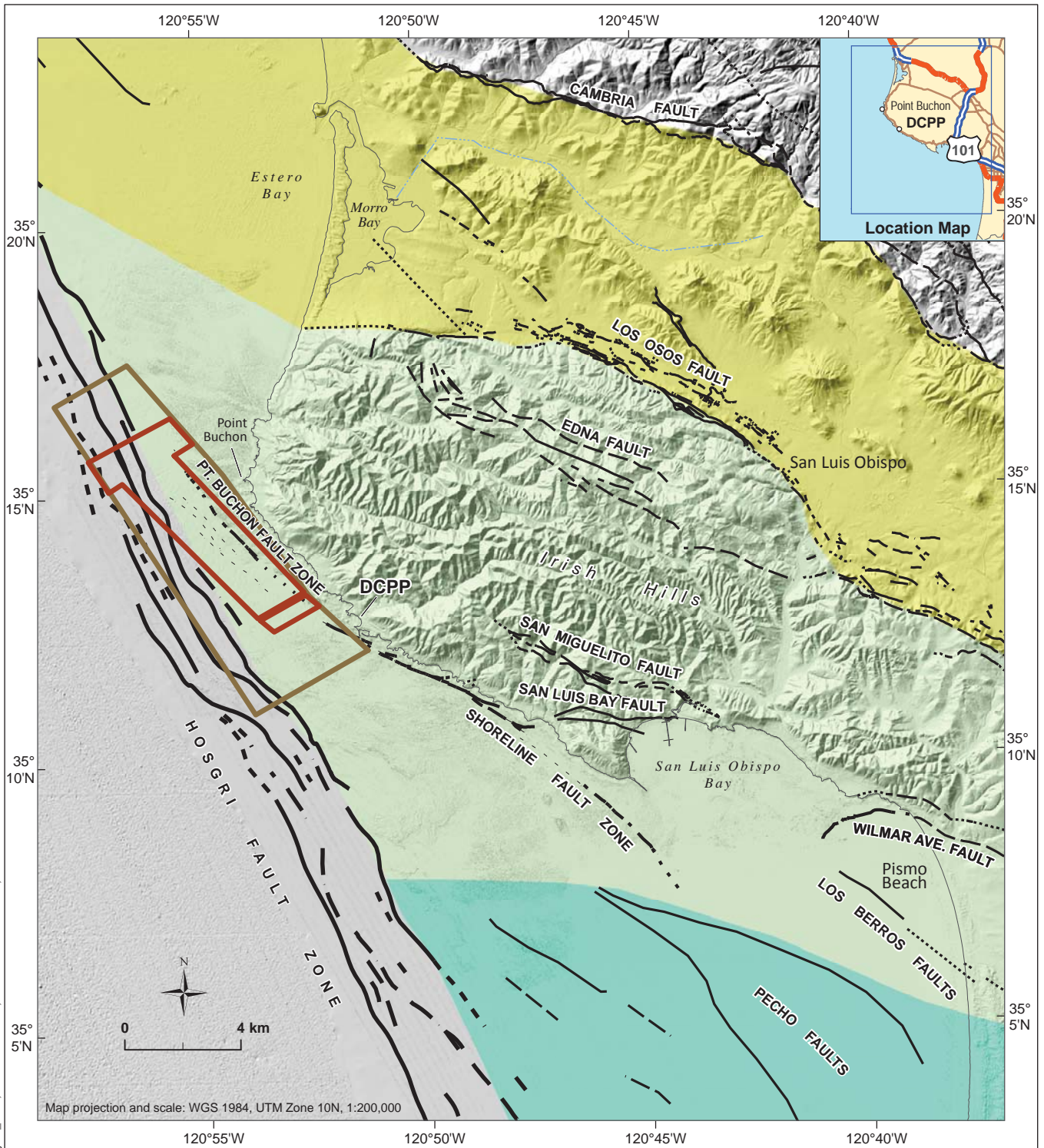
- Structural blocks within the Los Osos domain*
- A = Casmalia
 - C = Cambria
 - H = Solomon Hills
 - L = Los Osos
 - M = Santa Maria Valley
 - P = Purisima
 - S = San Luis/Pismo
 - V = Vandenberg/Lompoc

Source: PG&E (1988)

- Notes:
1. Brown box outlines the 3D/2D seismic reflection study area.
 2. Green line outlines the Los Osos domain.
 3. Hachures indicate uplifted structural blocks within the Los Osos domain.

Regional tectonic setting with faults and structural domains	
DCPP 3D/2D Seismic-Reflection Investigation	
Pacific Gas and Electric Company	Figure 1

File path: S:\13800\13838\13838\02\Figures\20120210_SIT\A\Figure_01.ai; Date: 07/09/2012; User: Jerome Chandler, LCI



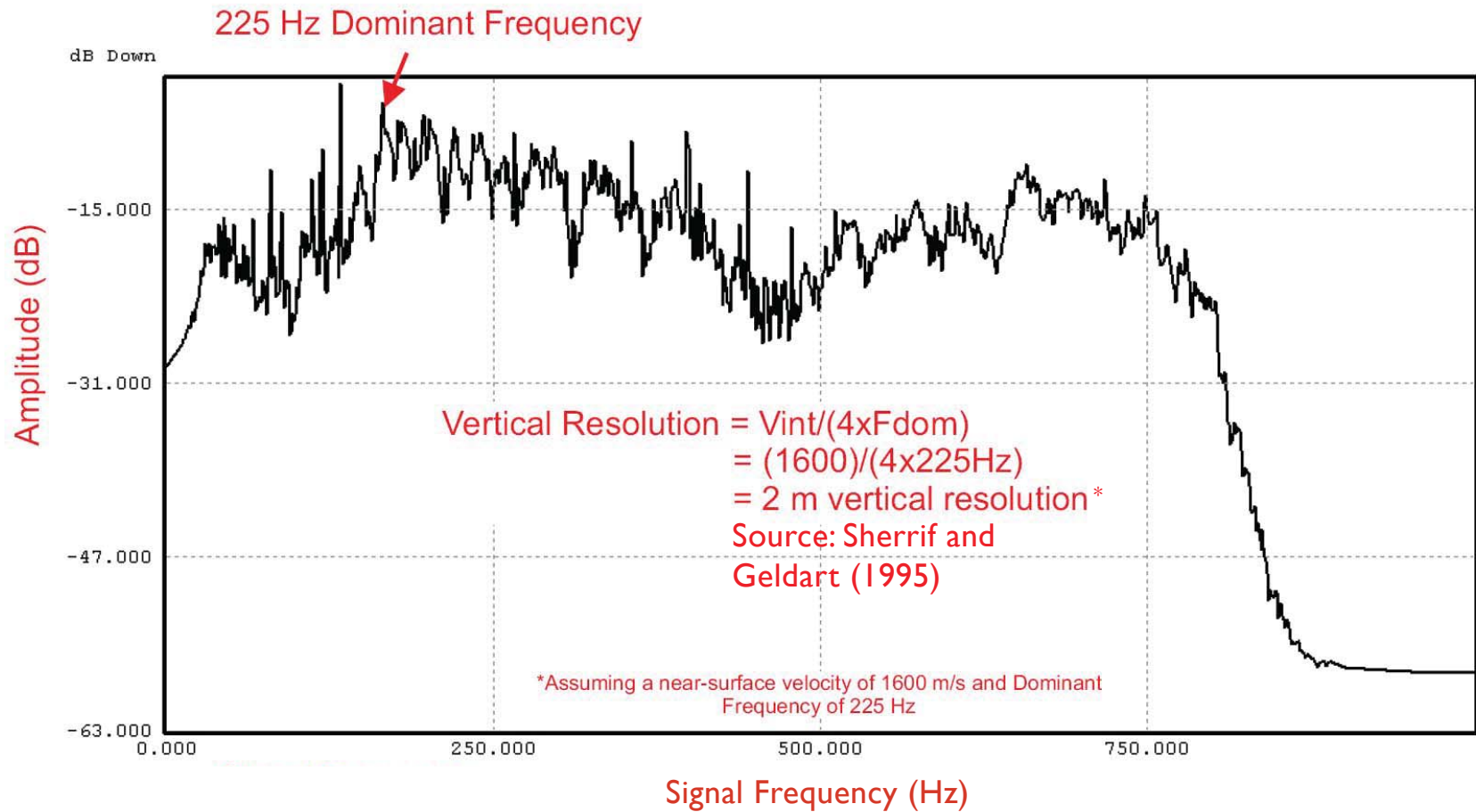
File path: S:\13800\13838\13838.002\Figures\20120210_SIT\AI\Figure_02.ai; Date: 07/27/2012; User: Jerome Chandler, LCI

Explanation

- Hosgri Fault Zone, slip rate >1mm/yr
- Fault with estimated slip rate <1mm/yr
- Los Osos Structural Block
- San Luis/Pismo Structural Block
- Santa Maria Valley Structural Block
- 2D Survey area extent
- 3D Survey area extent

Notes: 1. Locations of faults shown on map are from PG&E (2011b).
 2. Basemap is 2010 PG&E Project DEM.

Structural blocks and faults in the DCPP area	
DCPP 3D/2D Seismic-Reflection Investigation	
Pacific Gas and Electric Company	Figure 2



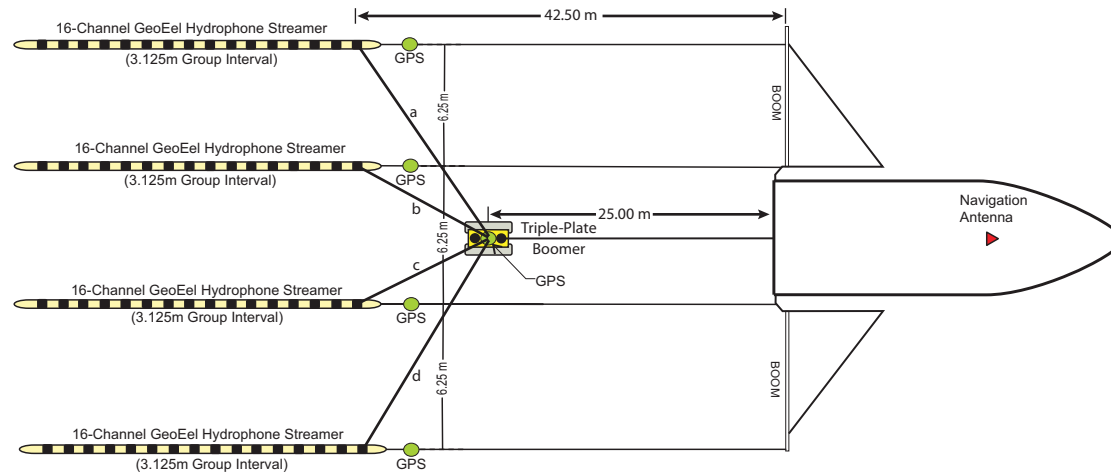
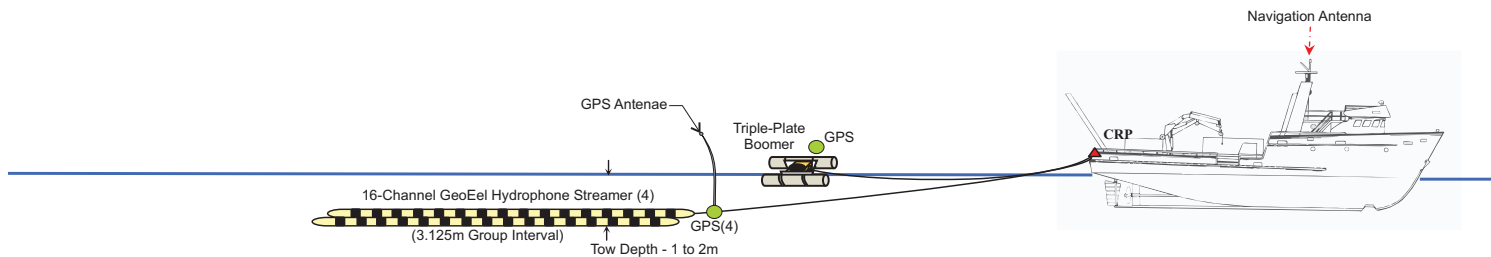
Frequency spectrum from 3D/2D seismic-reflection dataset showing dominant (fundamental) frequency of 200-225 Hz and calculated using 1600-1650 m/s to determine vertical resolution (2.00-2.06 and 1.78-1.83 m)

DCPP 3D/2D Seismic-Reflection Investigation



Pacific Gas and Electric Company

Figure 3



Distances from boomer to head of streamers:

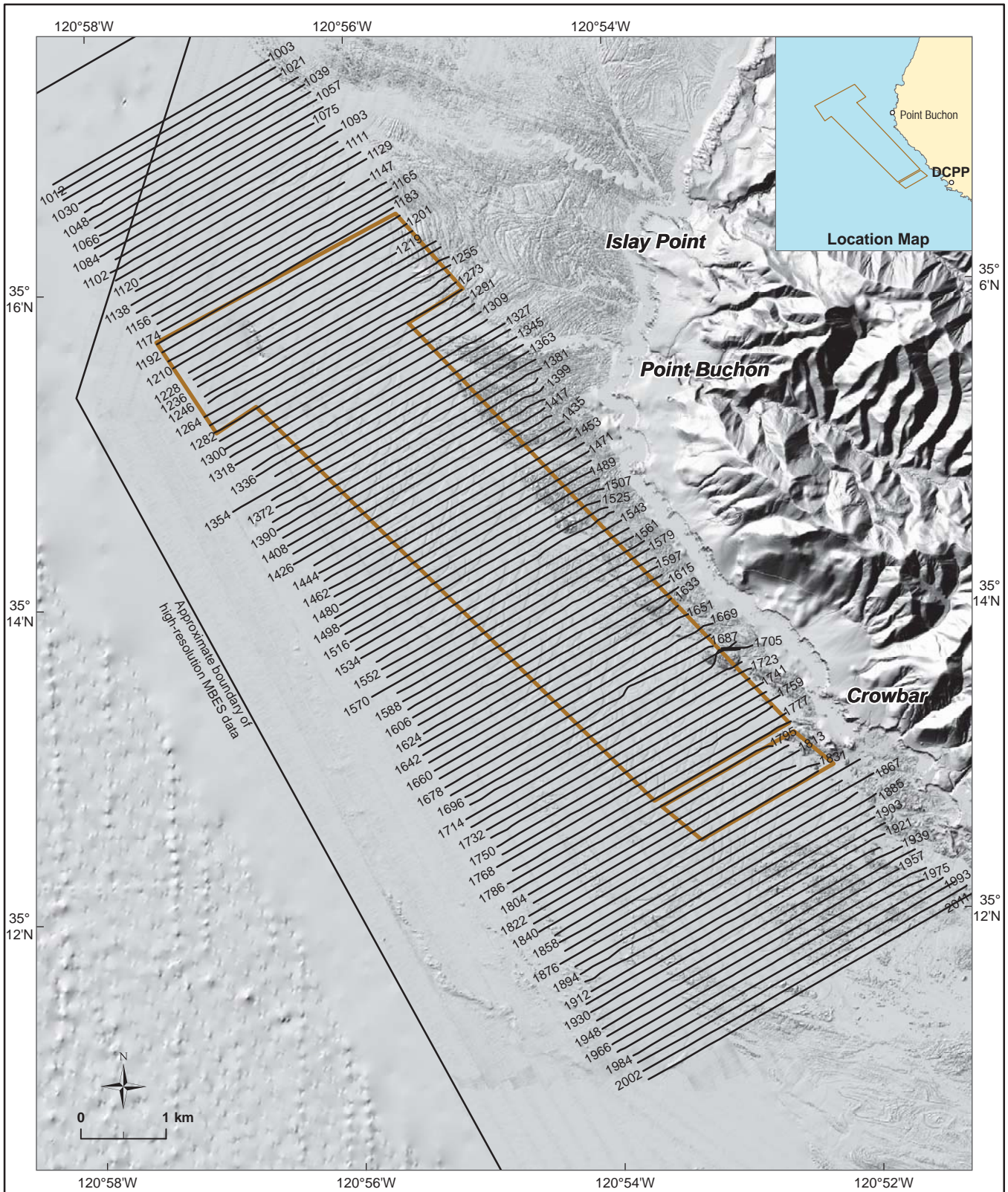
- a: 12.01 m
- b: 8.15 m
- c: 8.15 m
- d: 12.01 m

Notes:

CRP = Common Reference Point
 GPS = Global Positioning System

Streamer layout (layback diagram) for seismic source and receivers used in the collection of 3D/2D data from the M/V Michael Uhl

DCPP 3D/2D Seismic-Reflection Investigation



File path: S:\13800\13838\13838.002\Figures\20120210_SIT\A\Figure_06.ai; Date: 07/09/2012; User: Jereme Chandler, LCI

Explanation

- 2D survey trackline, approximately 100 m spacing
- ▭ Data boundary for 3D seismic reflection surveys

Map projection: WGS 1984, UTM Zone 10N
 MBES Data Source: Seafloor Mapping Lab, CSUMB

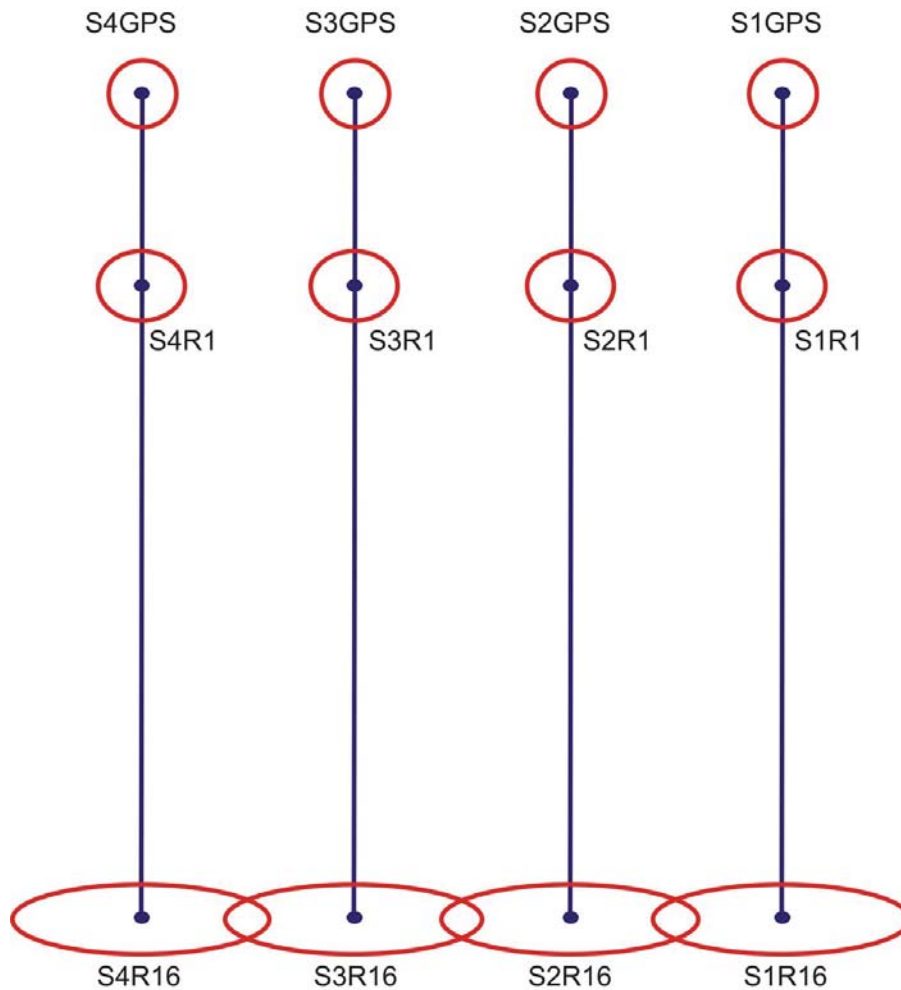
Trackline map of 2D seismic-reflection lines and boundary of 3D survey area

DCPP 3D/2D Seismic-Reflection Investigation



Pacific Gas and Electric Company

Figure **5**



Notes:

Ellipses represent working error of positioning; head end of streamers have a 1 m positioning accuracy whereas a 3 m positioning accuracy occurs at the tail ends, resulting in an overall horizontal resolution of ~2-3 m.

Codes at dots indicate the following: S1-4 = streamer number, S1GPS-S4GPS = position of GPS unit at head of each streamer, S1-4R1-16 = receiver number in streamer.

Schematic diagram of streamer array showing navigation positioning accuracy during 3D/2D seismic-reflection survey

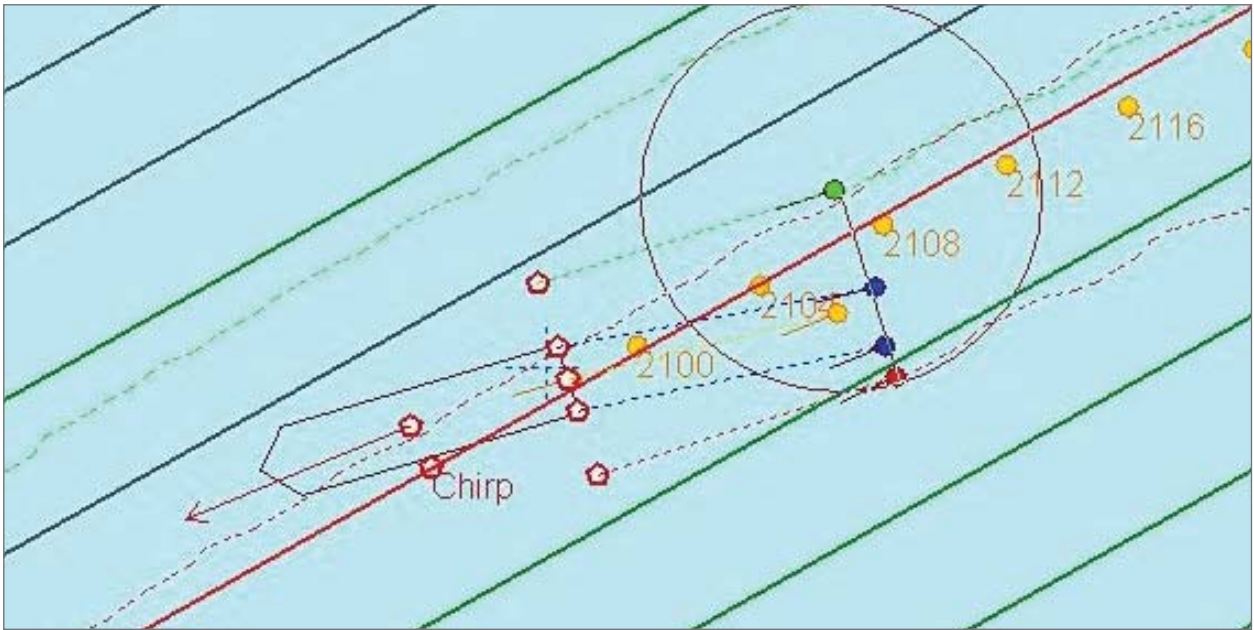
DCPP 3D/2D Seismic-Reflection Investigation



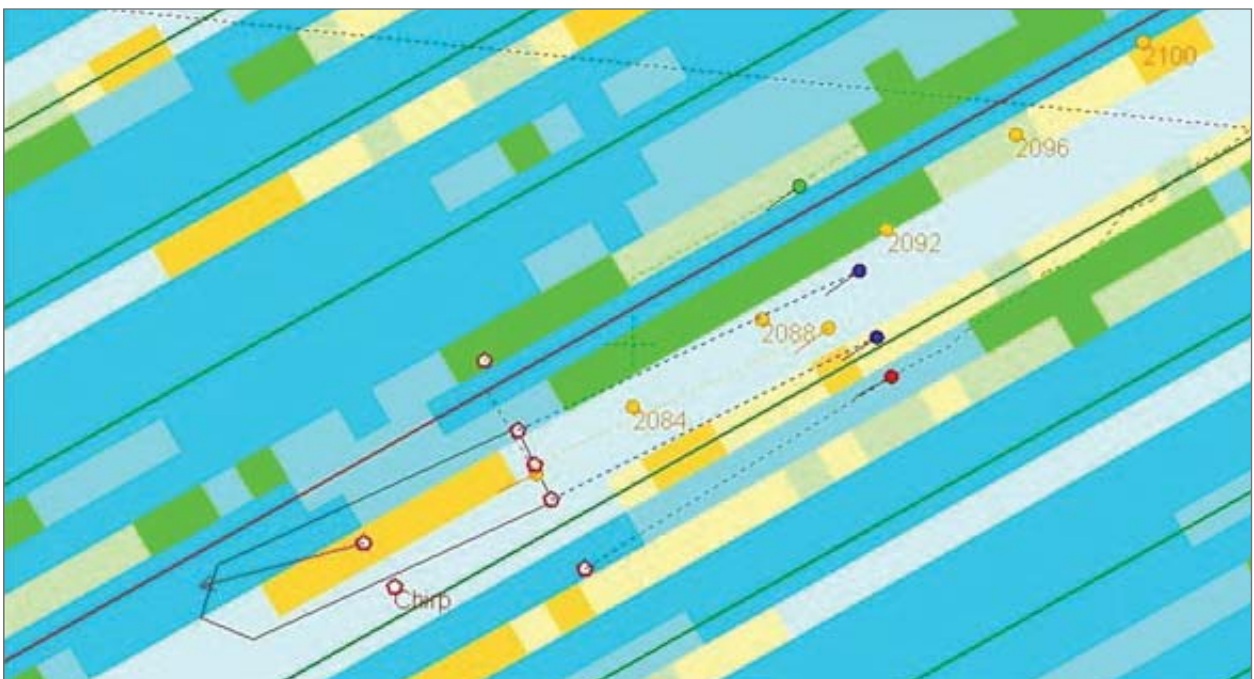
Pacific Gas and Electric Company

Figure 6

a.



b.



Notes:

a) Geometry of array in relation to line orientation (Data Coverage), and b) example of coverage obtained and geometry of array during gap filling operations (Bin Infilling)

In a) red circles represent locations of GPS sensors on vessel, at the source and at head ends of streamers, green (starboard or right), blue (inner) and red (port or left) color-filled circles represent ends of streamers, and numbers along the red line (active navigation line) represent shot points; green lines are pre-programmed navigation lines.

In b) blue color represent 4 or more fold coverage while, green is 3 fold, yellow is 2 fold and gray is 0 coverage.

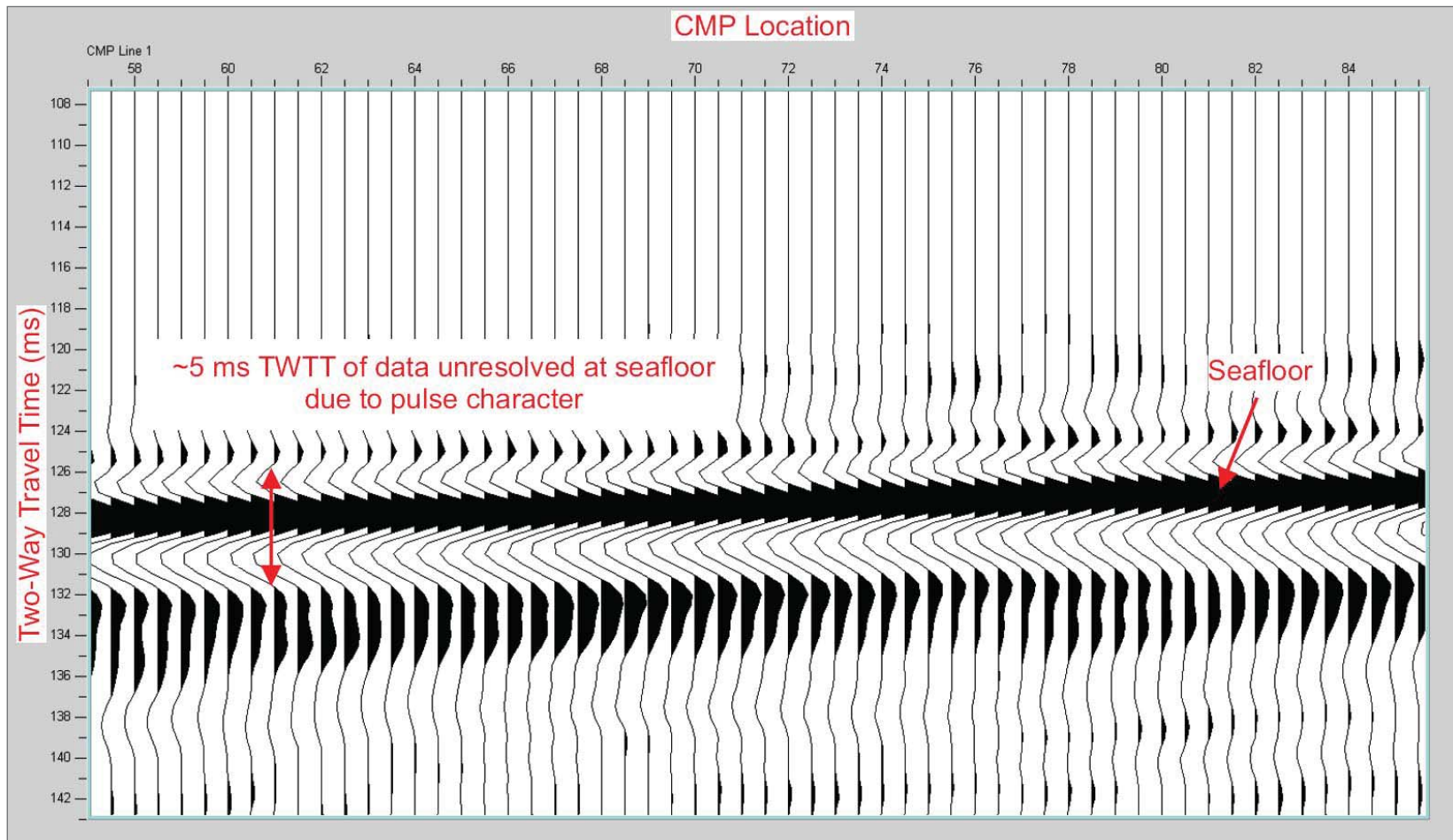
Schematic diagram illustrating skewed geometry of streamer array during times of adverse weather conditions resulting in irregular coverage

DCPP 3D/2D Seismic-Reflection Investigation



Pacific Gas and Electric Company

Figure 7



Note:

CMP = Common Mid Point or Shot Point location

Example of “bubble-pulse” recorded during 3D/2D seismic-reflection survey showing ~5 ms (~4 m) thick shallow subsurface section not resolvable due to masking of legitimate reflectors by pulse width

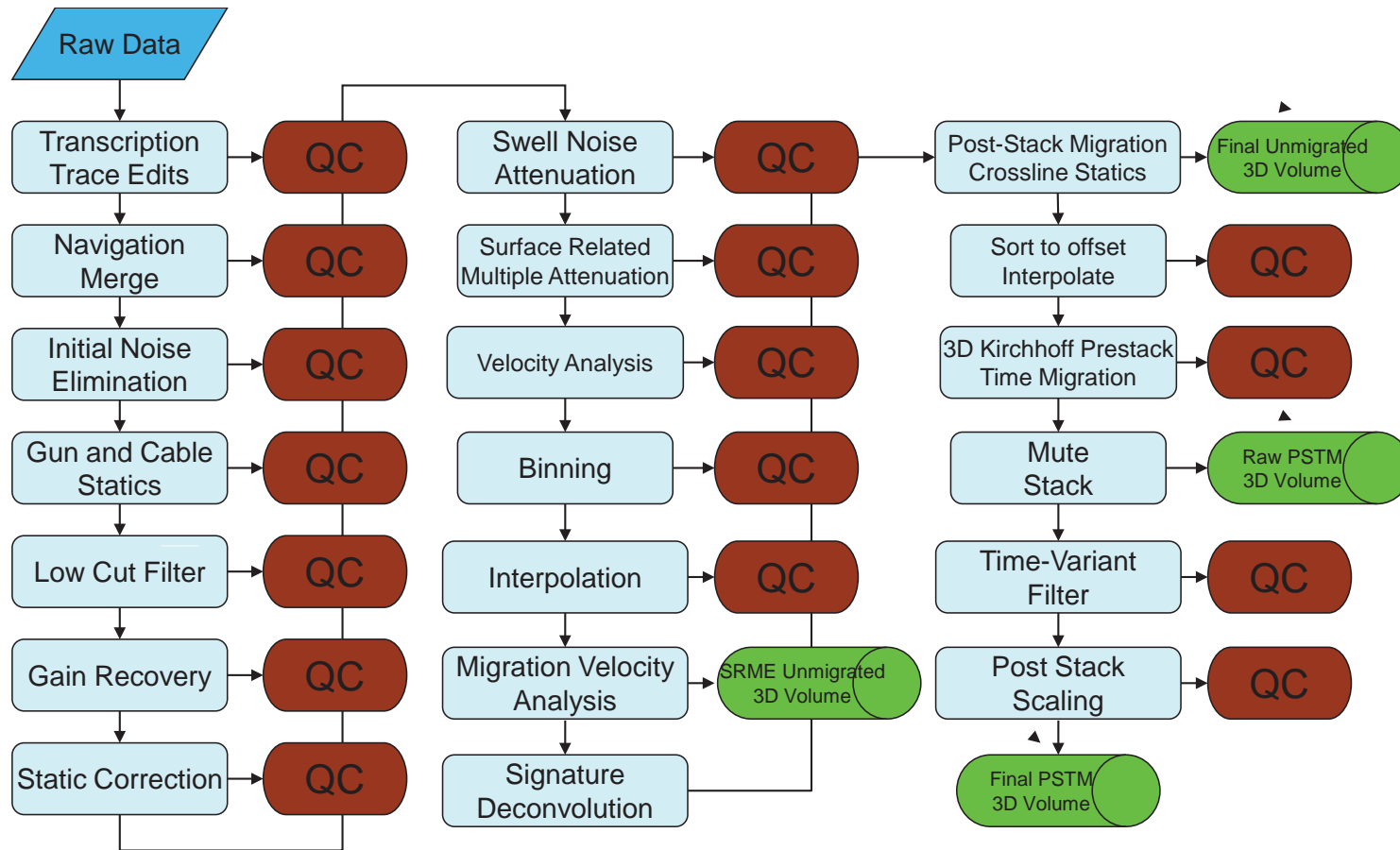
DCPP 3D/2D Seismic-Reflection Investigation



Pacific Gas and Electric Company

Figure 8

Processing Flow



Note:
All Quality Control (QC) assessments were made prior to advancing to the next step of processing.

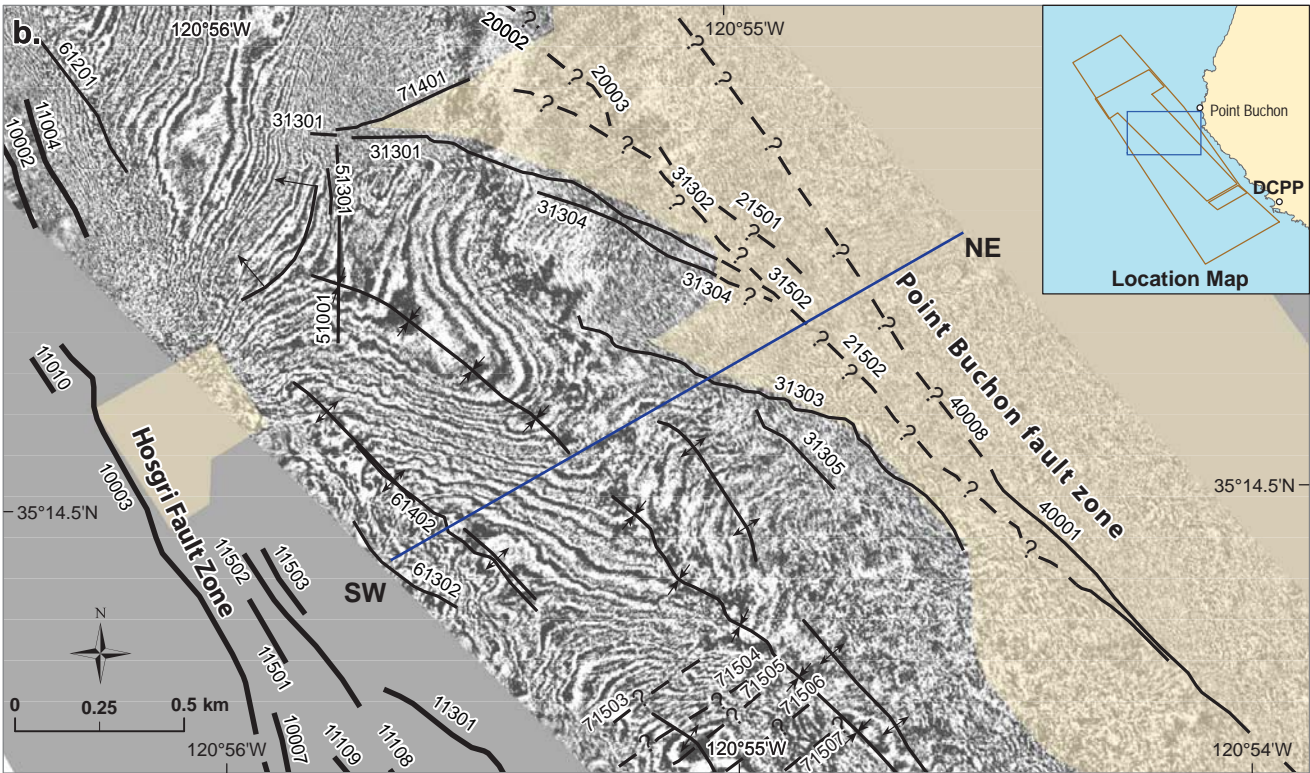
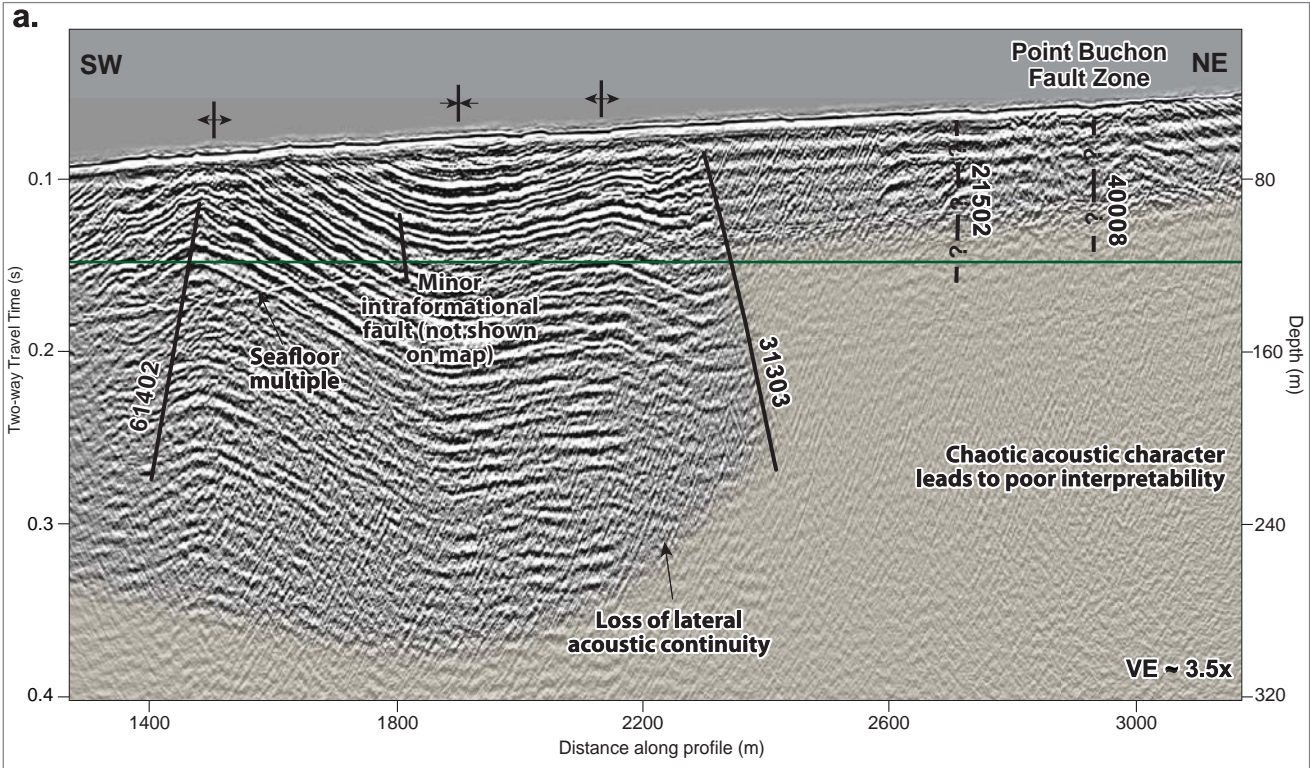
Flow chart showing procedures and steps undertaken in the processing of the 3D data

DCPP 3D/2D Seismic-Reflection Investigation



Pacific Gas and Electric Company

Figure 9



Explanation

- Time slice horizon
- Area of poor interpretability
- Location of seismic profile shown on Plate 3b
- - ? - - Faults, solid where well located, dashed where inferred or approximately located, queried where uncertain, dotted where buried by more than 20 milliseconds of undeformed strata
- ↕ Syncline
- ↔ Anticline
- ↗ Monocline



Note: Depth values on seismic profile assume a velocity of 1600 m/sec.

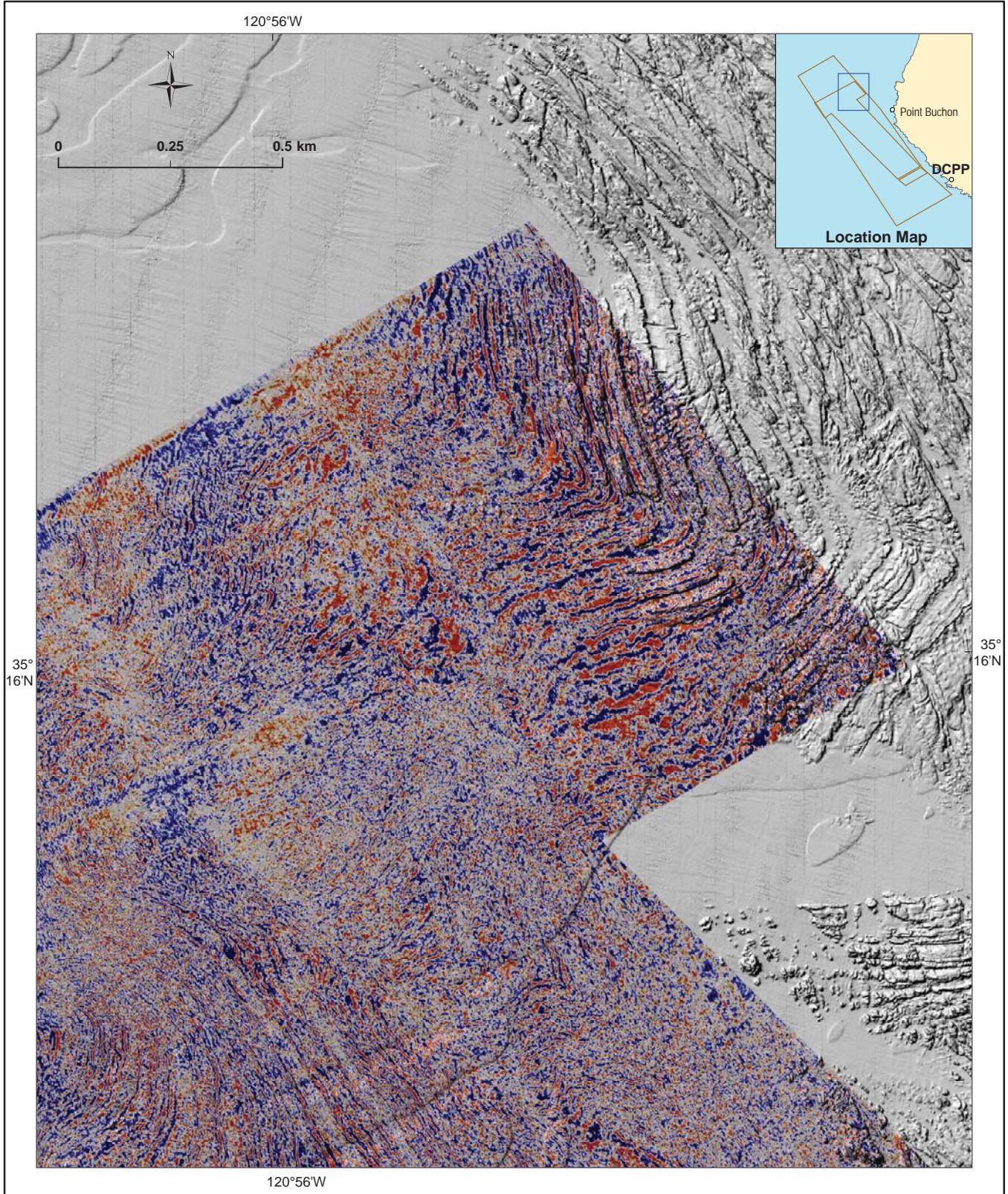
Examples of data quality (interpretability) shown in (a) 3D seismic-reflection profile line 12120 and (b) on amplitude time slice at 150 ms (TWTT)

DCPP 3D/2D Seismic-Reflection Investigation

Pacific Gas and Electric Company

Figure **10**

File path: S:\138001\38381\3838.002\Figures\20120210_SITVA\Figure_10.ai; Date: 07/09/2012; User: Jerome Chandler, LCI



File path: S:\13800\13838\13838.02\Figures\20120210_SITVA\Figure_11.ai; Date: 07/09/2012; User: Jerome Chandler, LCI

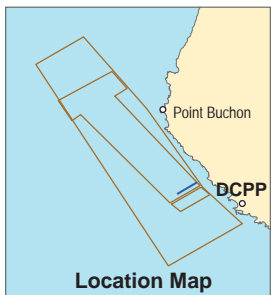
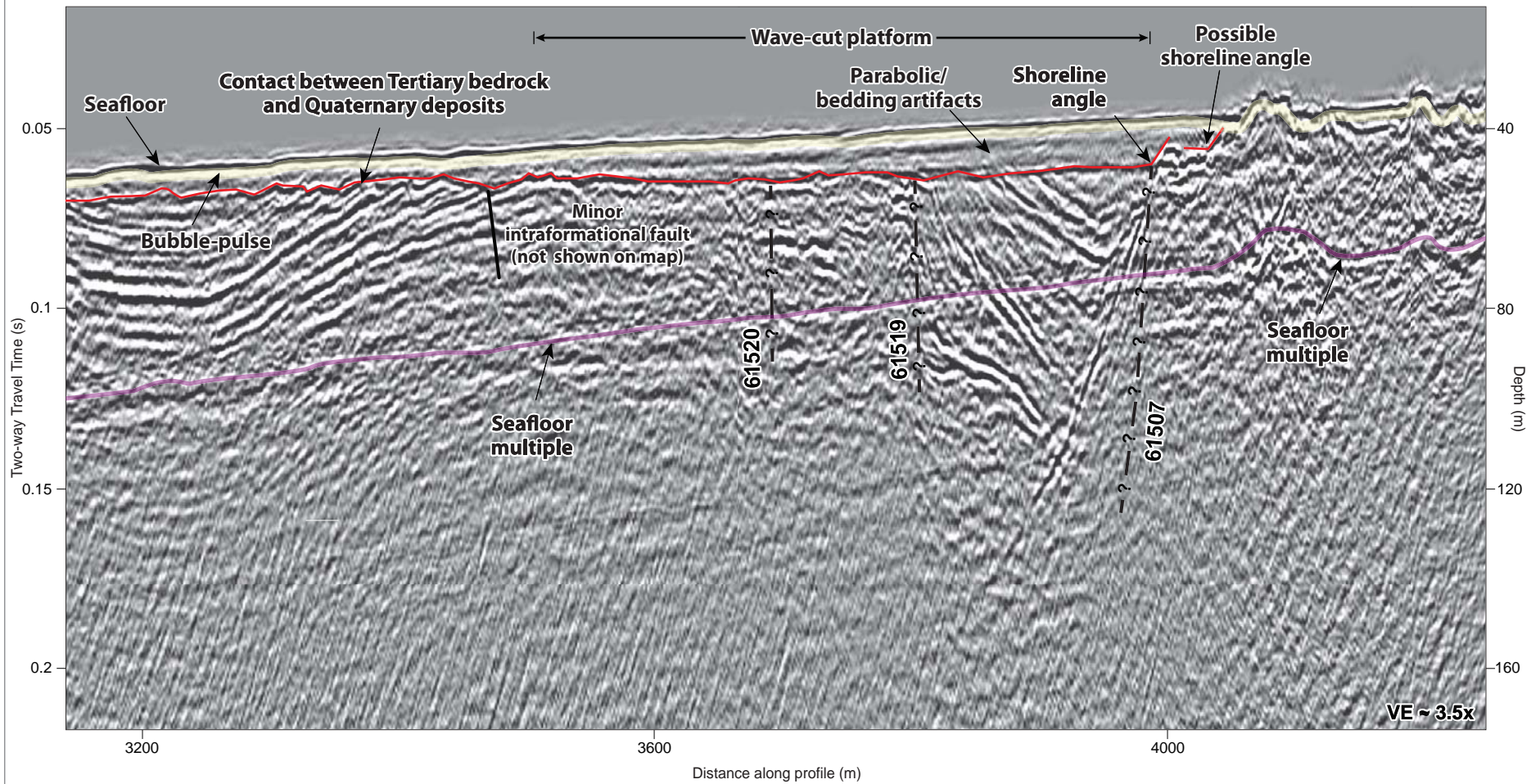
Time Slice Explanation



Note: Good correlation of reflectors in the time slice with ridges imaged in bathymetry suggests that 3D survey is correctly aligned with MBES survey

MBES bathymetry overlaid upon 3D amplitude time slice at 138 ms (TWTT) showing a good correlation between two data sets

DCPP 3D/2D Seismic-Reflection Investigation

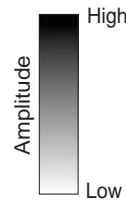


Explanation

- ?--- Faults, solid where well located, dashed where inferred or approximately located, queried where uncertain, dotted where buried by more than 20 milliseconds of undeformed strata
- Erosional surface (top of Tertiary rock)
- Location of seismic profile shown on Plate 3b

Notes:

1. Depth values on seismic profile assume a velocity of 1600 m/sec.
2. Minor intraformational fault displayed on profile is not mapped and shown on fault maps or included within the fault database.



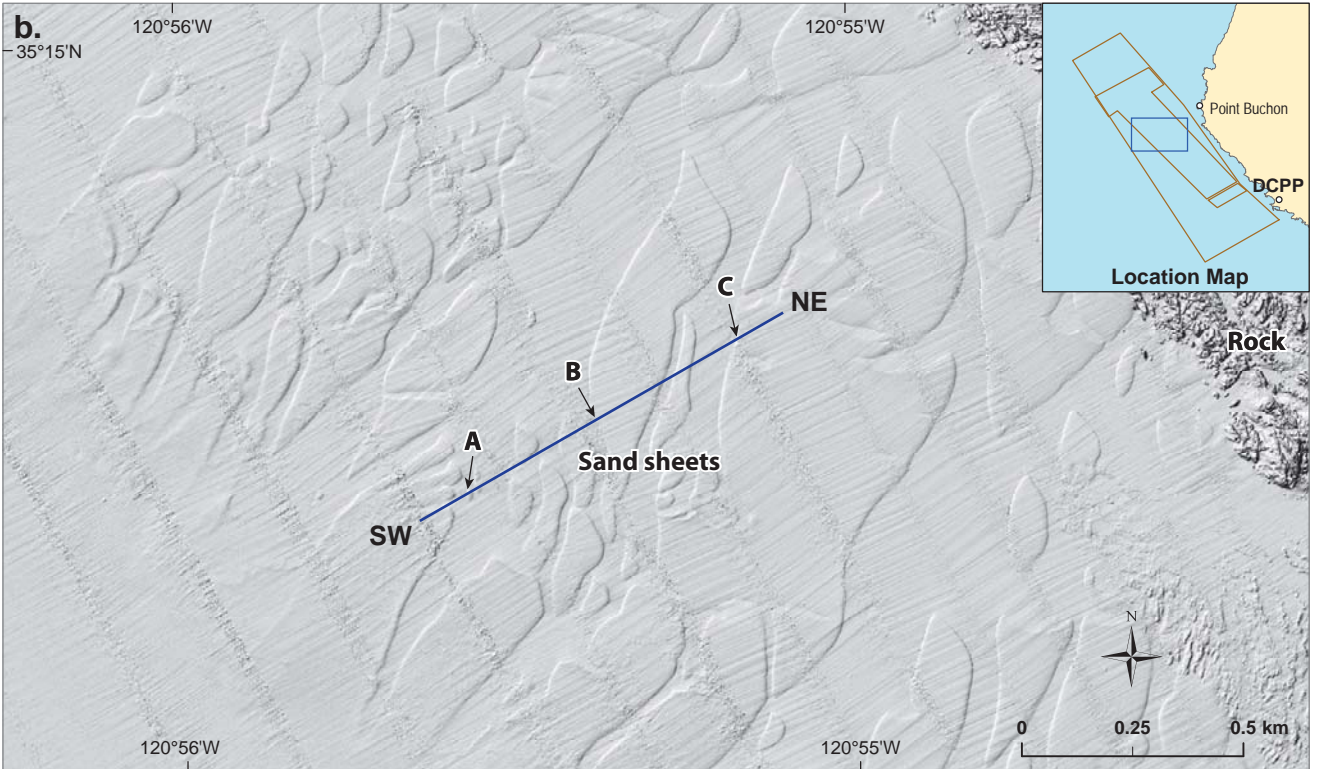
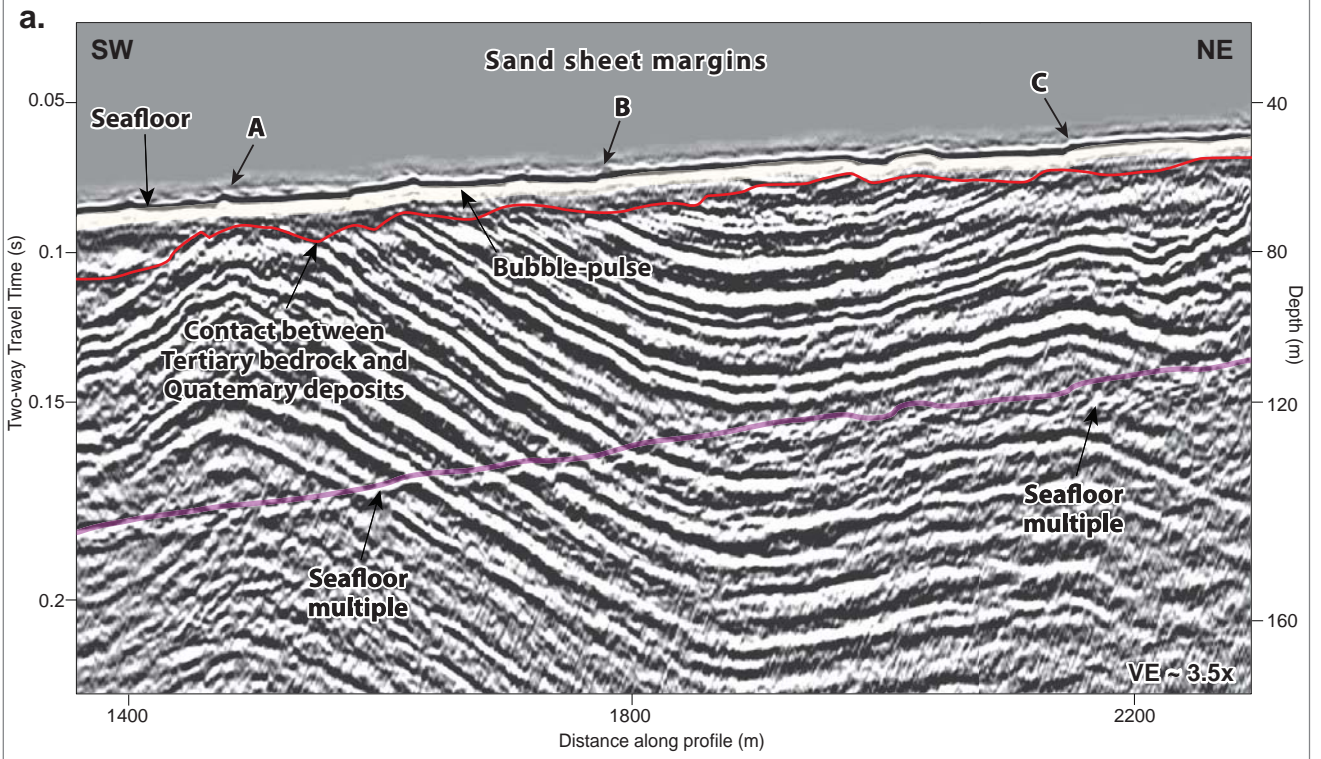
Example of a wave-cut platform and shoreline angles illustrated in 3D seismic-reflection profile 13340

DCPP 3D/2D Seismic-Reflection Investigation



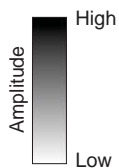
Pacific Gas and Electric Company

Figure **12**



Explanation

- Location of seismic profile shown on Plate 3b
- Erosional surface (top of Tertiary rock)
- ↙ ↘ Location of mobile sand sheet margins



Note: Depth values on seismic profile assume a velocity of 1600 m/sec.

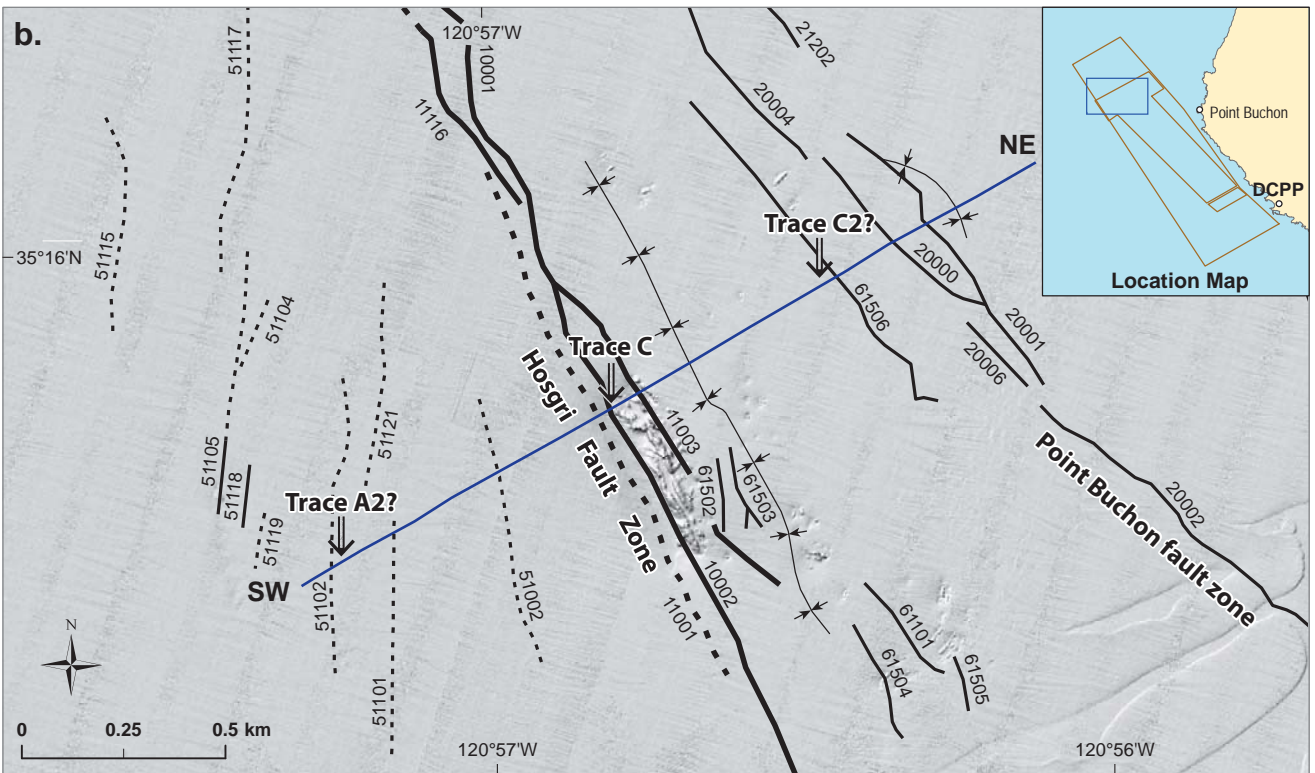
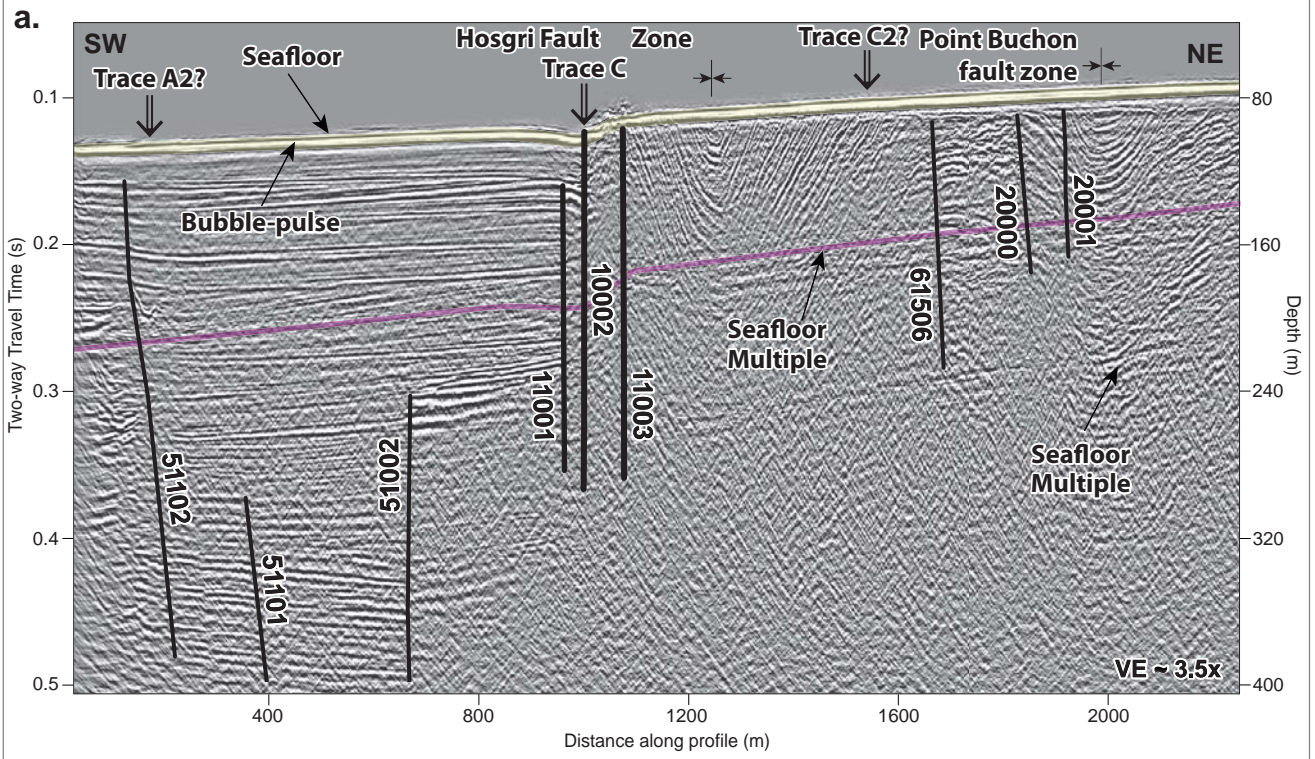
Illustrations of mobile sand sheets shown in (a) 3D seismic-reflection profile 1210 and (b) on MBES shaded relief bathymetry map

DCPD 3D/2D Seismic-Reflection Investigation



Pacific Gas and Electric Company

Figure **13**



Explanation

- Location of seismic profile shown on Plate 3b
 - ····· Faults, solid where well located, dashed where inferred or approximately located, dotted where buried by more than 20 milliseconds of undeformed strata
 - Approximate positions of Hosgri fault traces from PG&E (2011b)
 - Syncline
 - Anticline
- Amplitude

High
Low

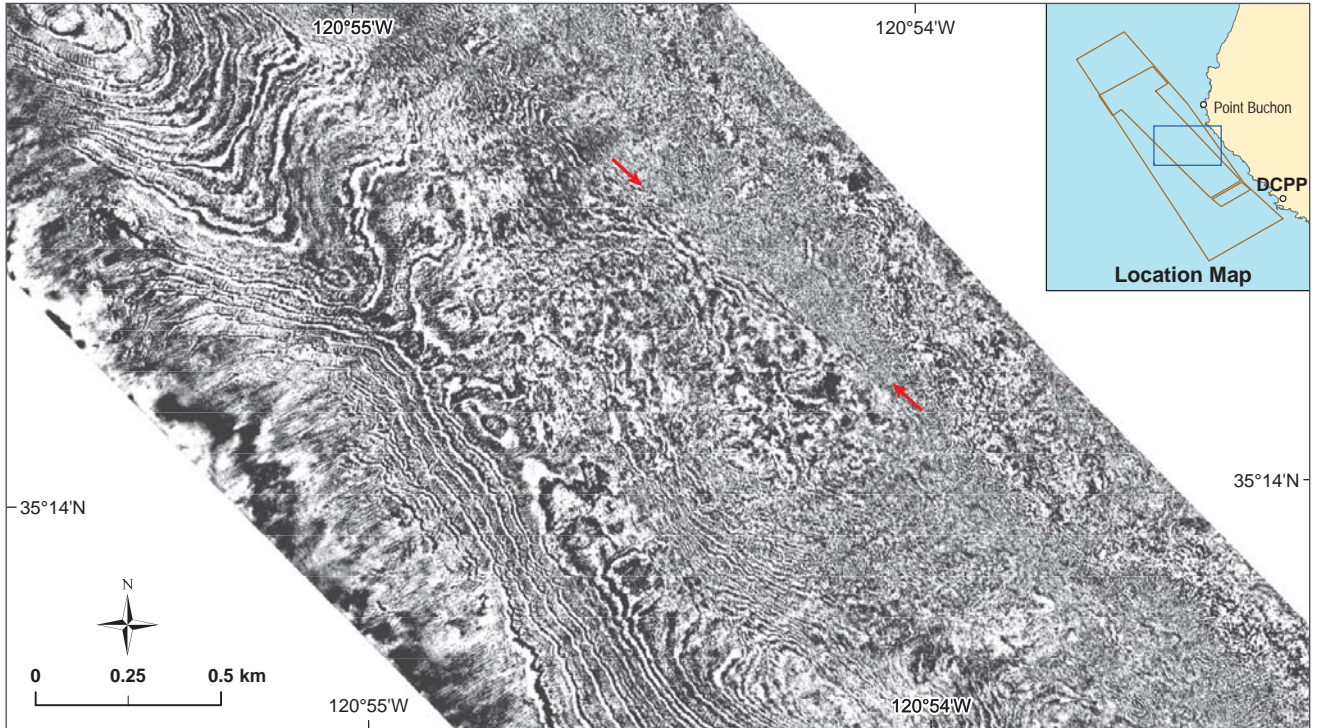
Note: Depth values on seismic profile assume a velocity of 1600 m/sec.

Vertical and horizontal geometry of Hosgri Fault Zone strands in (a) 3D seismic-reflection profile 11180 and (b) on MBES bathymetry map within northern part of survey area

DCPP 3D/2D Seismic-Reflection Investigation

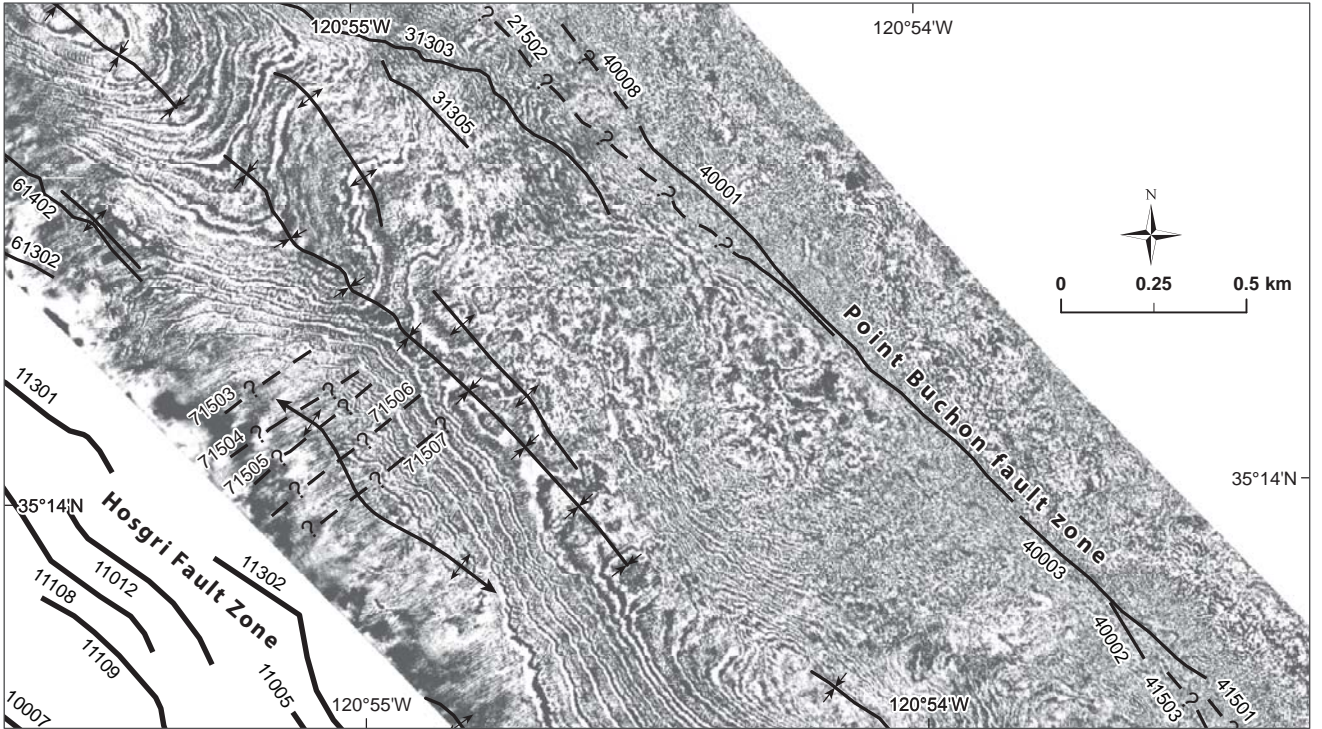
a.

Uninterpreted



b.

Interpreted



Explanation

—?— Faults, solid where well located, dashed where inferred or approximately located, queried where uncertain, dotted where buried by more than 20 milliseconds of undeformed strata



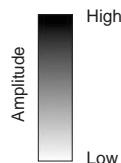
Syncline



Anticline



Point Buchon Fault Lineament



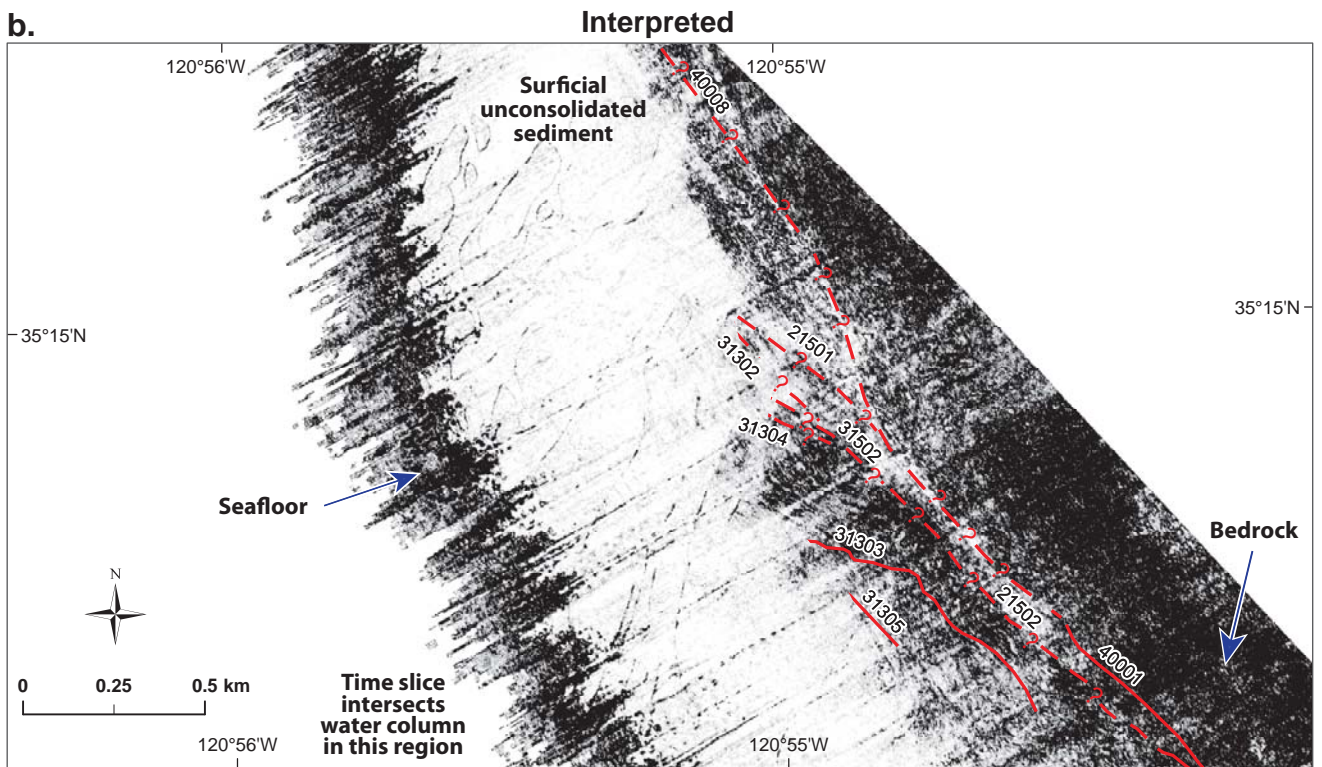
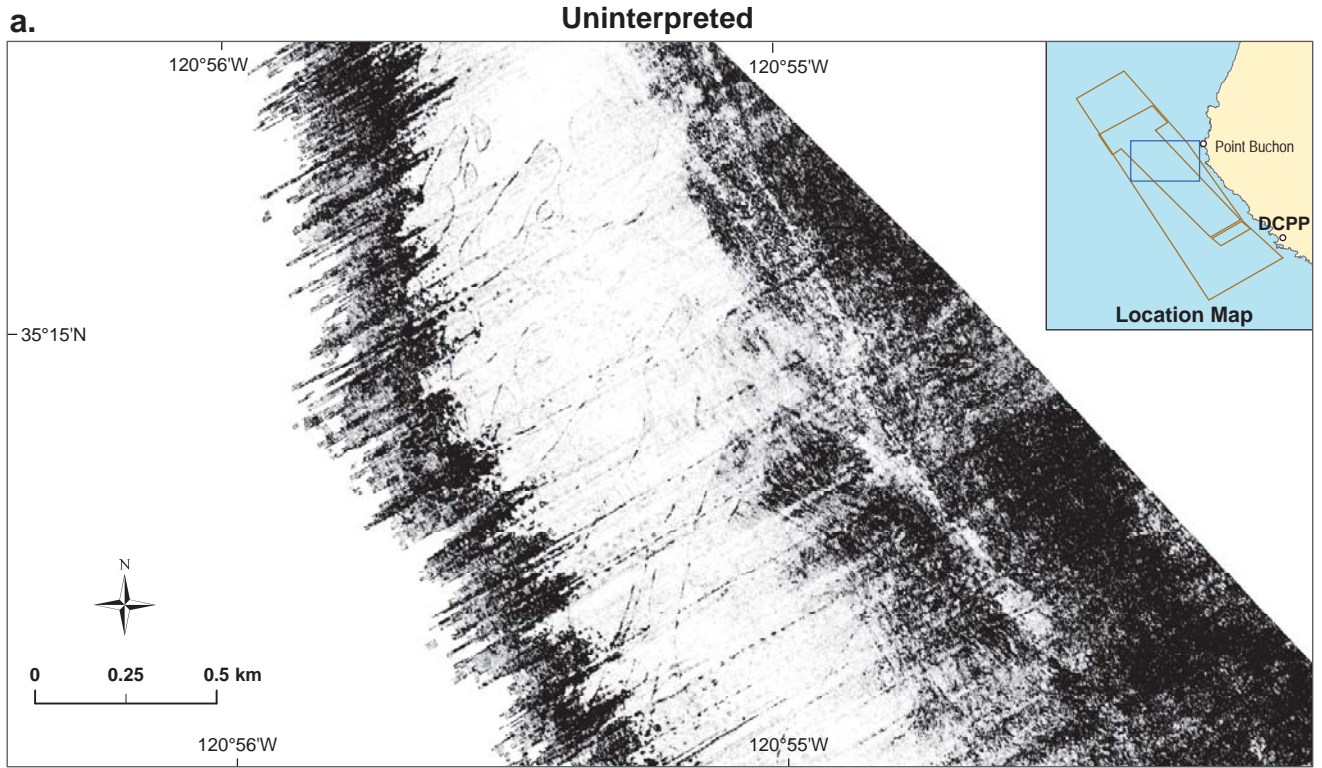
Amplitude time slice maps at 95 ms (TWTT) in the southern part of the 3D study area showing (a) uninterpreted and (b) interpreted strands of the Point Buchon fault zone

DCPP 3D/2D Seismic-Reflection Investigation



Pacific Gas and Electric Company

Figure 15

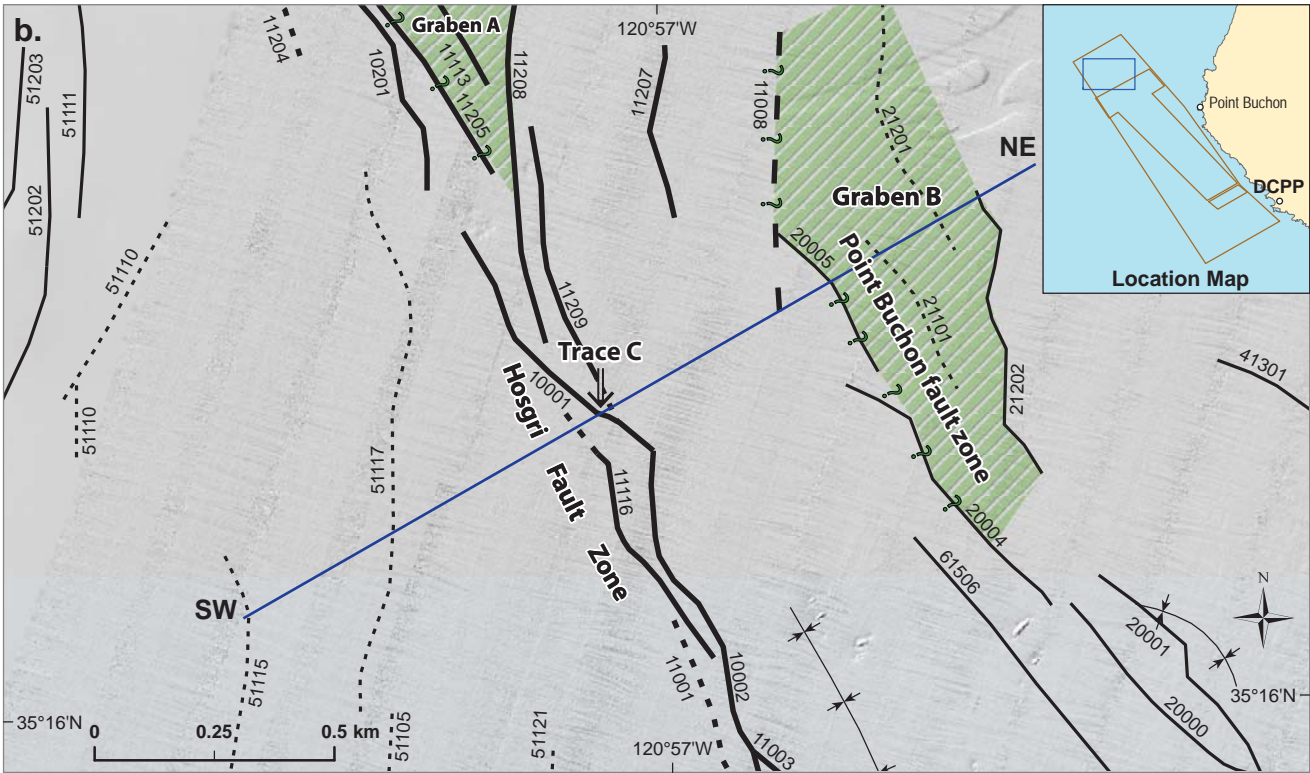
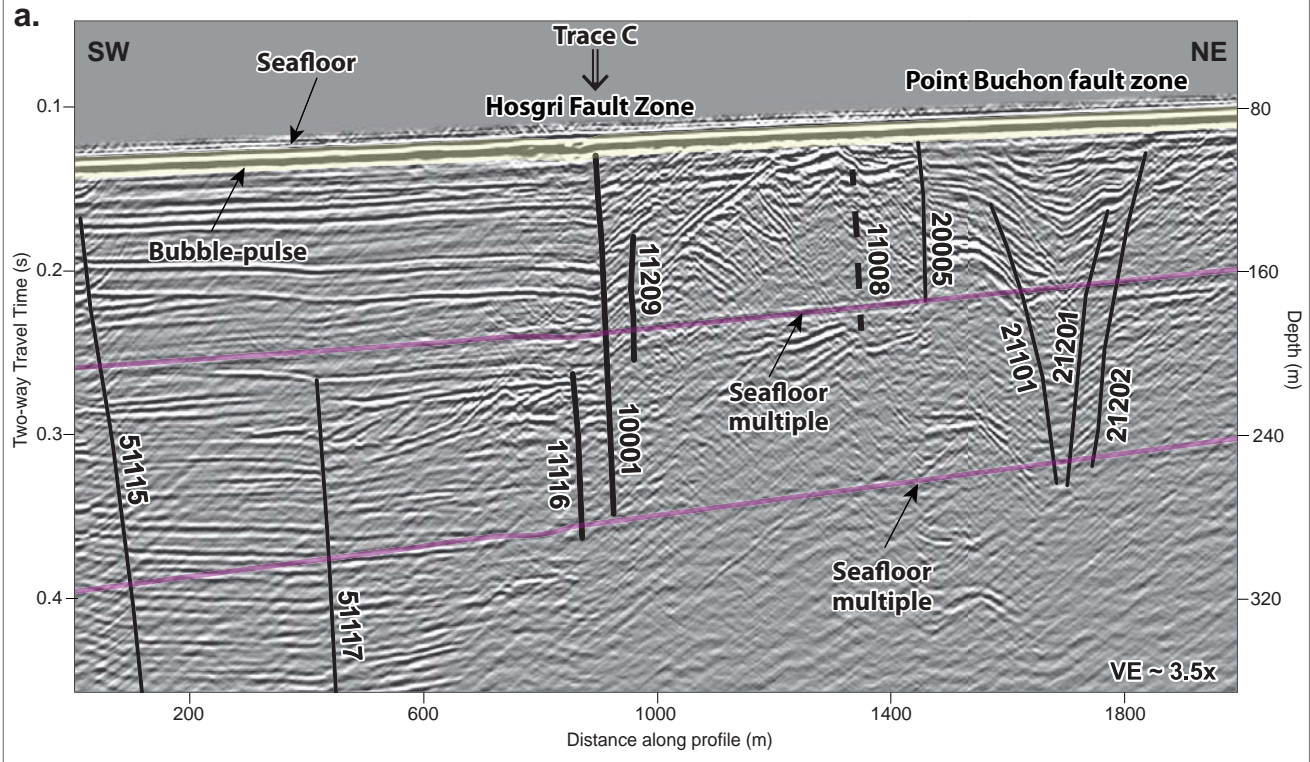


Explanation

---?--- Faults, solid where well located, dashed where inferred or approximately located, queried where uncertain, dotted where buried by more than 20 milliseconds of undeformed strata

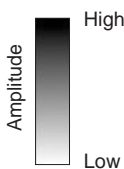
Fault strands associated with the fault intersection of the Point Buchon fault zone shown in (a) uninterpreted and (b) interpreted similarity time slices at 74 ms (TWTT)

DCPP 3D/2D Seismic-Reflection Investigation



Explanation

-  Location of seismic profile shown on Plate 3b
-  Faults, solid where well located, dashed where inferred or approximately located, dotted where buried by more than 20 milliseconds of undeformed strata
-  Graben, queried where full extent is uncertain

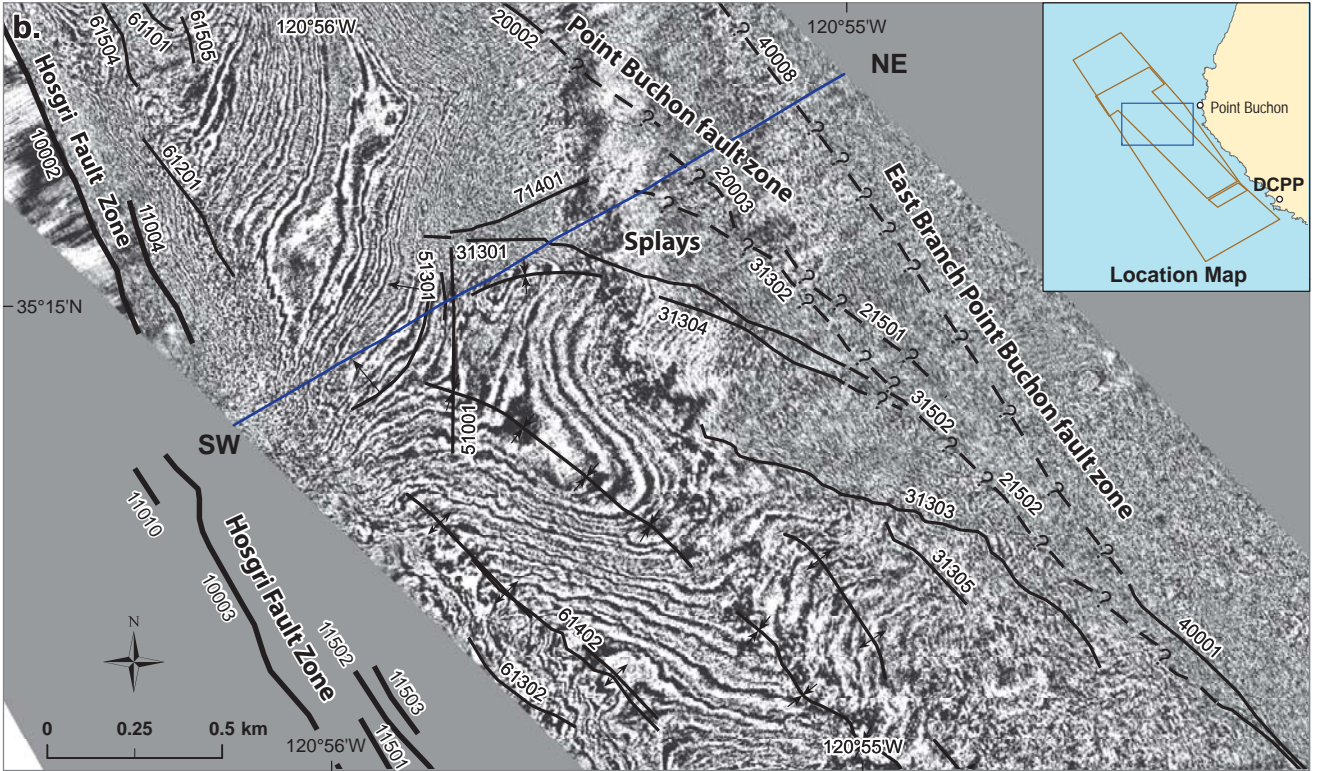
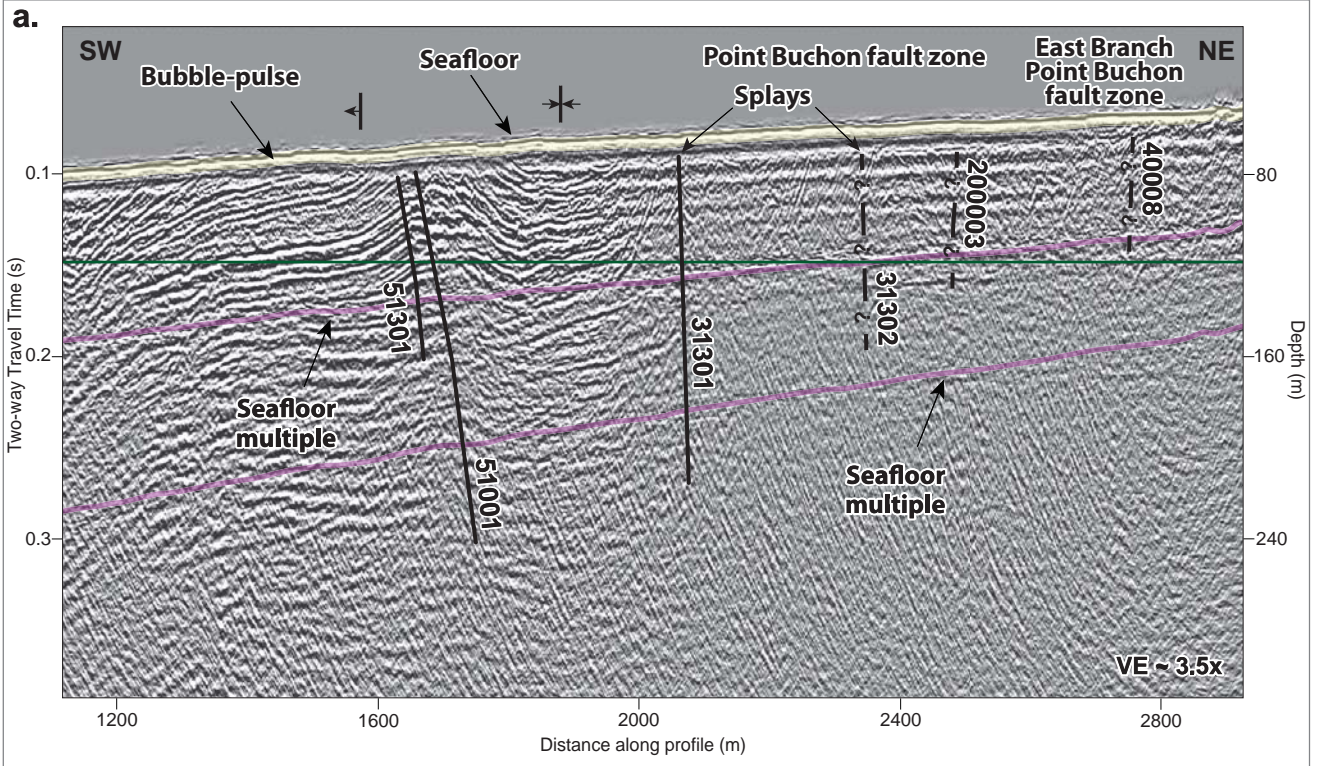


Note: Depth values on seismic profile assume a velocity of 1600 m/sec.

Graben at northern end of Point Buchon fault zone shown on (a) 2D seismic-reflection profile 1120, and (b) MBES bathymetry

DCPP 3D/2D Seismic-Reflection Investigation

File path: S:\13800\13838\13838.02\Figures\20120210_SIT\A\Figure_17.ai; Date: 07/09/2012; User: Jereme Chandler, LCI



Explanation

- Location of seismic profile
 - Time slice horizon
 - Faults, solid where well located, dashed where inferred or approximately located, queried where uncertain, dotted where buried by more than 20 milliseconds of undeformed strata
 - ↕ Syncline ↕ Anticline ↕ Monocline
- Amplitude
- High

Low

Note: Depth values on seismic profile assume a velocity of 1600 m/sec.

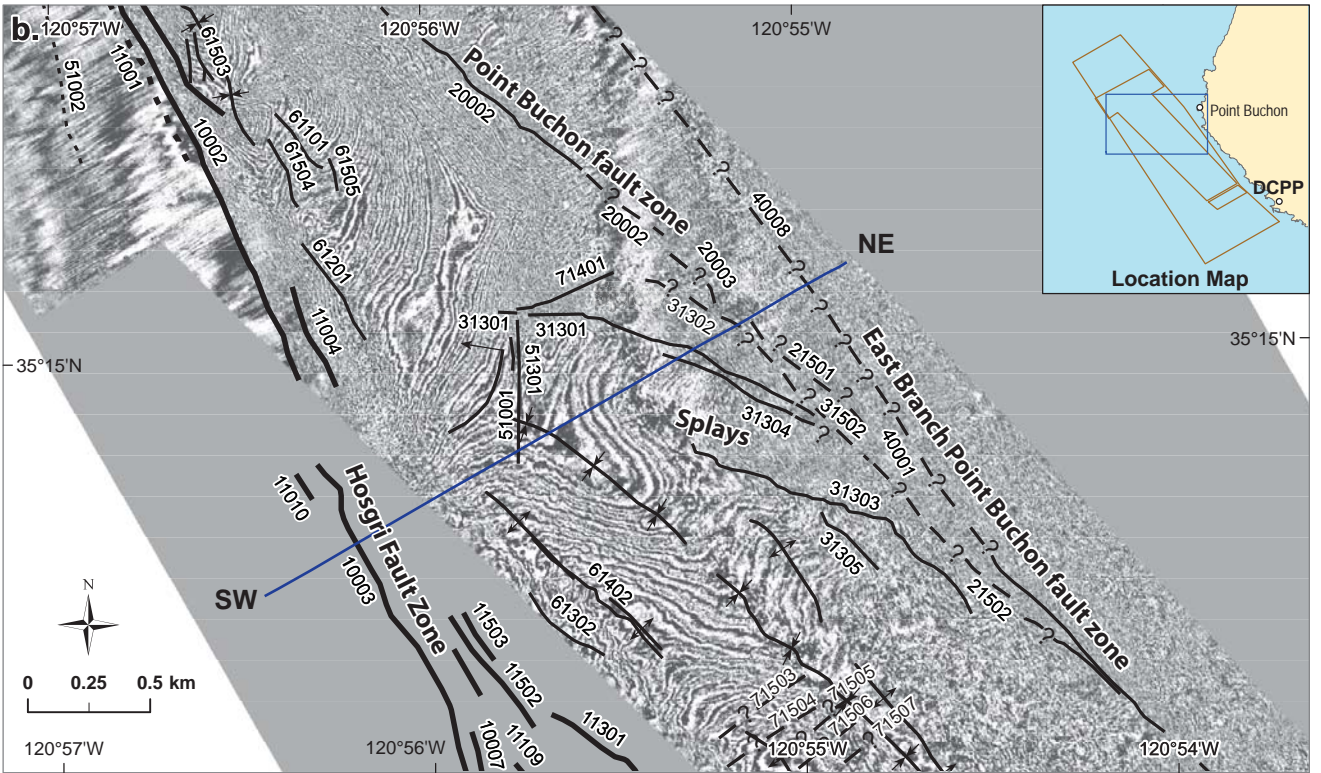
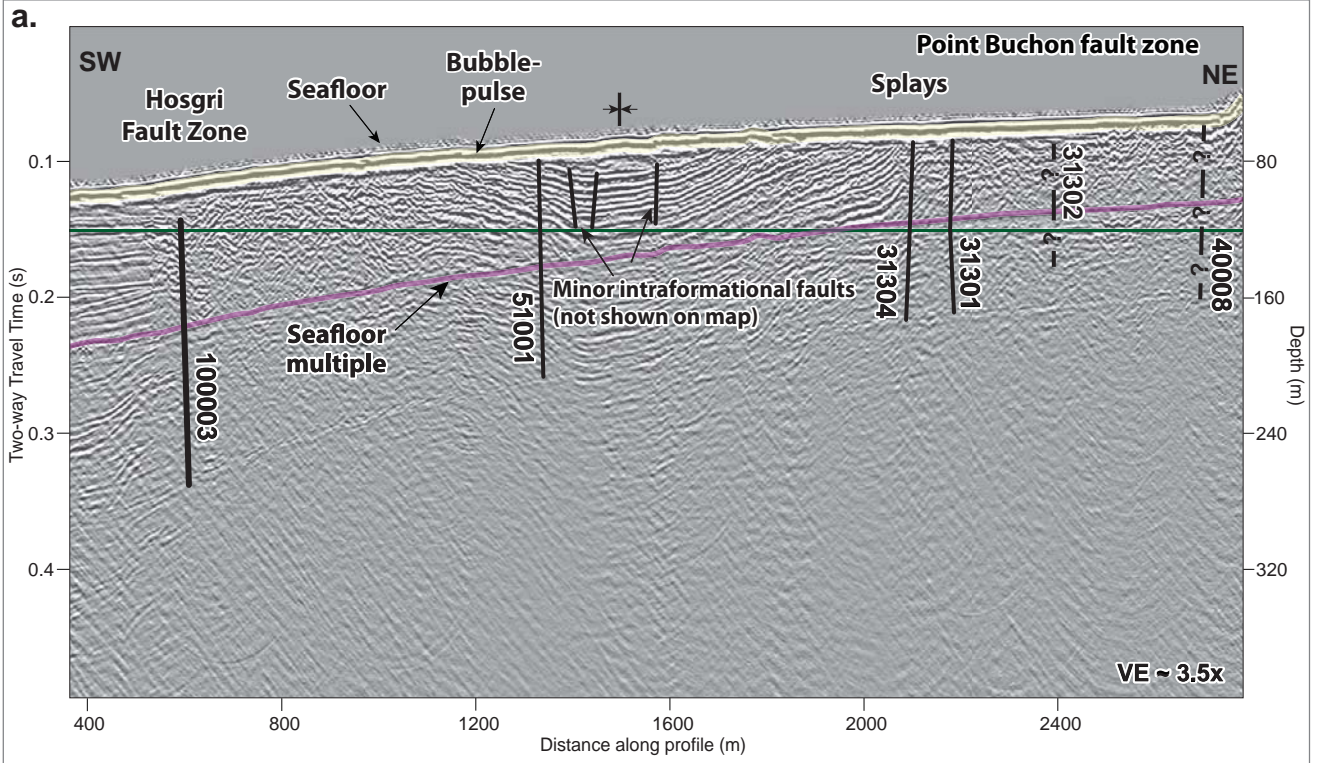
Structure associated with the northern part of the Point Buchon fault zone shown in (a) 3D seismic-reflection profile 11820 and (b) in amplitude time slice at 150 ms (TWTT)

DCPP 3D/2D Seismic-Reflection Investigation



Pacific Gas and Electric Company

Figure 18



Explanation

- Location of seismic profile shown on Plate 3b
 - Time slice horizon
 - Faults, solid where well located, dashed where inferred or approximately located, queried where uncertain, dotted where buried by more than 20 milliseconds of undeformed strata
 - Syncline
 - Anticline
 - Monocline
- Amplitude

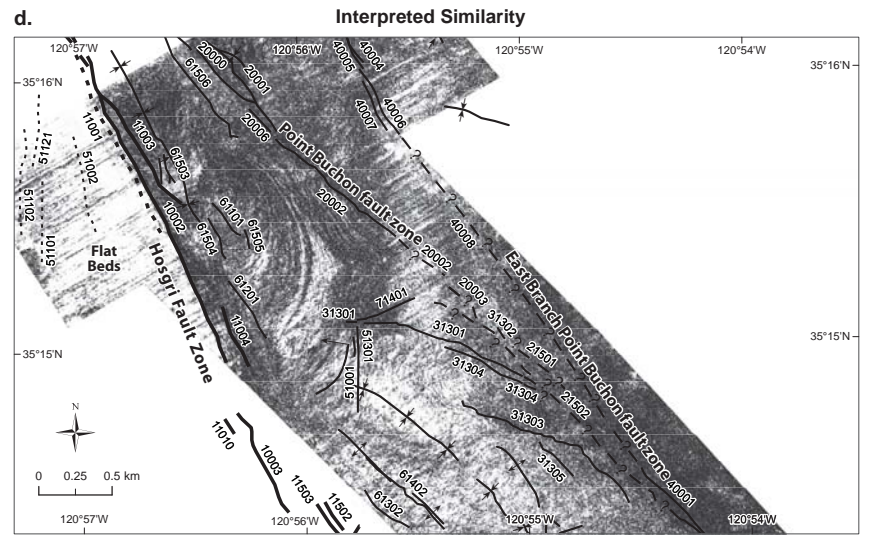
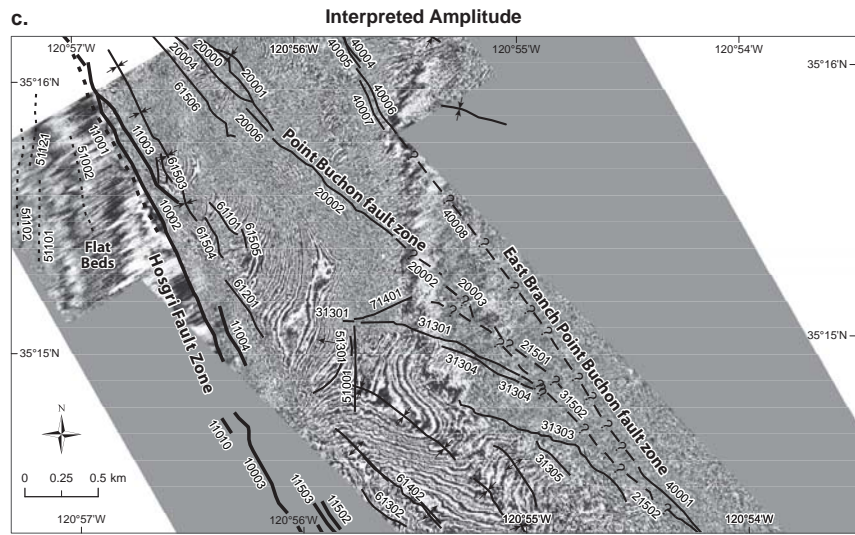
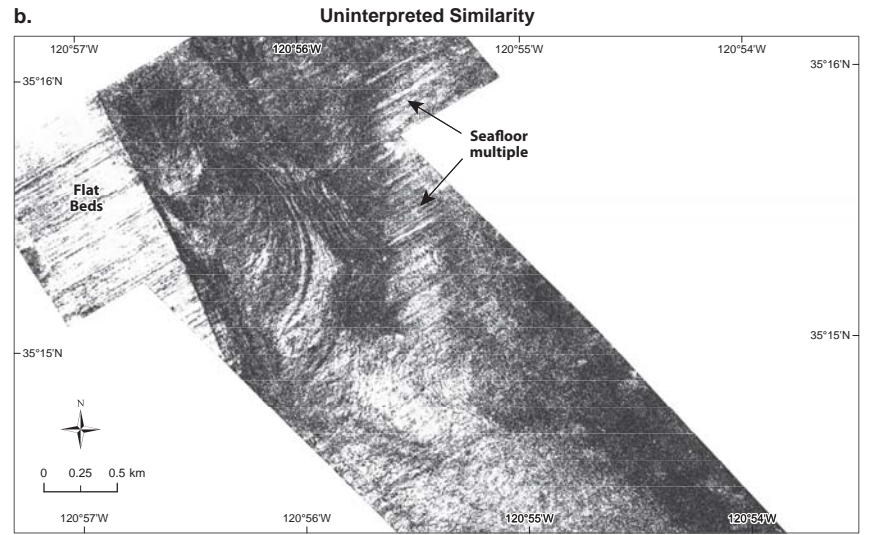
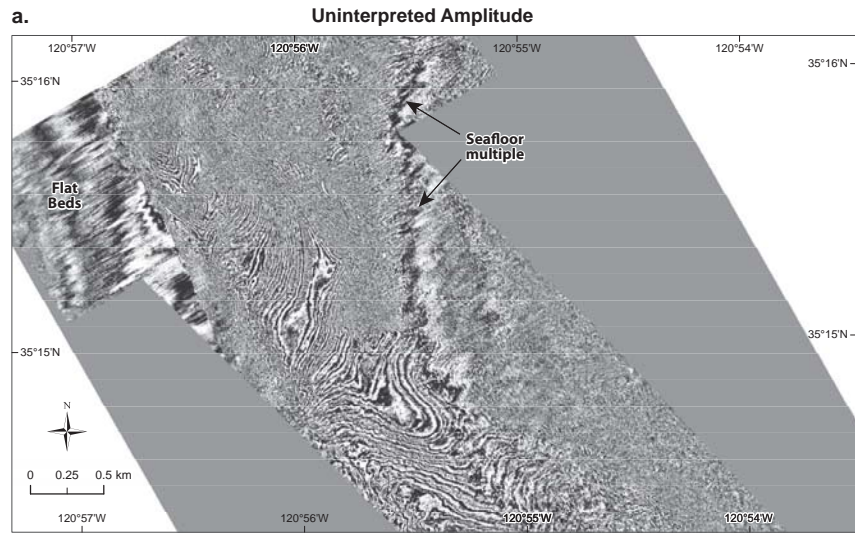
Note: Depth values on seismic profile assume a velocity of 1600 m/sec.

Principal structural elements in the northern part of the study area showing faults and folds in (a) 2D seismic-reflection profile 1399 and (b) on amplitude time slice map at 150 ms (TWTT)

DCPP 3D/2D Seismic-Reflection Investigation

Pacific Gas and Electric Company

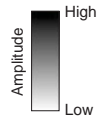
Figure **19**



Map projections: UTM Zone 10N, WGS84

Explanation

- ?--- Faults, solid where well located, dashed where inferred or approximately located, queried where uncertain, dotted where buried by more than 20 milliseconds of undeformed strata
- ⋈ Syncline
- ⋈ Anticline
- ⋈ Monocline

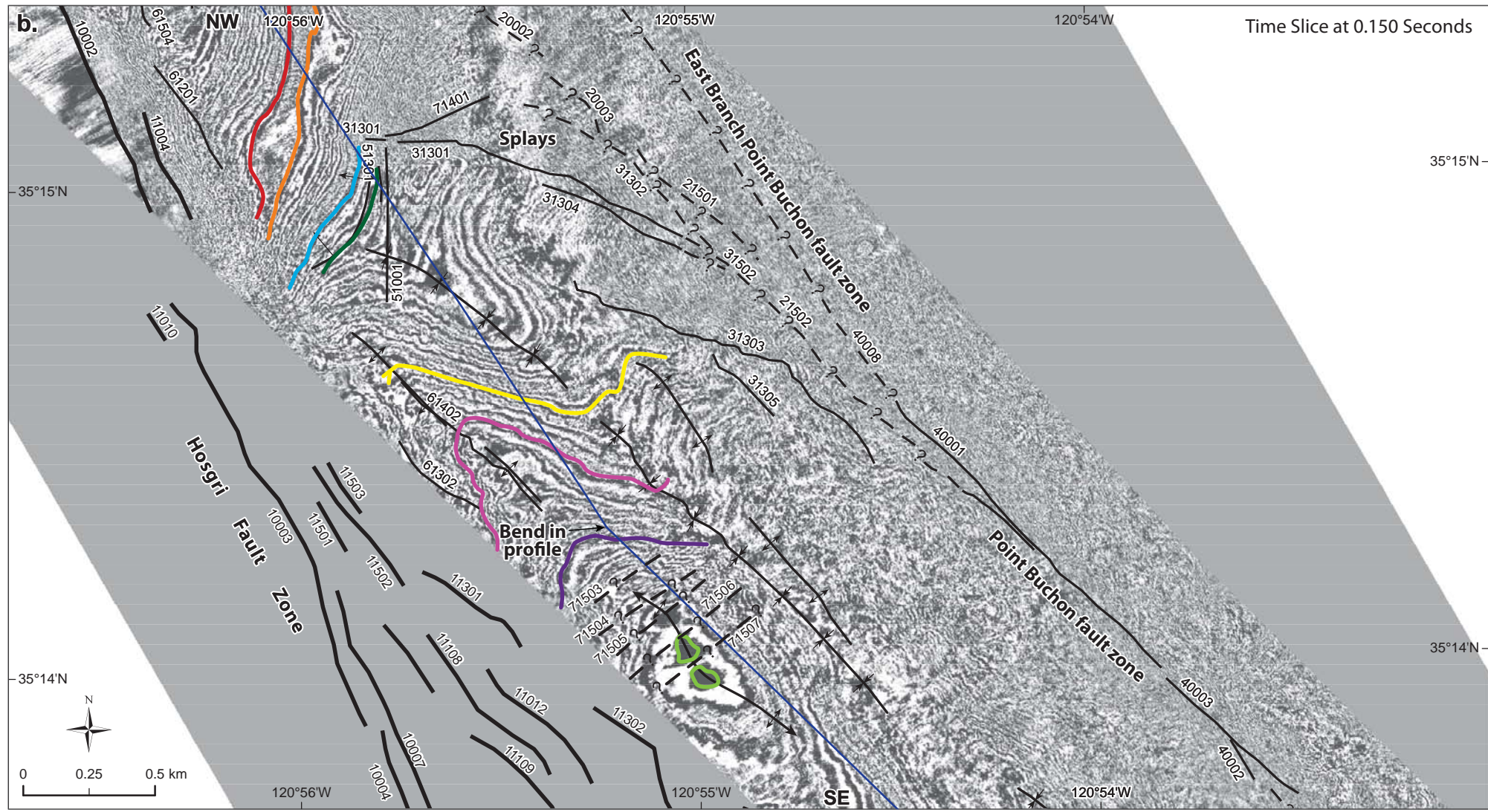
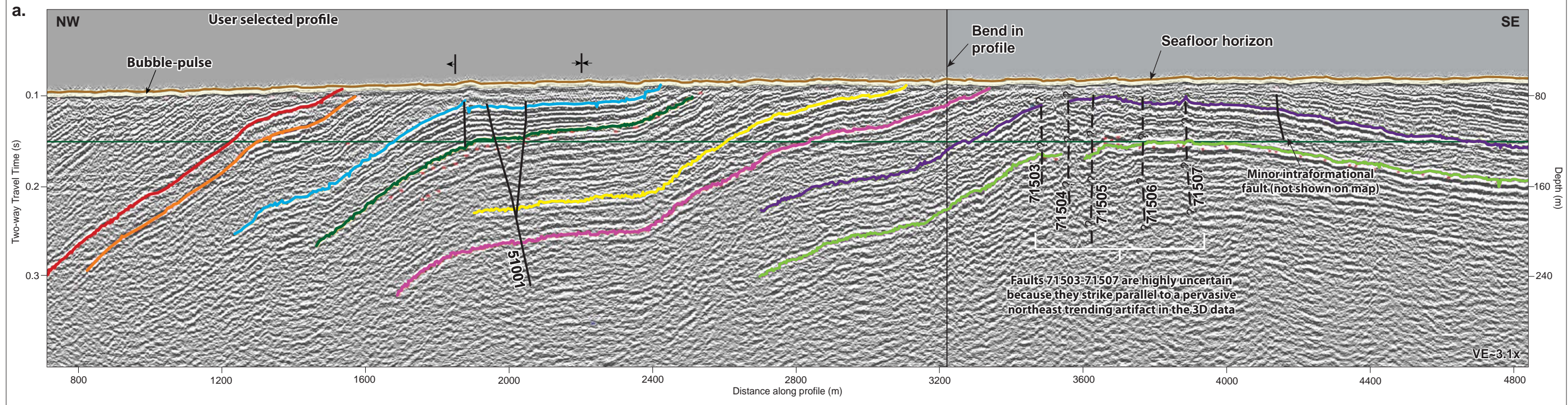


Comparison of amplitude and similarity time slices at 150 ms showing uninterpreted data (a and b) and interpreted maps (c and d)

DCPP 3D/2D Seismic-Reflection Investigation

Pacific Gas and Electric Company

Foldout **A**



Explanation

Location of seismic profile shown on Plate 3b

Time slice horizon

---?--- Faults, solid where well located, dashed where inferred or approximately located, queried where uncertain, dotted where buried by more than 20 milliseconds of undeformed strata

Horizon Name

- H05A
- H05B
- H15
- H20
- H25
- H30
- H35
- H40

Monocline

Anticline

Syncline

Amplitude

High

Low

Note: Depth values on seismic profile assume a velocity of 1600 m/sec.

Location Map

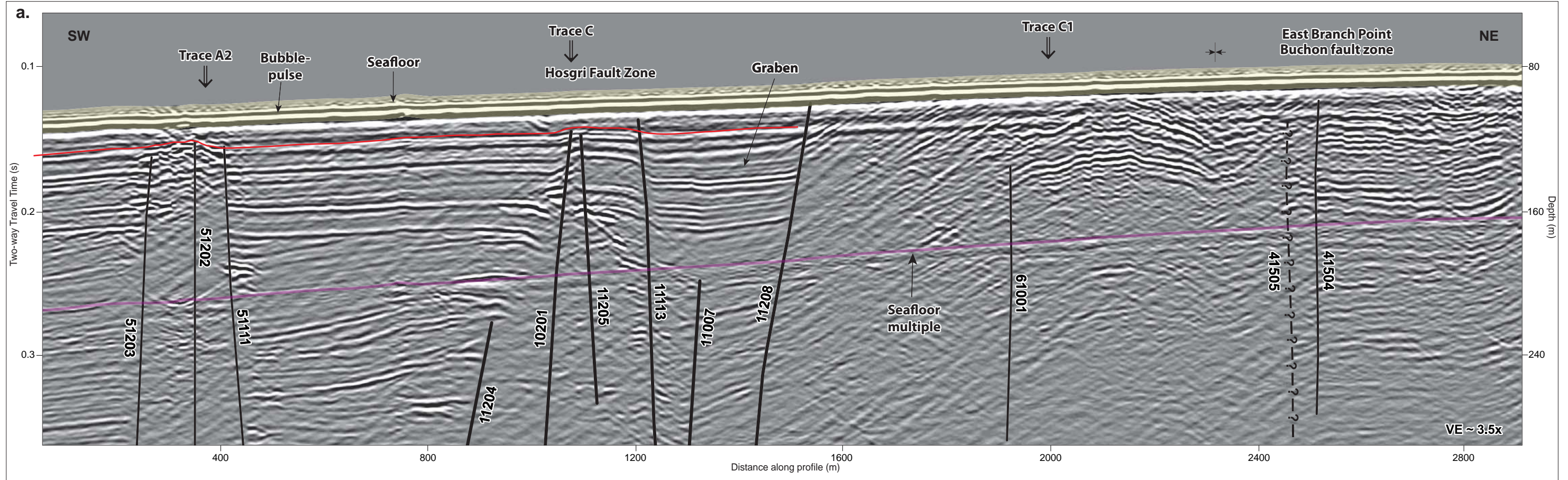
Marker horizons identified in (a) user-selected 3D strike line and (b) mapped on amplitude time slice at 150 ms (TWTT)

DCPP 3D/2D Seismic-Reflection Investigation

Pacific Gas and Electric Company

Foldout **B**

File path: S:\136001\38381\38381\Figures\20120210_SIT\AI\Foldout_B.ai; Date: 07/09/2012; User: Jerome Chandler, LCI



Explanation

- Location of seismic profile as shown on Plate 3b
- Shallow unconformity described in text
- Faults, solid where well located, dashed where inferred or approximately located, queried where uncertain, dotted where buried by more than 20 milliseconds of undeformed strata
- Approximate location of Hosgri fault traces from PG&E (2011b)
- Graben, queried where full extent is uncertain
- Syncline
- Anticline
- Monocline

Amplitude: High (black) to Low (white)

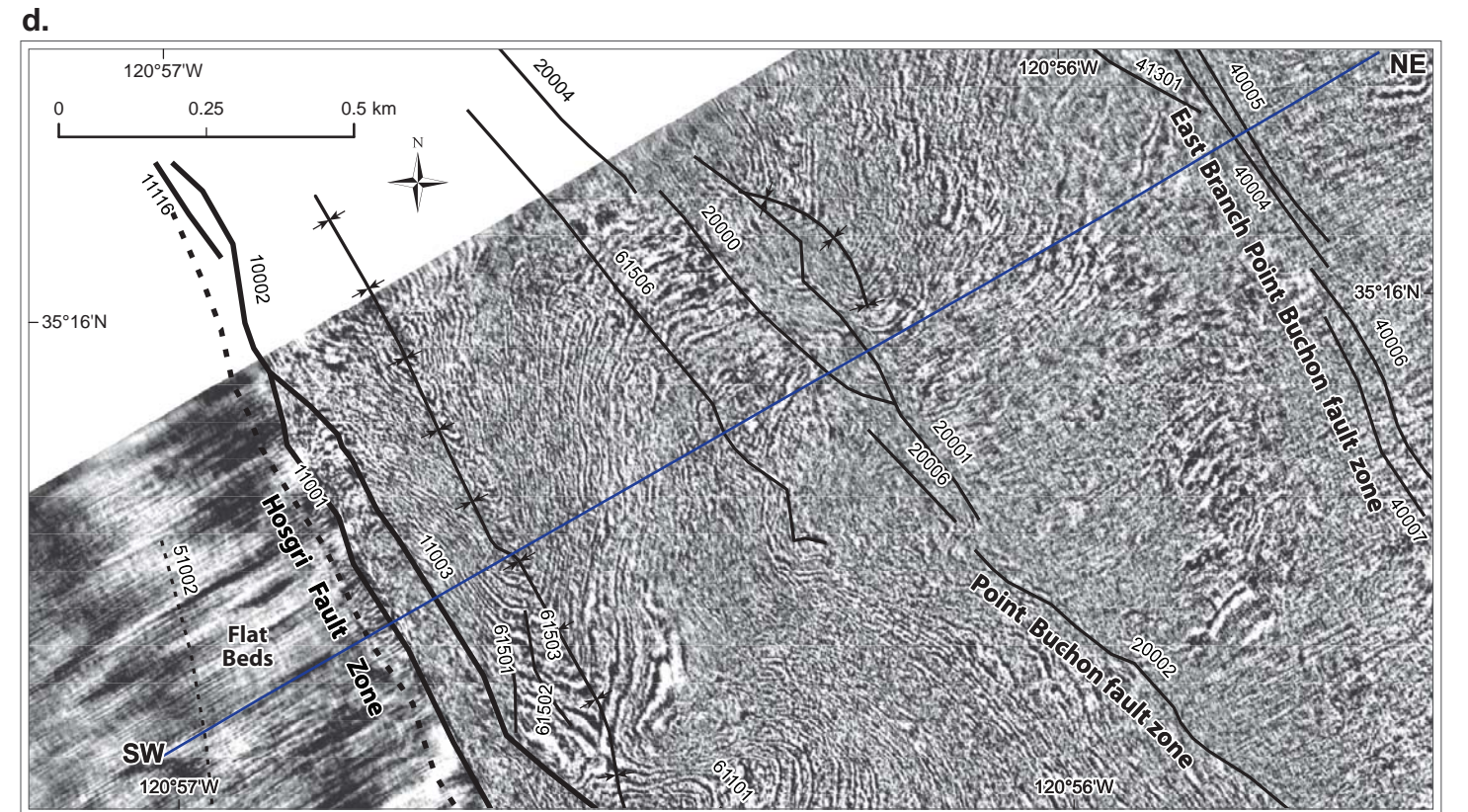
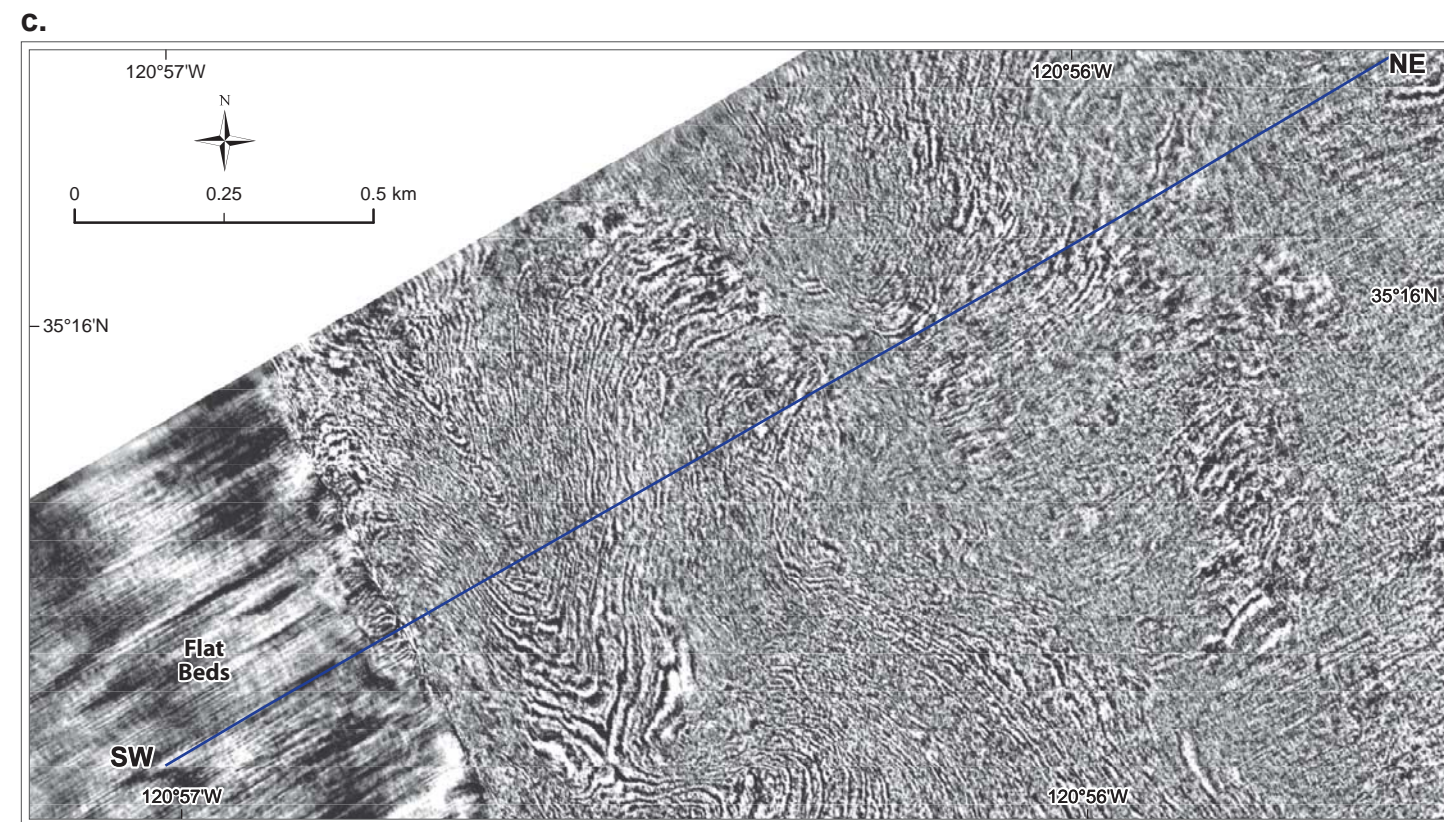
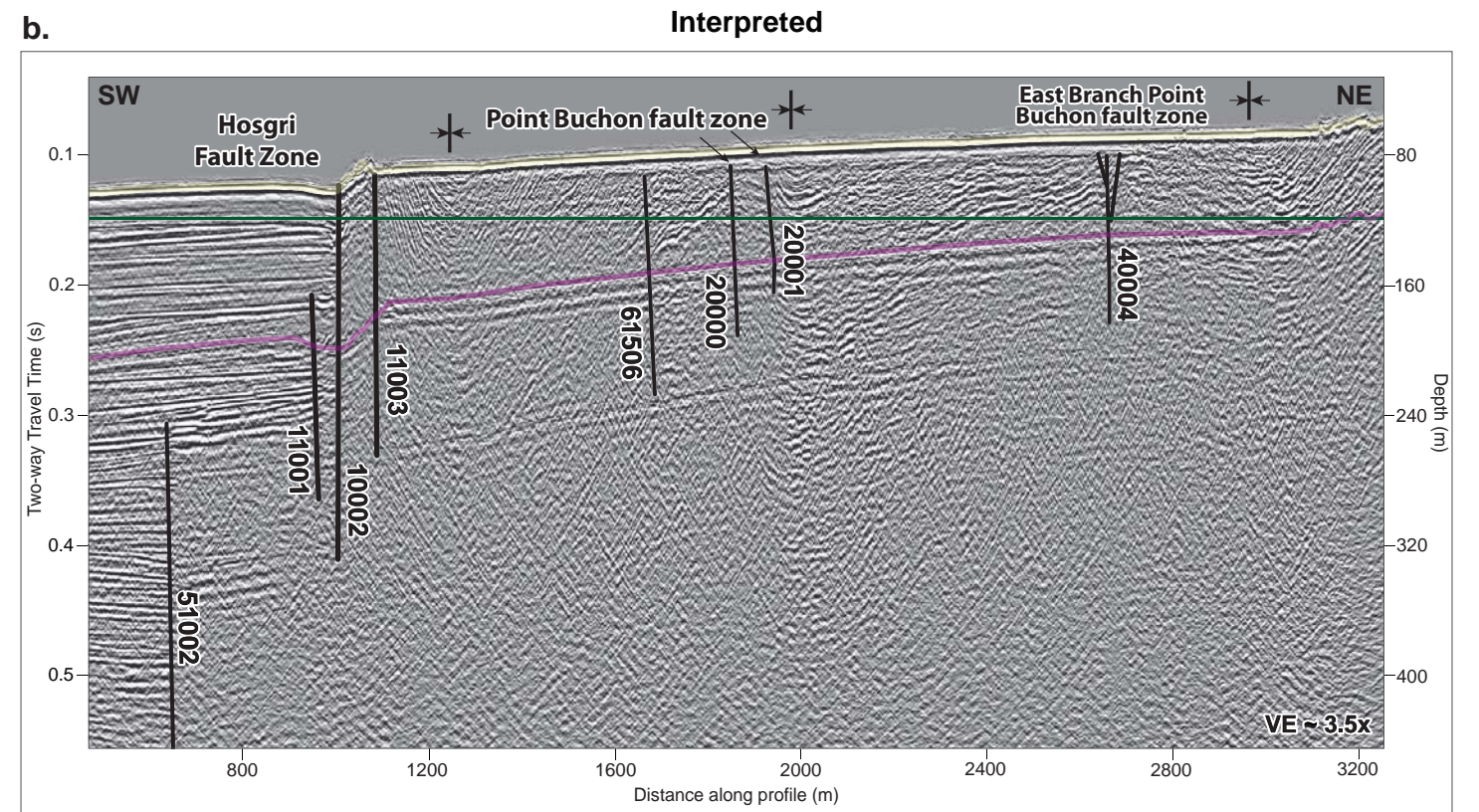
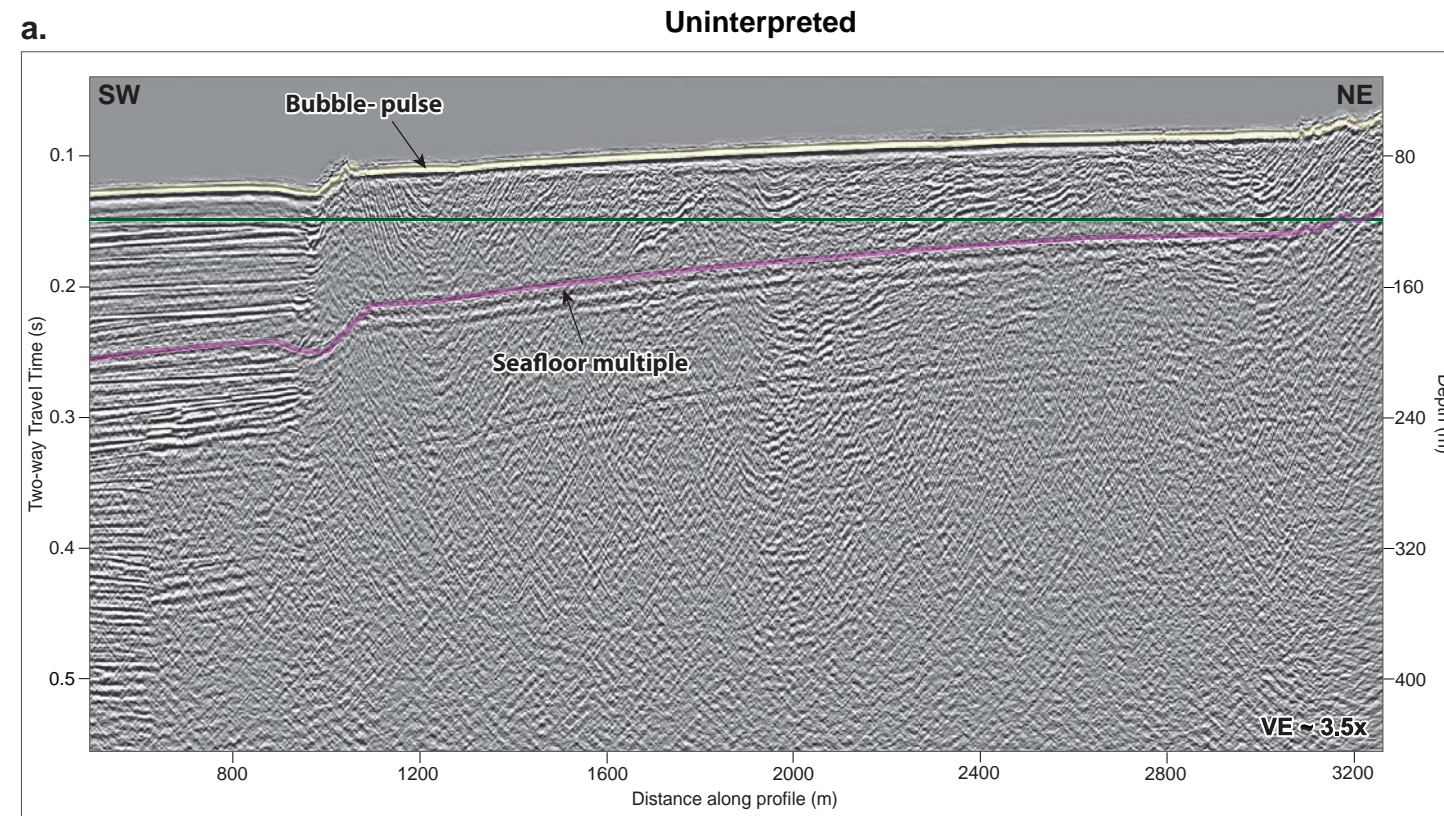
Note: Depth values on seismic profile assume a velocity of 1600 m/sec.

Graben associated with Hosgri Fault Zone:
 (a) 2D seismic-reflection profile 1039 showing fault boundaries and sediment fill and (b) map view showing faults, graben, and MBES bathymetry

DCPP 3D/2D Seismic-Reflection Investigation

Pacific Gas and Electric Company

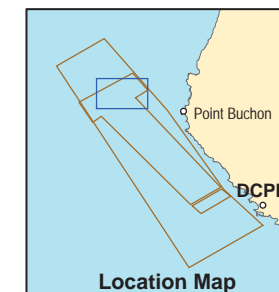
Foldout **C**



Explanation

- Location of seismic profile shown on Plate 3b
- Time slice horizon
- Faults, solid where well located, dashed where inferred or approximately located, queried where uncertain, dotted where buried by more than 20 milliseconds of undeformed strata
- Anticline
- Syncline
- Amplitude: High to Low

- Notes:
1. Depth values on seismic profile assume a velocity of 1600 m/sec.
 2. Map projections: UTM Zone 10N, WGS84

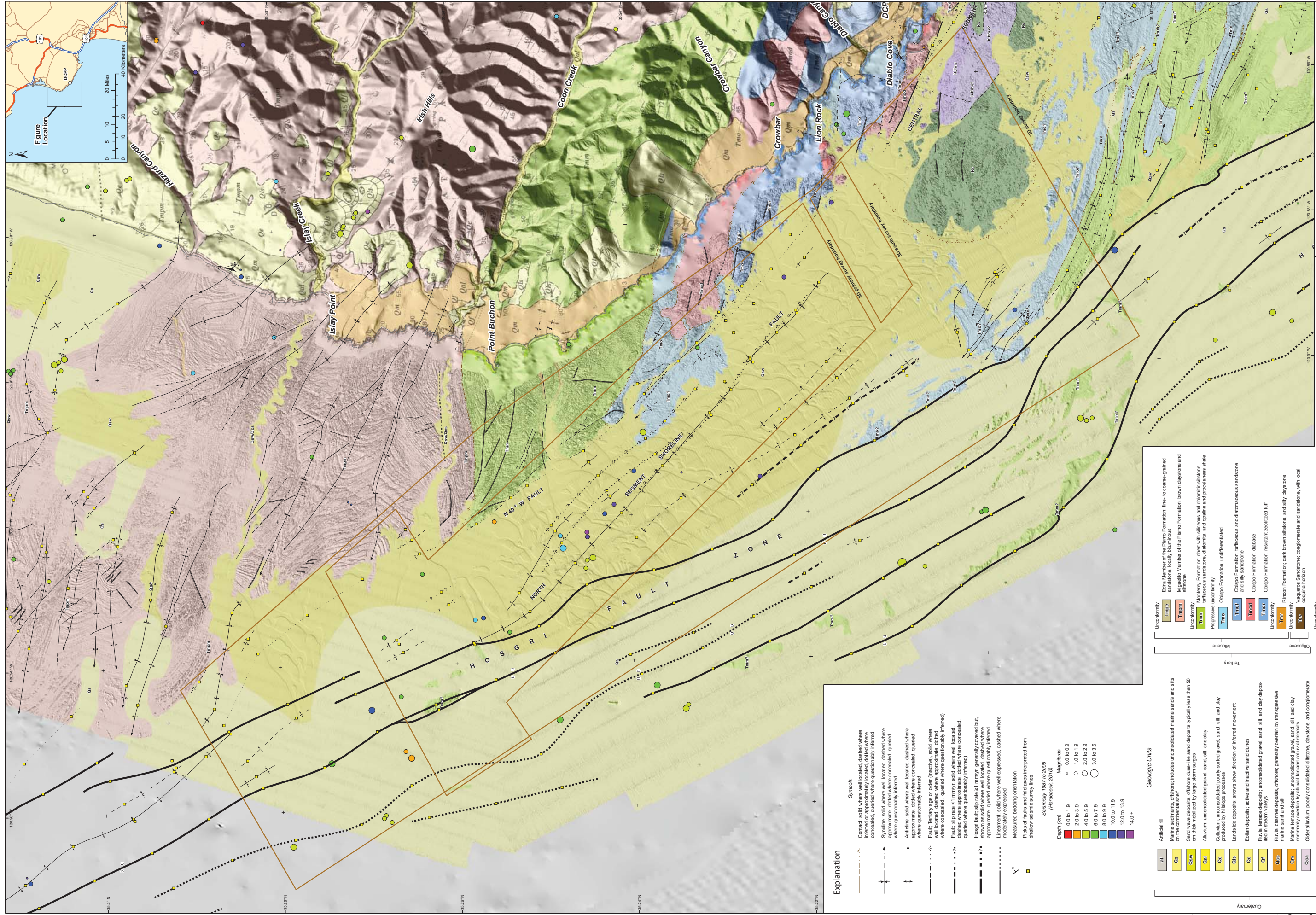


Relationship of the Hosgri and Point Buchon fault zones in the northern part of the survey area: (a) uninterpreted and (b) interpreted 3D profile 11200; (c) uninterpreted and (d) interpreted amplitude time slice at 150 ms (TWTT)

DCPP 3D/2D Seismic-Reflection Investigation

Pacific Gas and Electric Company

Foldout **D**



Geology of Interpreted Offshore Structures from the 2011 Shoreline Fault Zone Report (PG&E, 2011b)

Note: Geologic map shown here is an excerpt of Plate 1 from PG&E (2011b). Not all geologic units in the explanation are present on the map

Map projection: NAD 1983, UTM Zone 10 North
 Map scale: 1:20,000
 0 1,000 2,000 4,000 feet
 0 500 1,000 Meters

Explanation

Symbols

- Contact: solid where well located, dashed where inferred or approximately located, dotted where concealed, queried where questionably inferred
- Syncline: solid where well located, dashed where approximate, dotted where concealed, queried where questionably inferred
- Anticline: solid where well located, dashed where approximate, dotted where concealed, queried where questionably inferred
- Fault: Tertiary-age or older (inactive), solid where well located, dashed where approximate, dotted where concealed, queried where questionably inferred
- Fault: slip rate < 1 mm/yr; solid where well located, dashed where approximate, dotted where concealed, queried where questionably inferred
- Hoopli fault: slip rate ≥ 1 mm/yr; generally covered but, shown as solid where well located, dashed where approximate, queried where questionably inferred
- Lineament: solid where well expressed, dashed where moderately expressed
- Measured bedding orientation
- Picks of faults and fold axes interpreted from shallow seismic survey lines

Seismicity 1987 to 2008 (Horsbeck, 2010)

Depth (km)

- 0.0 to 1.9
- 2.0 to 3.9
- 4.0 to 5.9
- 6.0 to 7.9
- 8.0 to 9.9
- 10.0 to 11.9
- 12.0 to 13.9
- 14.0 +

Magnitude

- 0.0 to 0.9
- 1.0 to 1.9
- 2.0 to 2.9
- 3.0 to 3.5

Geologic Units

Unit	Description
af	Artificial fill
Qs	Marine sediments, offshore; includes unconsolidated marine sands and silts on the continental shelf
Qsw	Shelf wave deposits, offshore; dune-like sand deposits typically less than 50 m in height by large storm surges
Qal	Alluvium; unconsolidated gravel, sand, silt, and clay
Qc	Colluvium; unconsolidated poorly-sorted gravel, sand, silt, and clay produced by hillslope processes
Qls	Landslide deposits; arrows show direction of inferred movement
Qa	Eolian deposits; active and inactive sand dunes
Qf	Fluvial terrace deposits; unconsolidated gravel, sand, silt, and clay deposited in stream valleys
Qcs	Fluvial channel deposits, offshore; generally overlain by transgressive marine sand and silt
Qm	Marine terrace deposits; unconsolidated gravel, sand, silt, and clay commonly overlain by alluvial fan and colluvial deposits
Qoa	Older alluvium; poorly consolidated siltstone, claystone, and conglomerate

Unconformity

- Unconformity: Piano Formation; undifferentiated to coarse-grained sandstone
- Local unconformity: Bellevue Member of the Piano Formation; sandy claystone, siltstone, claystone and fine-grained sandstone, diatomaceous horizons
- Gregg Member of the Piano Formation; fine- to medium-grained silty sandstone, rare diatomaceous siltstone, pebble conglomerate, and bluish sandstone
- Note: Geologic units are shaded by depth (e.g., QoaC3) indicate depth profiles in which the former unit overlies the latter.

Unconformity

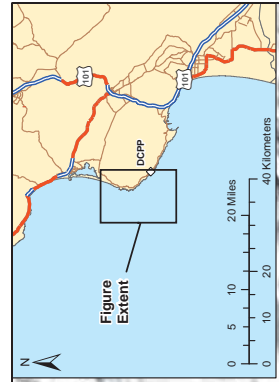
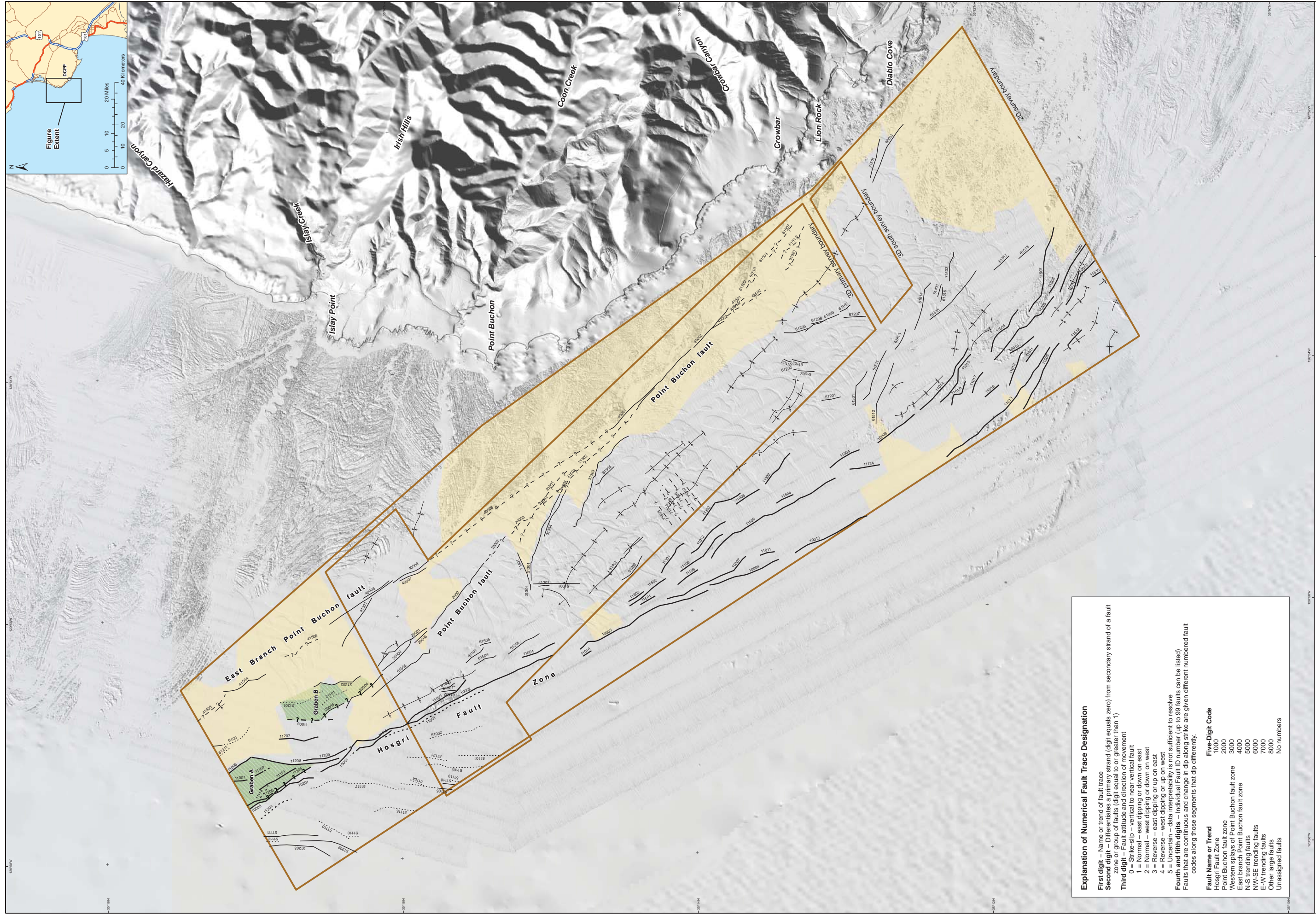
- Time: Edge Member of the Piano Formation; fine- to coarse-grained sandstone, locally bluish silty sandstone
- Time: Mugueta Member of the Piano Formation; brown claystone and siltstone
- Time: Monterey Formation; chert with siliceous and dolomitic siltstone, tuffaceous sandstone, diatomite, and opaline and proclastic shale
- Progressive unconformity: Obispo Formation, undifferentiated
- Time: Obispo Formation; tuffaceous and diatomaceous sandstone and silty sandstone
- Time: Obispo Formation; diabase
- Unconformity: Obispo Formation; resistant acidified tuff
- Time: Rincon Formation; dark brown siltstone, and silty claystone
- Unconformity: Vaqueros Sandstone; conglomerate and sandstone, with local caliche horizon
- Unconformity: Undifferentiated well bedded brown fine- to coarse-grained arkosic to lithic sandstone with shale

Franciscan Complex

- Franciscan Complex, undifferentiated
- Franciscan Complex rocks, pelagic, shaly shale, mudstone and siltstone with knobbies of graywacke, schist, conglomerate, metaclastic rocks, and green, white, or red chert
- Franciscan Complex, metaclastic rocks
- Franciscan Complex, ophiolite
- Serpentine

Approximate survey boundaries





Explanation of Numerical Fault Trace Designation

First digit – Name or trend of fault trace
Second digit – Differentiates a primary strand (digit equals zero) from secondary strand of a fault zone or group of faults (digit equal to or greater than 1)
Third digit – Fault attitude and direction of movement
 0 = Strike-slip – vertical to near vertical fault
 1 = Normal – east dipping or down on east
 2 = Normal – west dipping or down on west
 3 = Reverse – east dipping or up on east
 4 = Reverse – west dipping or up on west
 5 = Uncertain – data interpretability is not sufficient to resolve
Fourth and fifth digits – Individual Fault ID number (up to 99 faults can be listed)
 Faults that are continuous and change in dip along strike are given different numbered fault codes along those segments that dip differently.

Fault Name or Trend

- Hosgri Fault Zone
- Point Buchon fault zone
- Western splays of Point Buchon fault zone
- East branch Point Buchon fault zone
- N-S trending faults
- NW-SE trending faults
- E-W trending faults
- Other large faults
- Unassigned faults

Five-Digit Code

- 1000
- 2000
- 3000
- 4000
- 5000
- 6000
- 7000
- 8000
- No numbers

Explanation

- Faults, solid where well located, dashed where inferred or approximately located, queried where uncertain, dotted where buried by more than 20 milliseconds of undeformed strata
- Syncline axis
- Anticline axis
- Approximate survey boundaries
- Area of poor interpretability

Notes:

- Faults and fold axes are shown at the position where they intersect a time slice at 150 milliseconds. Faults that do not intersect the 150 millisecond time slice were projected vertically from their intersection with a time slice at either 80 milliseconds or 300 milliseconds as appropriate.
- Basemap is hillshade image developed from MBES bathymetry, taken from Shoreline Fault report, the PG&E (2010) coastal LIDAR survey, and the San Luis Obispo County 5 m DEM.

Map scale: 1:20,000
 Map projection: NAD 1983,
 UTM Zone 10 North

